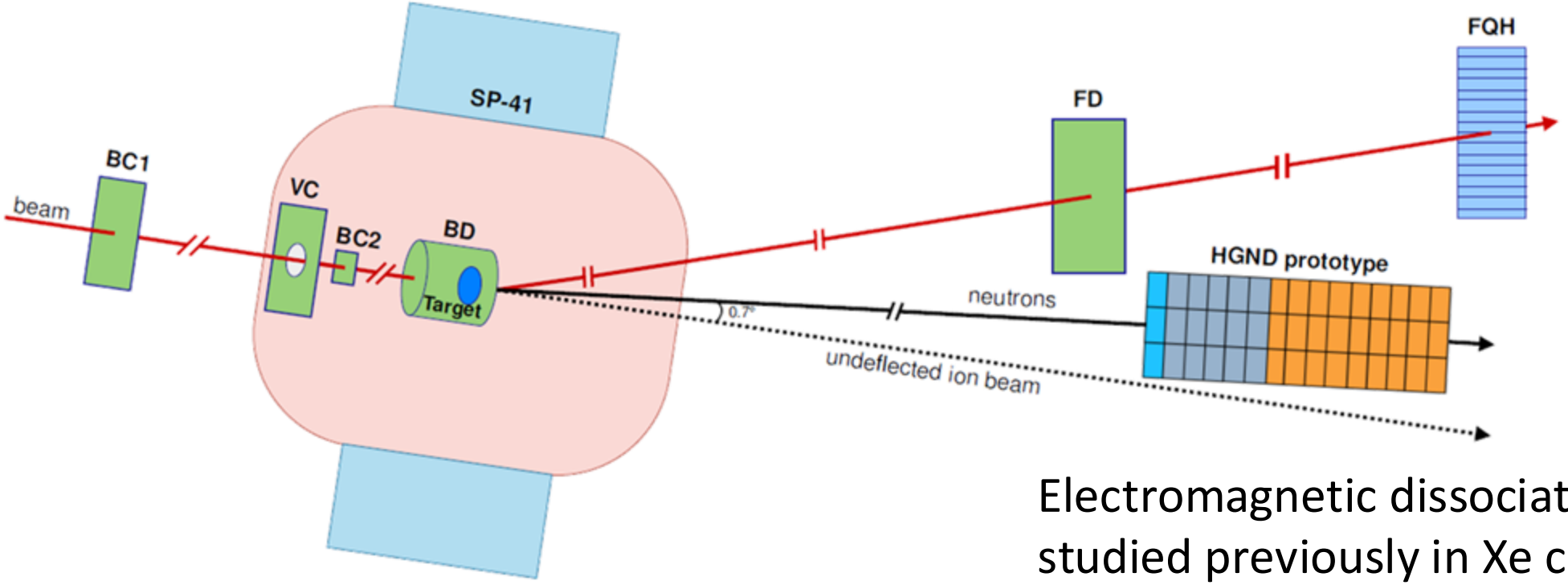
BM@N
Baryonic Matter at Nuclotron

Status of the analysis of spectator neutron yields in Run 8

A. Zubankov on behalf of the HGND group

12.05.2026

Introduction



To validate the concept of the full-scale HGND, small prototype was tested in ^{124}Xe+CsI at 3.8A GeV run at the BM@N.

Electromagnetic dissociation has not been studied previously in Xe collisions at 2–4A GeV.

HGND prototype can be used to study neutrons from ultra-peripheral collisions and spectator neutrons in beams from the Nuclotron.

First measurements of forward neutrons from projectile fragmentation for central and semi-central collisions and for electromagnetic dissociation (EMD) of ^{124}Xe will be demonstrated.

Analysis note: https://bmn.jinr.int/wp-content/uploads/2026/05/Note_forward_neutrons_HGND.pdf

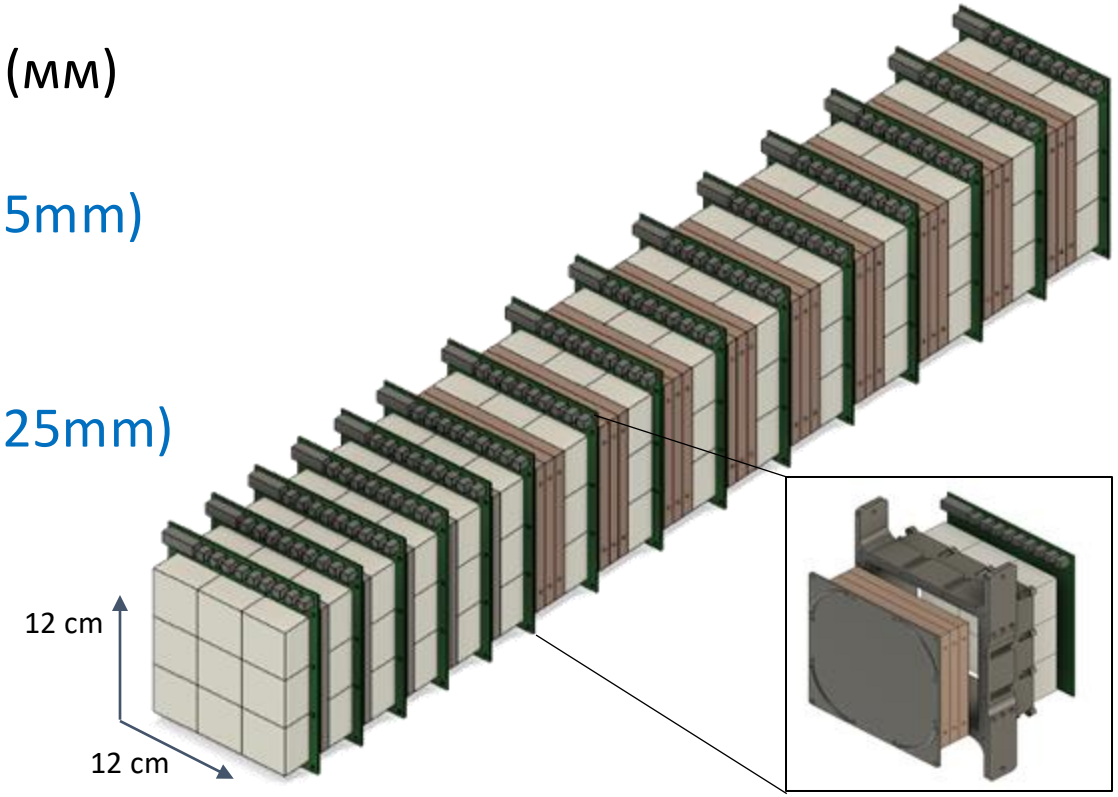
Outline

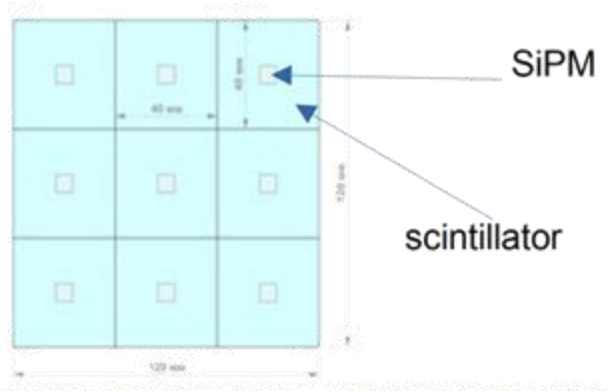
1. Measurements of distributions of kinetic energies of forward neutrons
2. Unfolding of kinetic energy spectra of neutrons
3. Validation of the background from simulations
4. Measurements of differential cross section of forward neutron emission
5. Comparison with LAND ALADIN 600A MeV Sn+Sn data

HGND prototype design

- Scint. layer **Veto** 120x120x25 (мм)
- 1st (electromagnetic) part:
  5 layers: **Pb (8mm)** + Scint. (25mm)
  + PCB + air
- 2nd (hadronic) part:
  9 layers: **Cu (30mm)** + Scint. (25mm)
  + PCB + air

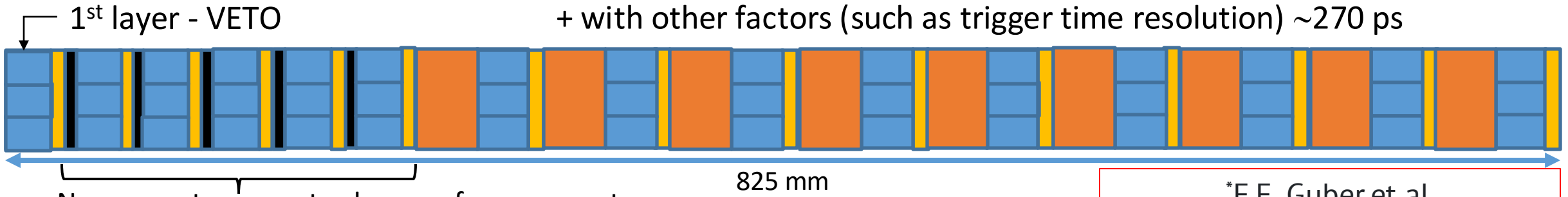
Scint. cell – 40 x 40 x 25 mm^3
Total number of cells – 135
Total size – 12 x 12 x 82.5 cm^3
Total length ~ 2.5 λ_{int}





Hamamatsu S13360- 6050PE
Photosensitive area – 6x6 mm^2
Number of pixels – 14400
Pixel size – 50 μm
Gain – 1.7×10^6
PDE – 40%

Time resolution of cell ~200 ps*,
+ with light collection heterogeneity ~240 ps,
+ with other factors (such as trigger time resolution) ~270 ps

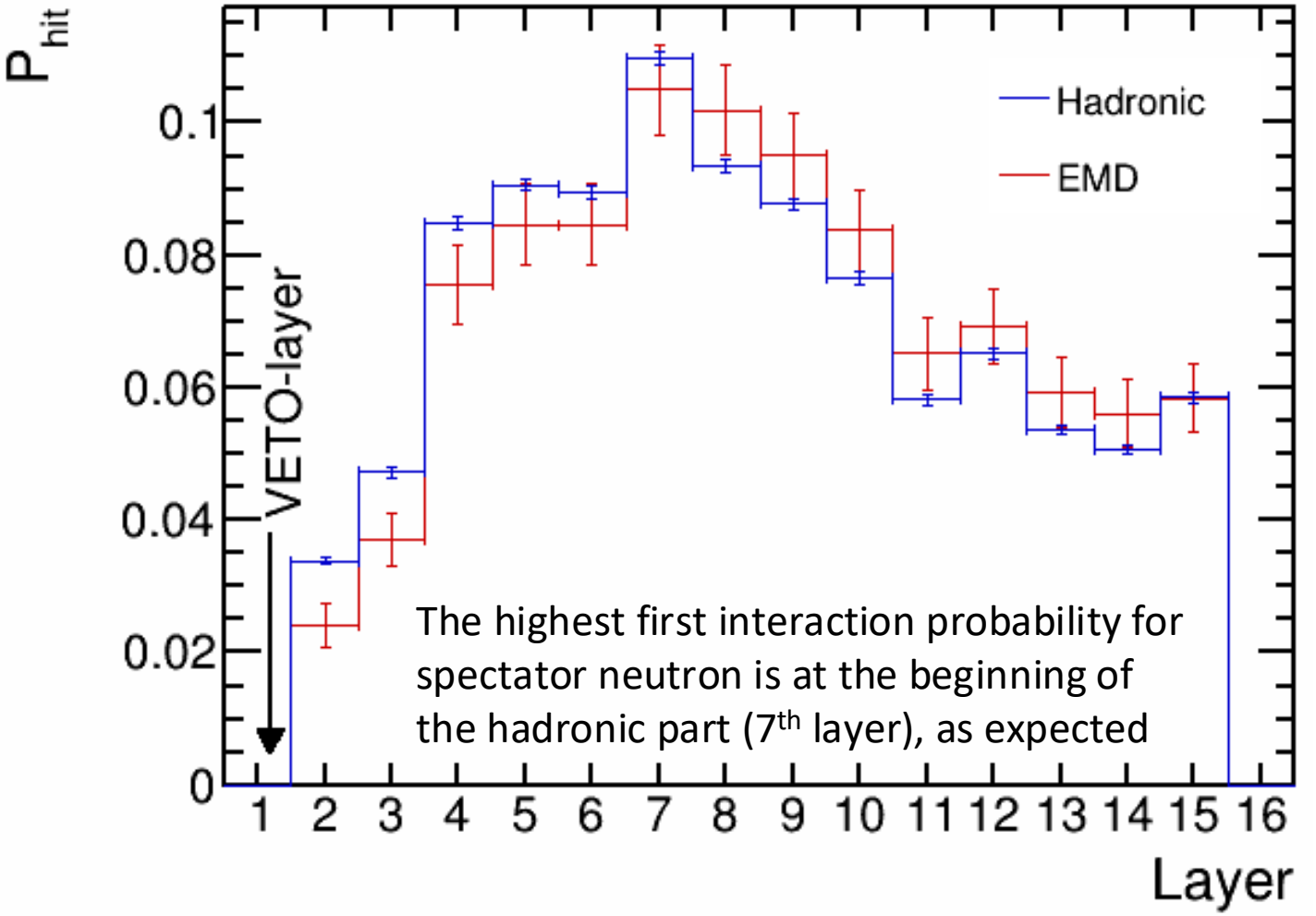


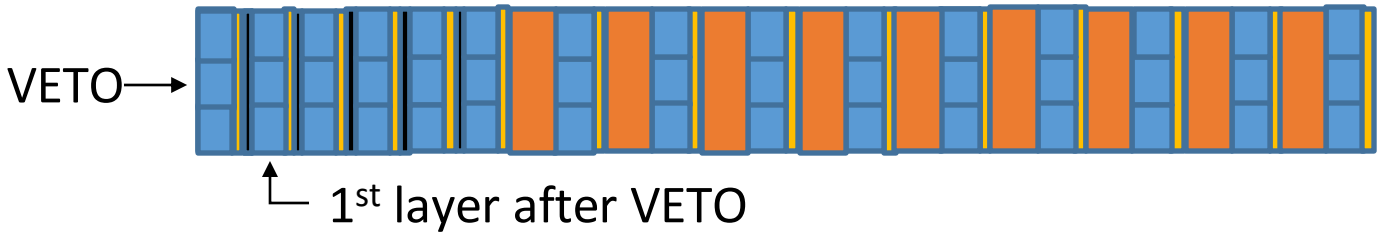
*F.F. Guber et al.
10.1134/S0020441223030065

1. Measurements of distributions of kinetic energies of forward neutrons

Selection of spectator neutrons

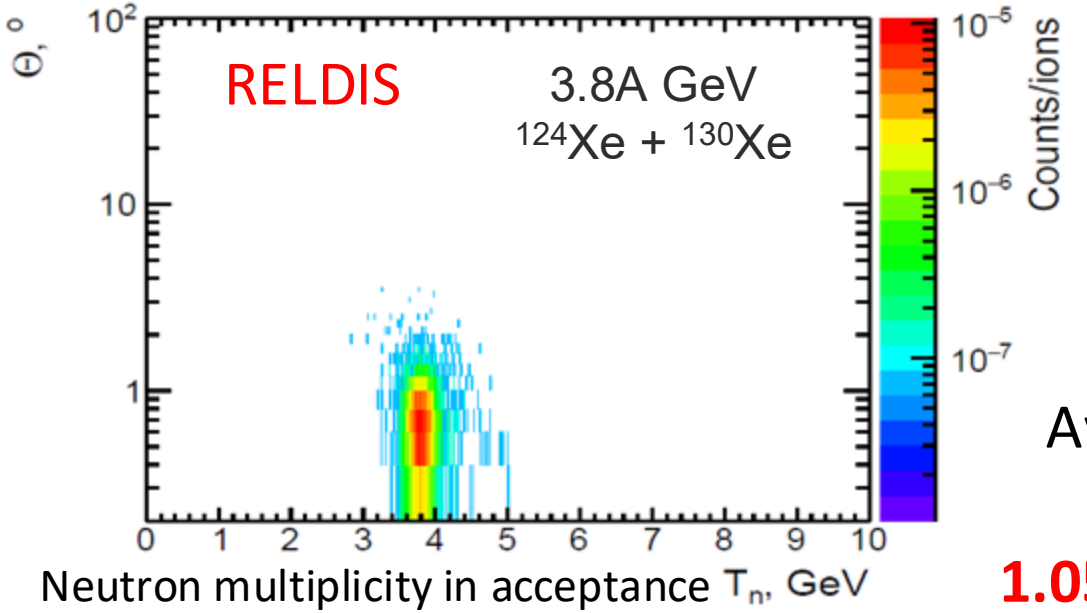
- Only single Xe ion in target
- CCT trigger
- Selection of events without charged particles using **VETO**
- Photon rejection using **1st layer after VETO** (1.55 X_0 or 0.11 λ_{int})
- Reconstruction of energy by **maximum velocity**
- Scaled by incident ion beam rate measured by **Beam Trigger BT**





Zubankov, A., Afanasiev, S., Golubeva, M. *et al.* Performance study of the Highly Granular Neutron Detector prototype in the BM@N experiment. *NUCL SCI TECH* **36**, 226 (2025).

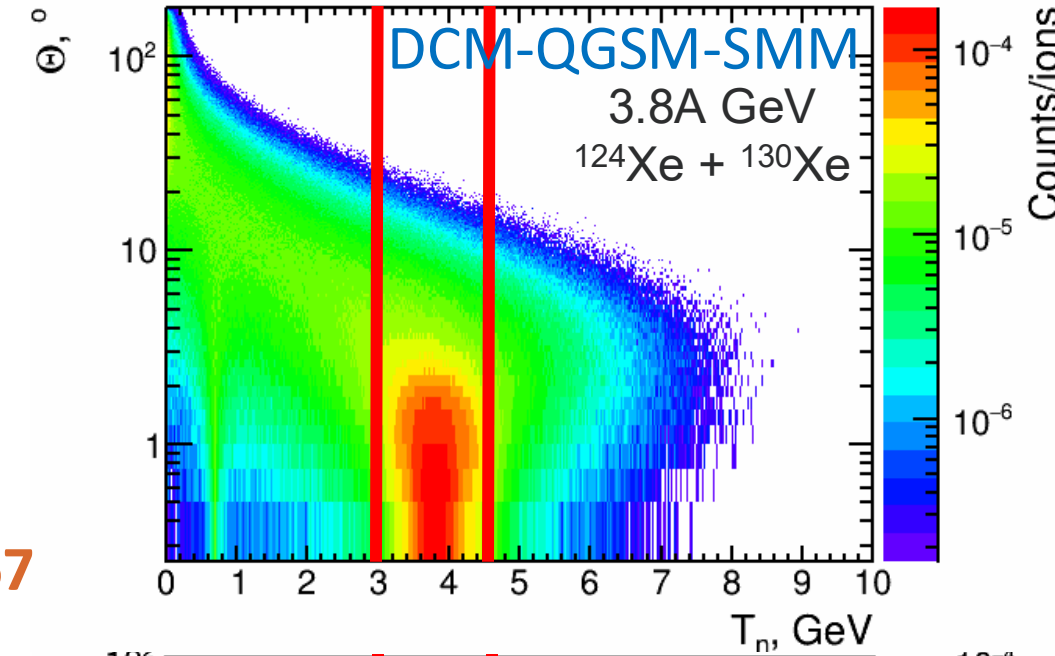
EMD vs hadronic interactions

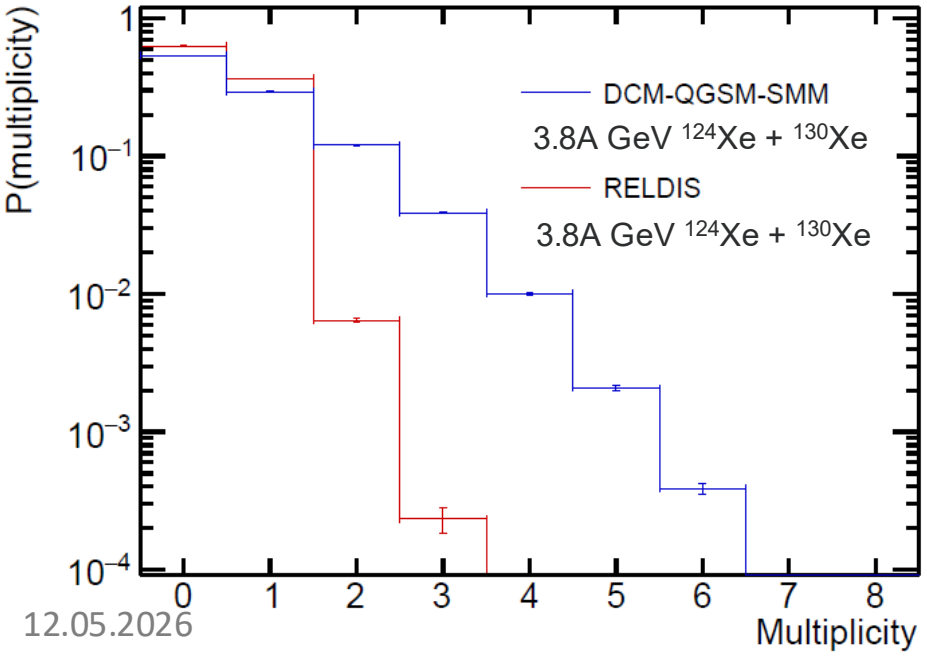


Neutron multiplicity in acceptance of the HGND prototype

Average neutron multiplicity

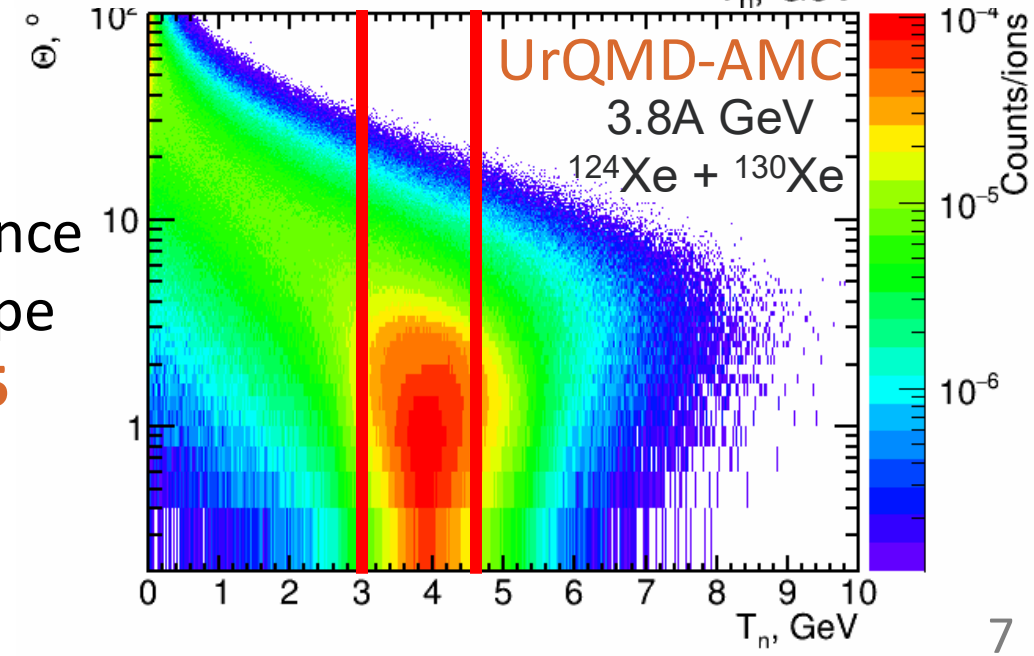
1.05 **13.56** **17.67**



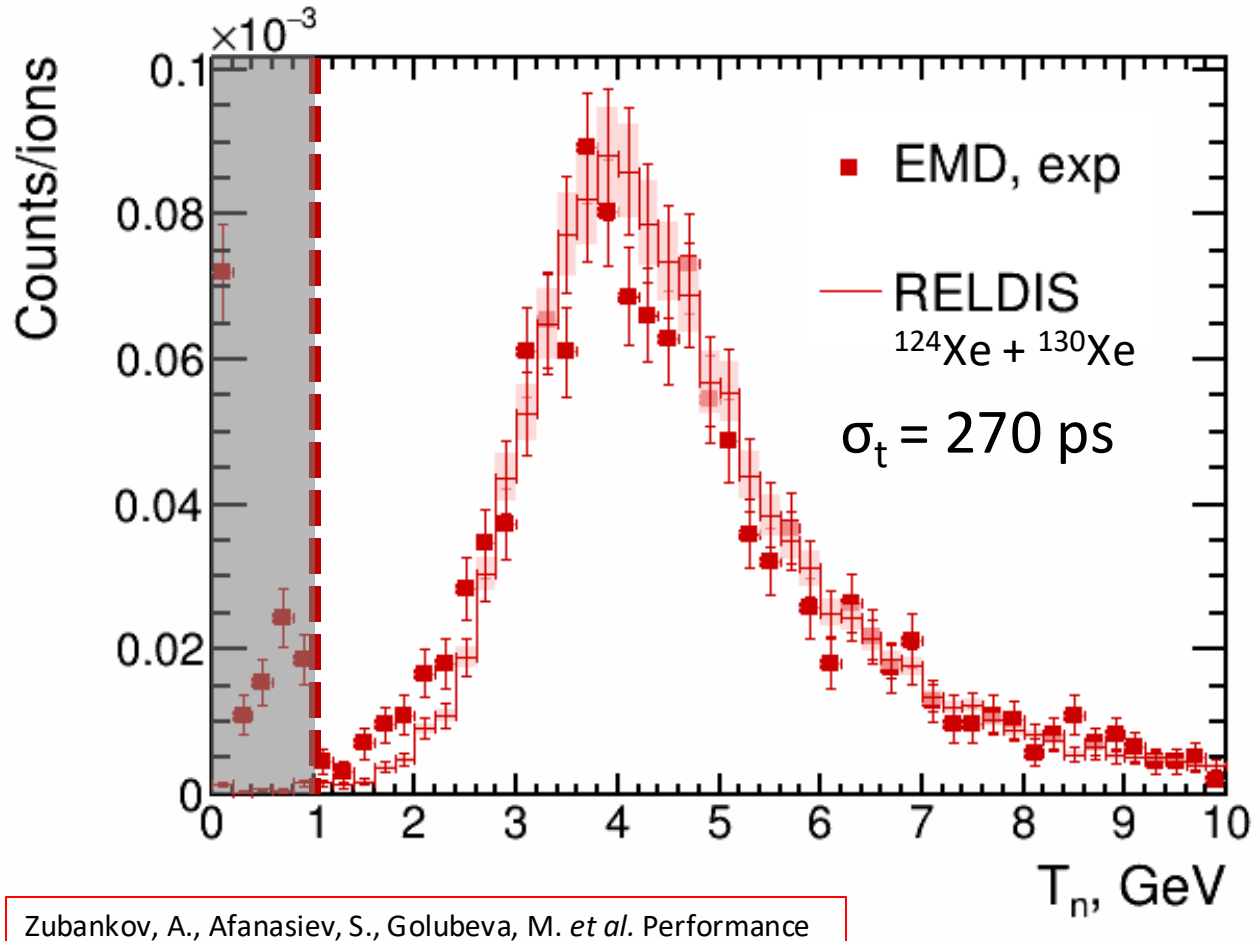


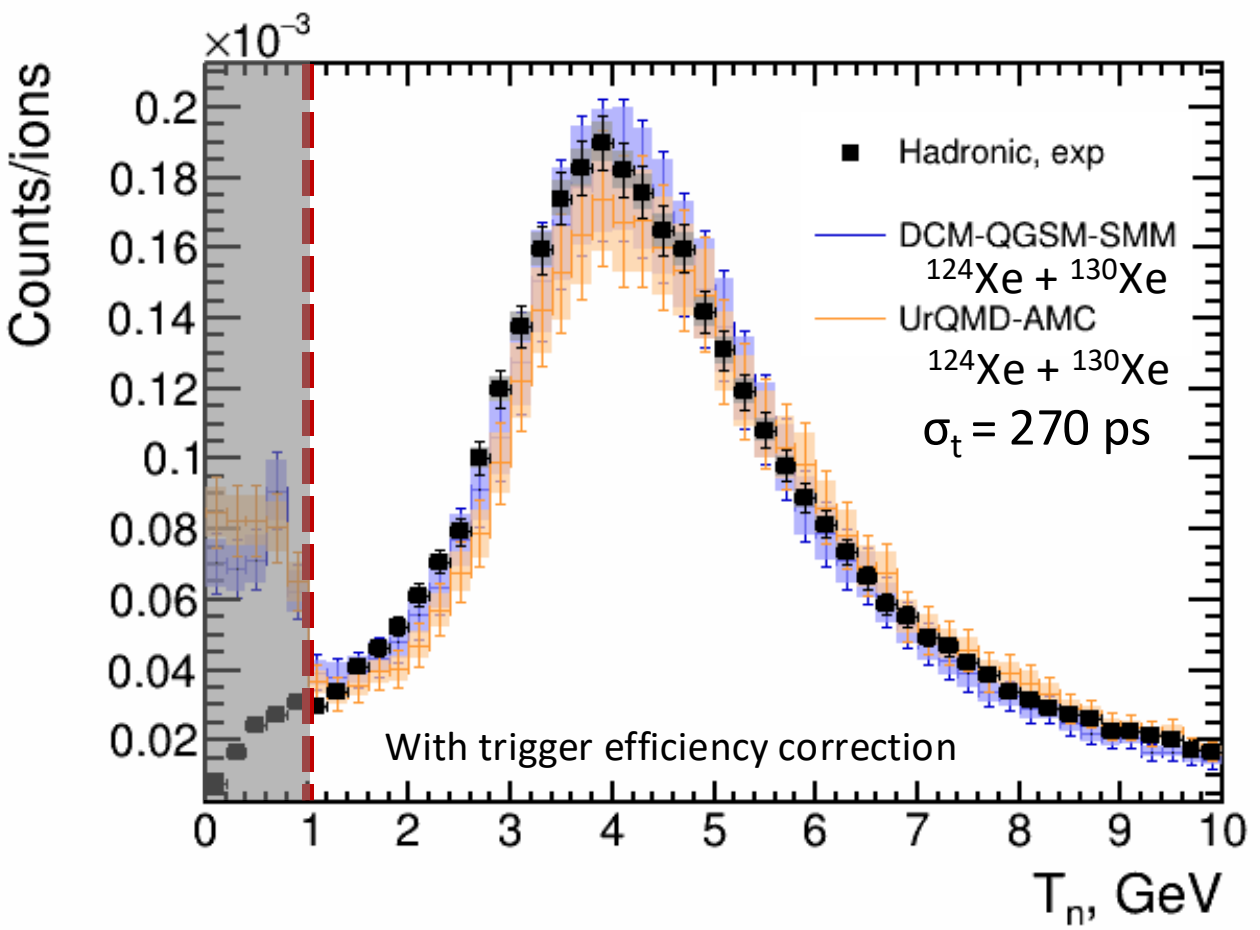
Average neutron multiplicity in acceptance of the HGND prototype

1.02 **1.38** **1.35**



Comparison of measurements (before unfolding) and simulations





Zubankov, A., Afanasiev, S., Golubeva, M. *et al.* Performance study of the Highly Granular Neutron Detector prototype in the BM@N experiment. *NUCL SCI TECH* **36**, 226 (2025).

Ω_n, %	ε_n, %	Ω_n x ε_n, %
34.56 ± 0.26	55.47 ± 0.42	19.17 ± 0.15

$$\Omega_n = \frac{N_{hit}}{N_{gen}} \qquad \varepsilon_n = \frac{N_{rec}}{N_{hit}}$$

Plotnikov, V.A., Kapishin, M.N. Evaluation of Trigger Efficiency in the BM@N Experiment Session with a Beam of Xenon Ions with a Kinetic Energy of 3.8 AGeV. *Phys. Part. Nuclei Lett.* **22**, 1406–1415 (2025).

Ω_n, %	ε_n, %	Ω_n x ε_n, %
3.26 ± 0.02	49.25 ± 0.16	1.61 ± 0.01
2.45 ± 0.01	50.03 ± 0.27	1.22 ± 0.01

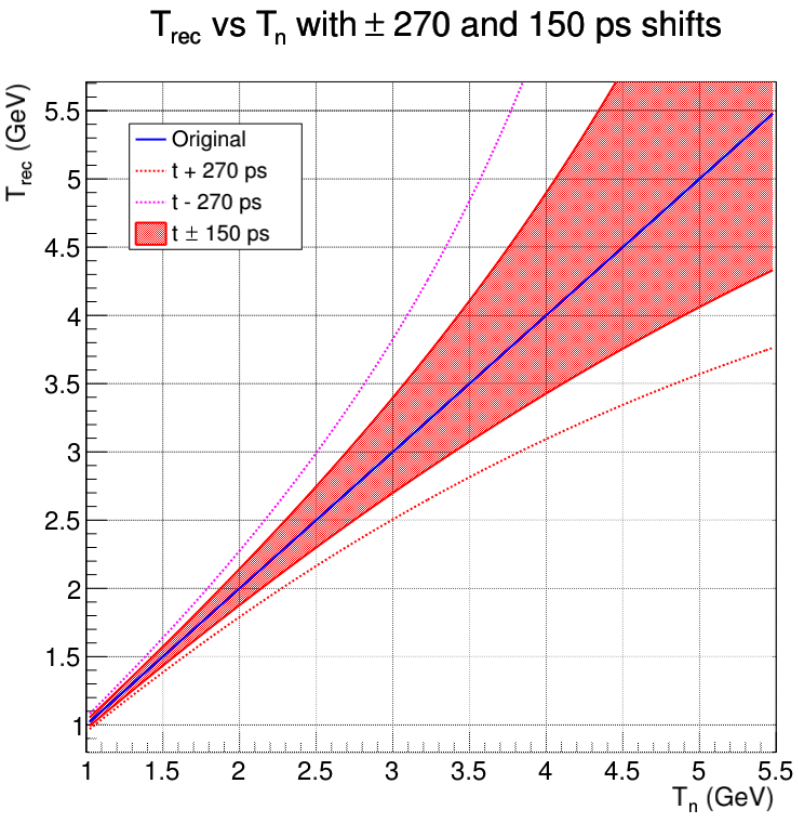
2. Unfolding of kinetic energy spectra of neutrons

Unfolding of neutron kinetic energy distributions

Unfolding makes possible to account for a limited time resolution of the detectors.
We use the RooUnfold framework of ROOT to calculate true kinetic energies of neutrons.
https://gitlab.cern.ch/RooUnfold/RooUnfold

$$\mu = R^{-1}(\nu - \beta)$$

- μ: true kinetic energy of neutrons
- R^{-1}: response matrix
- ν: reconstructed kinetic energy
- β: background

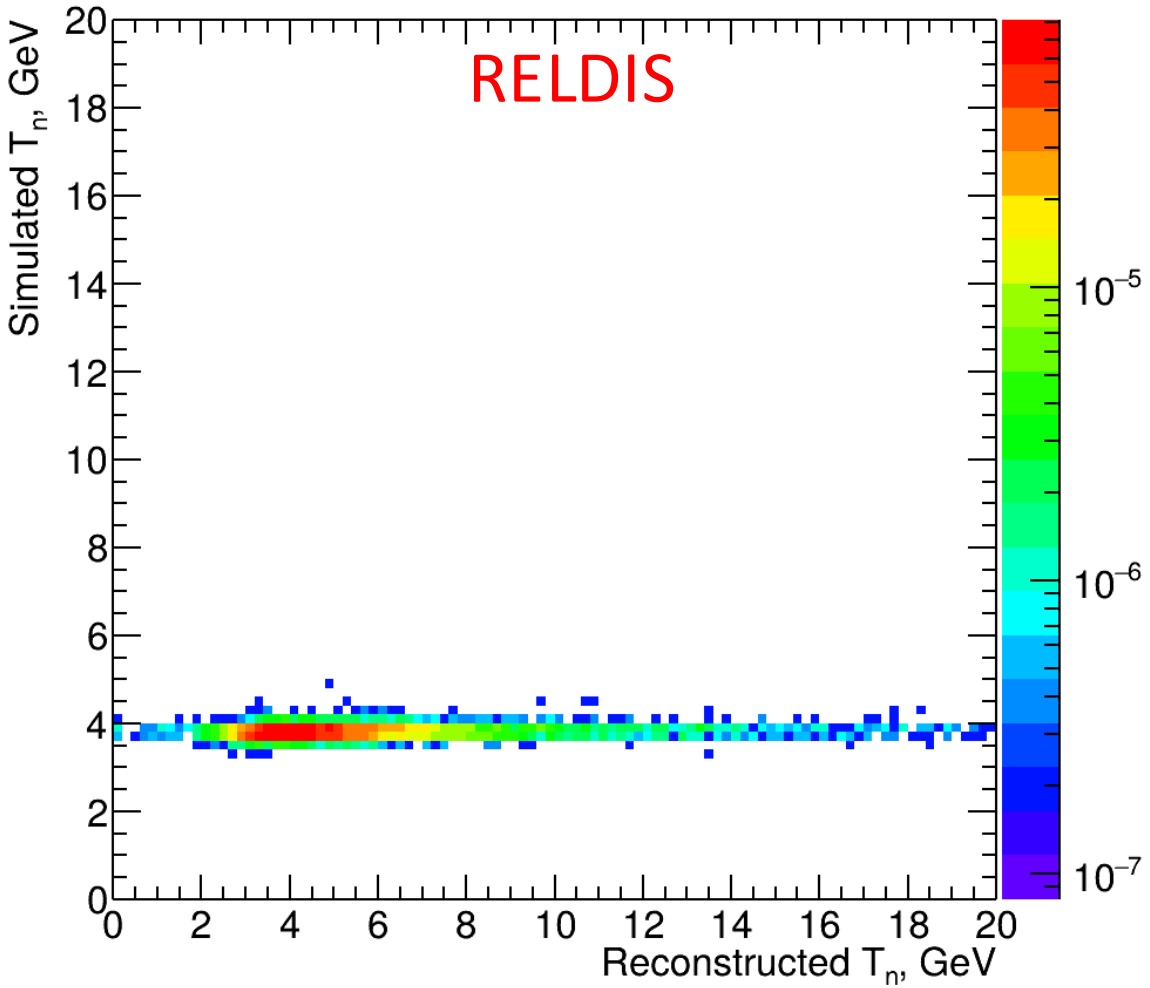


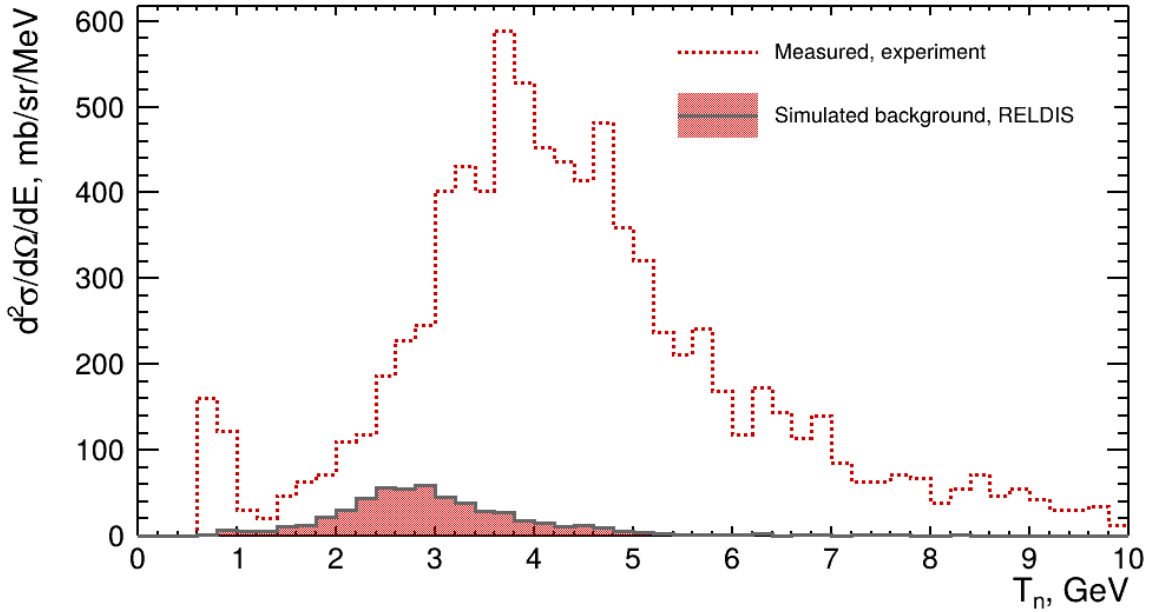
The response matrix **R** is obtained by simulating the response of the HGND prototype to neutrons.

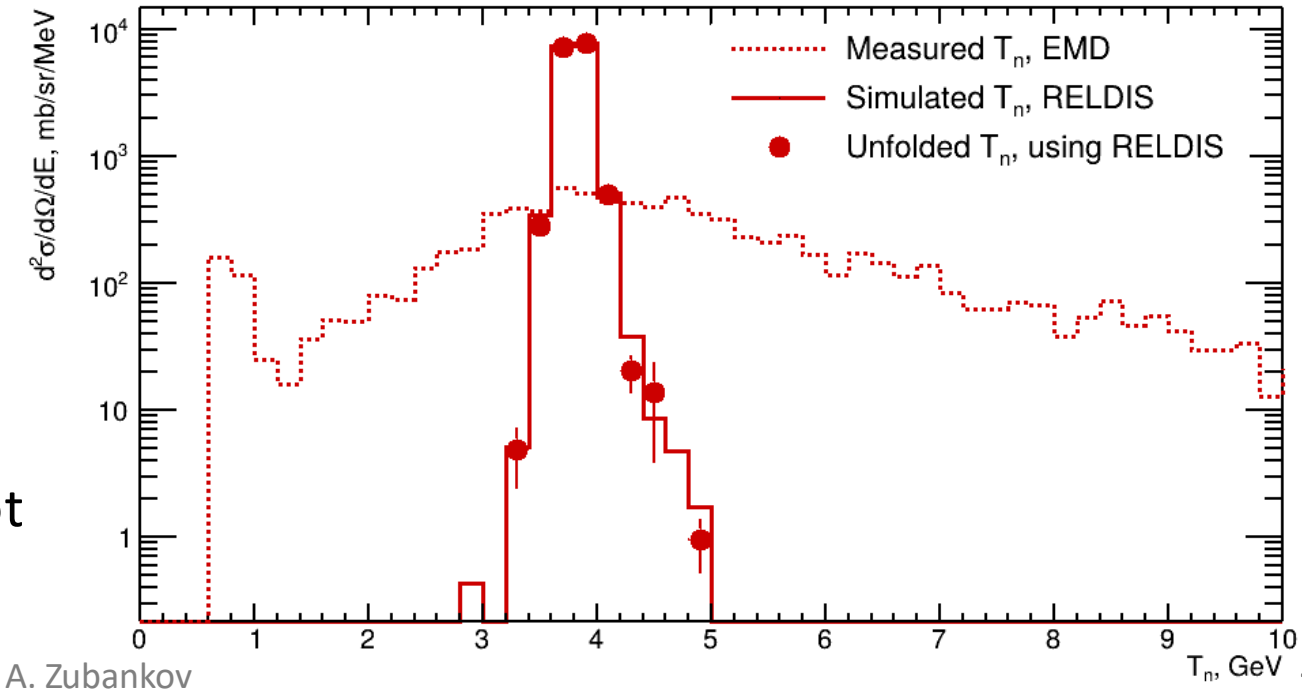
The iterative Bayesian method is used. In other fields, this approach is known as Richardson-Lucy deconvolution.

Comparison of unfolding methods using RooFitUnfold., L. Brenner et al., International Journal of Modern Physics A, Vol. 35, No. 24, 2050145 (2020)

Unfolding using the response matrix from RELDIS

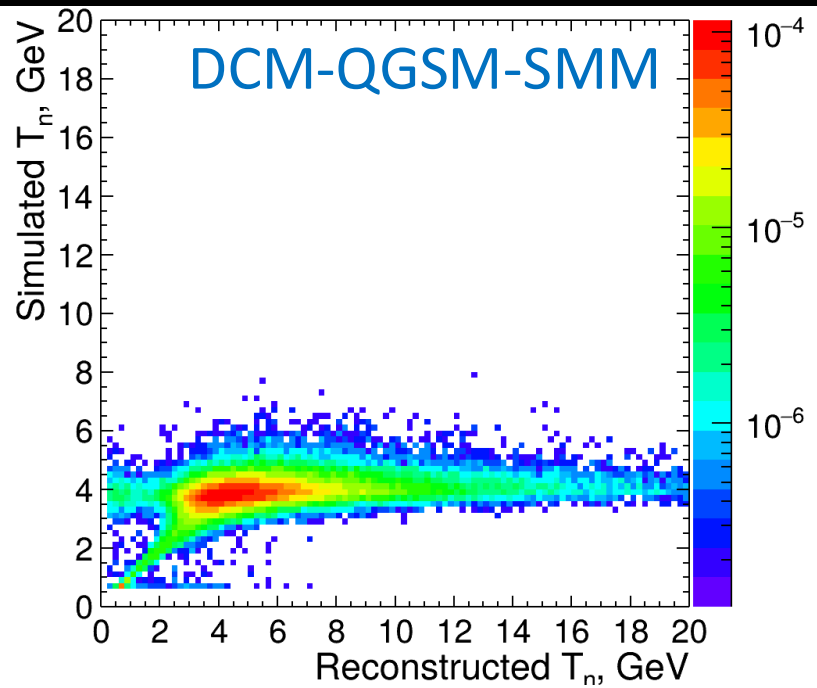


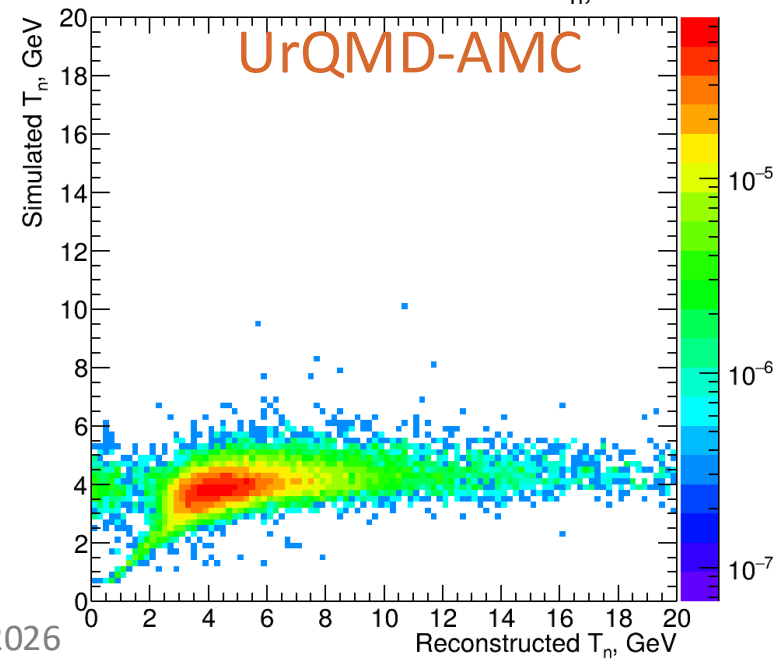


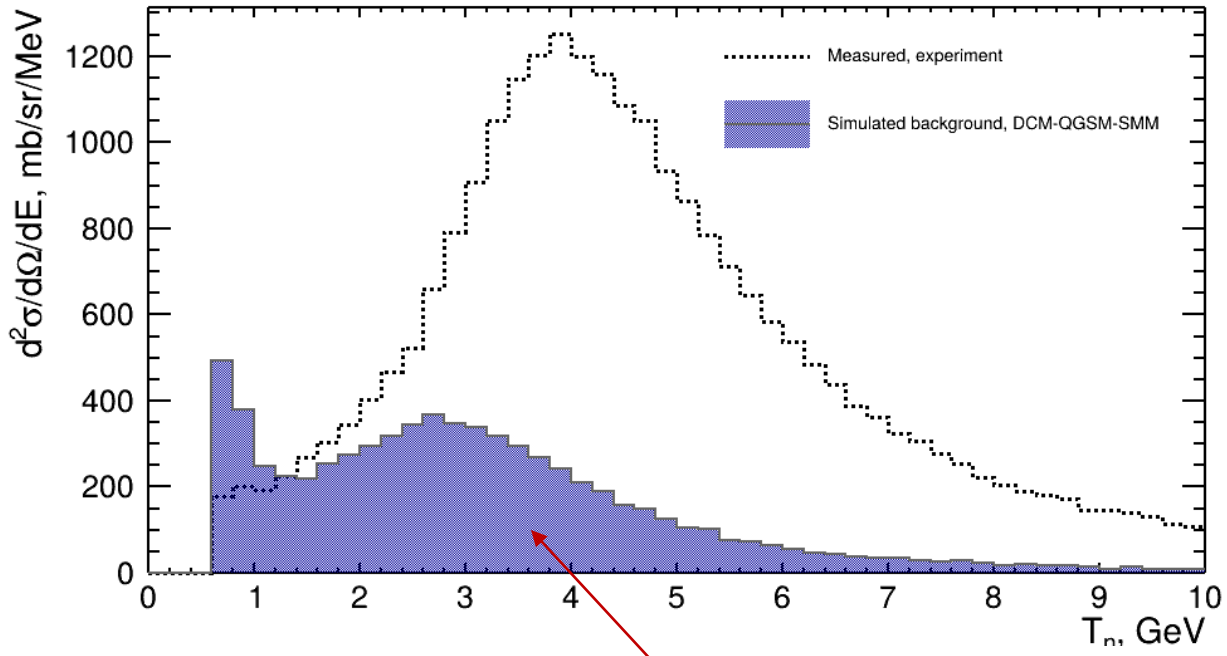


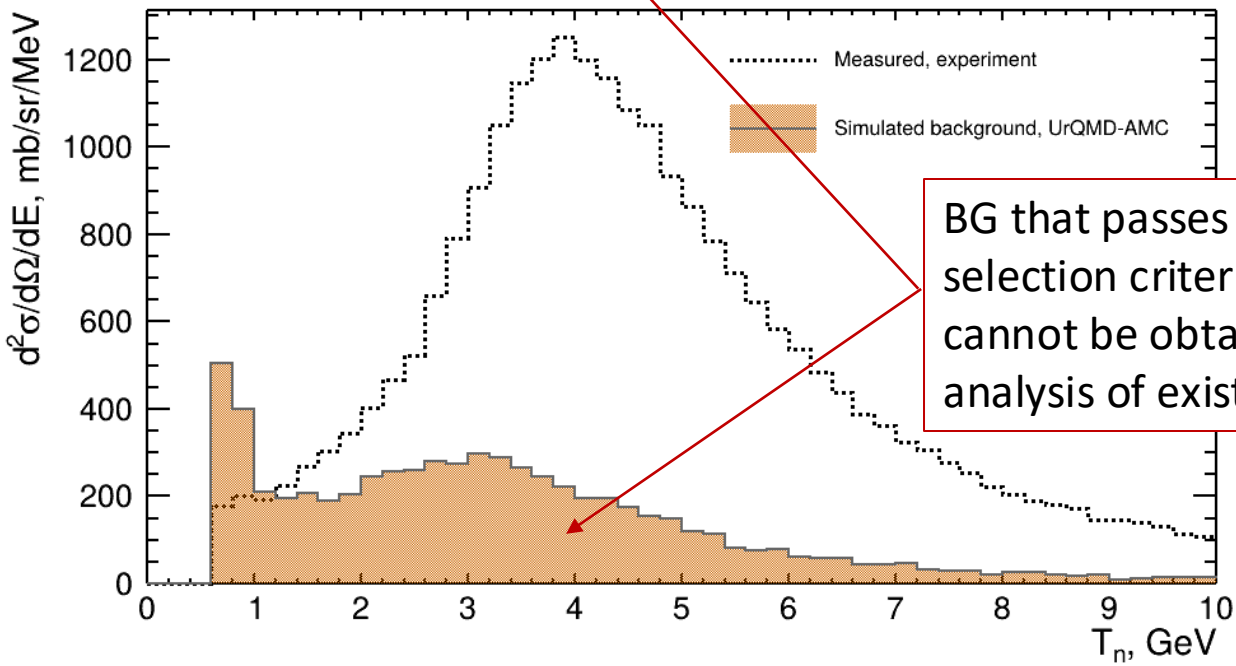
- Good agreement in the peak region.
- Disagreement in the tails because they are not covered by a narrow response function.

Unfolding using the response matrices from DCM-QGSM-SMM & UrQMD-AMC





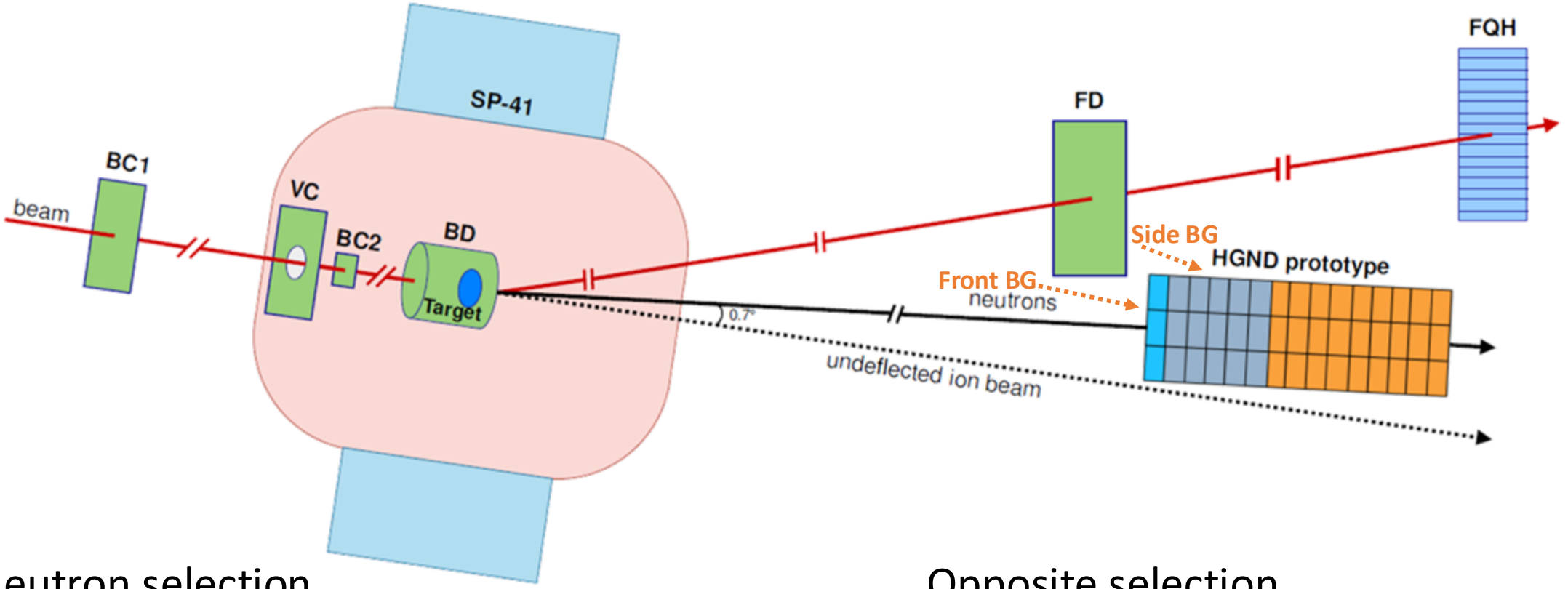




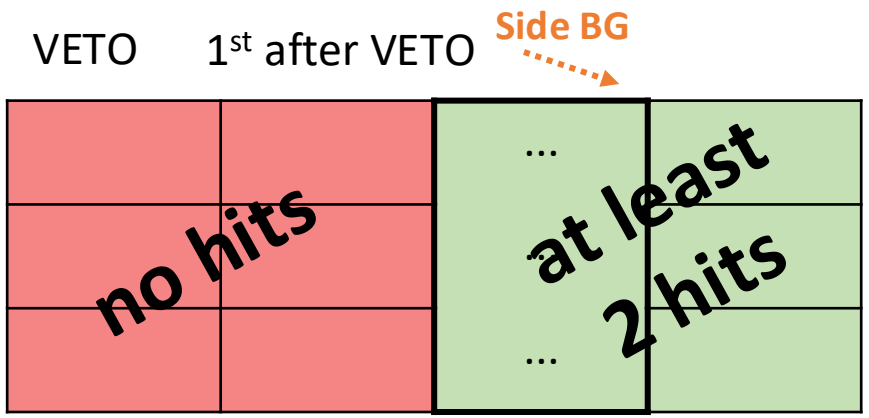
BG that passes the neutron selection criteria and cannot be obtained by analysis of existing data

3. Validation of the background from simulations

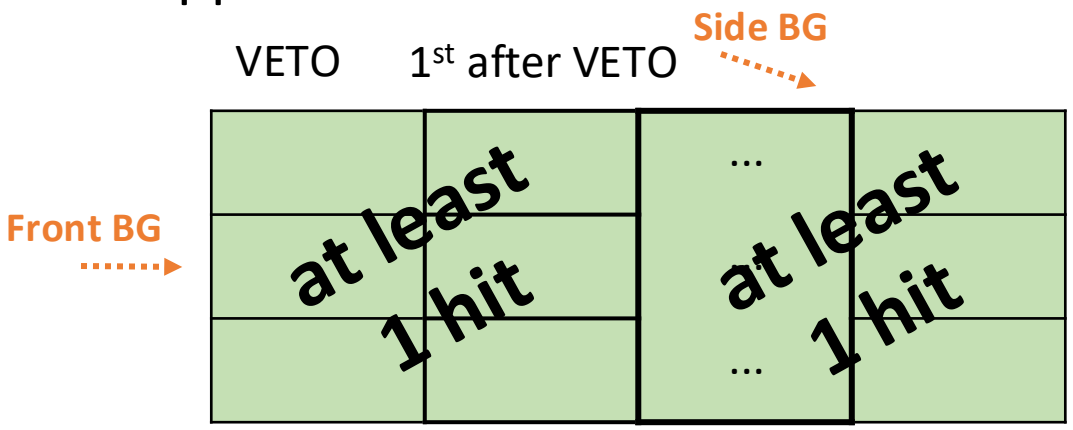
Background validation from simulation using opposite selection



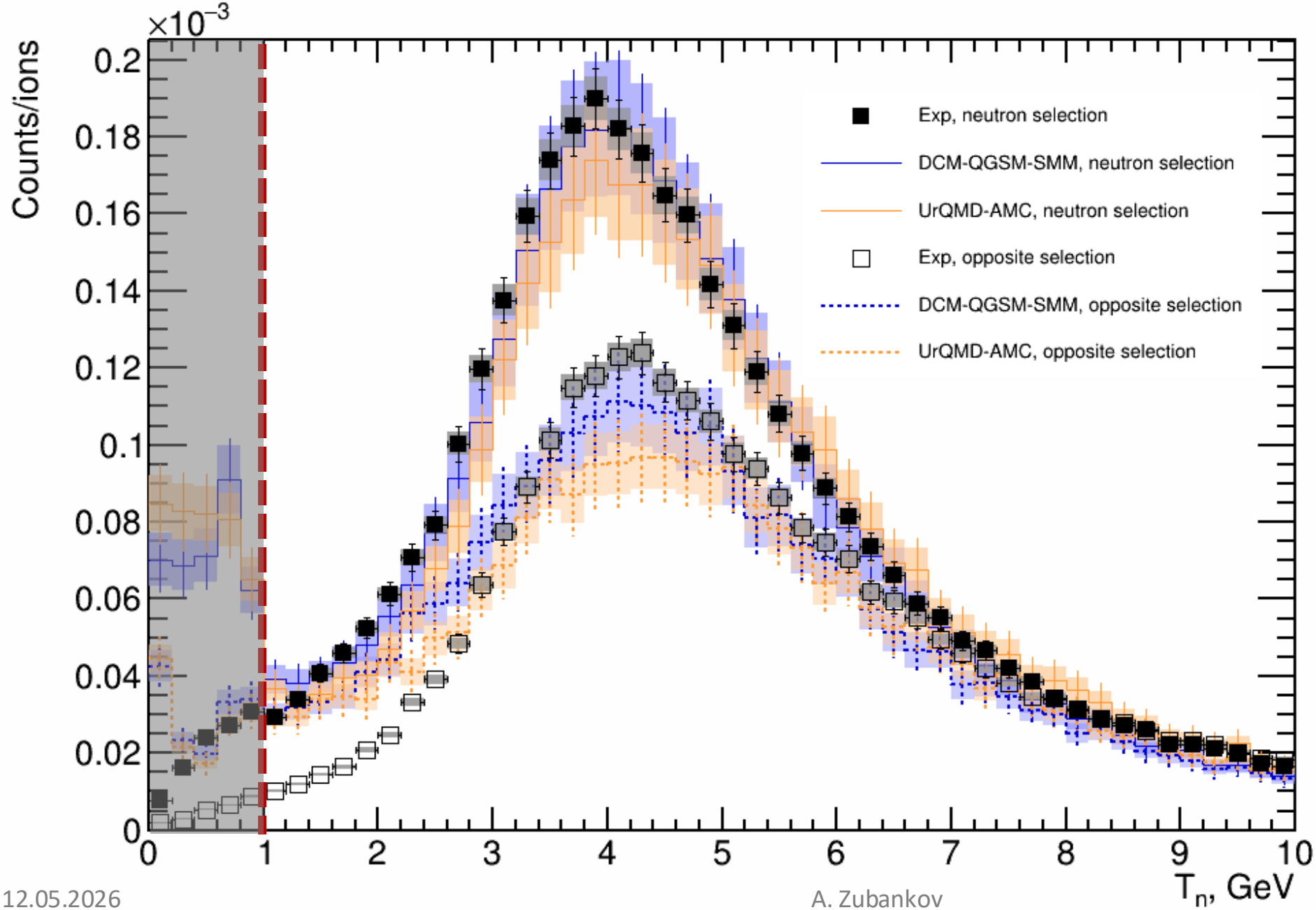
Neutron selection



Opposite selection



Background validation from simulation using opposite selection

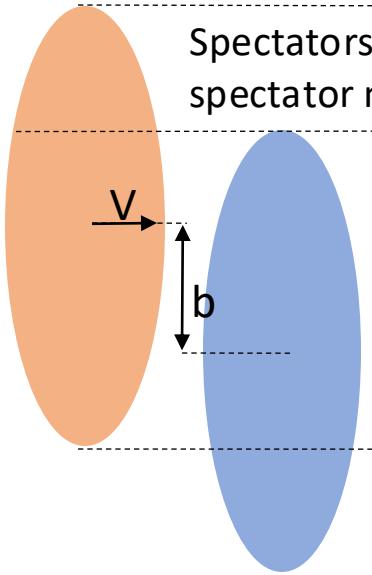


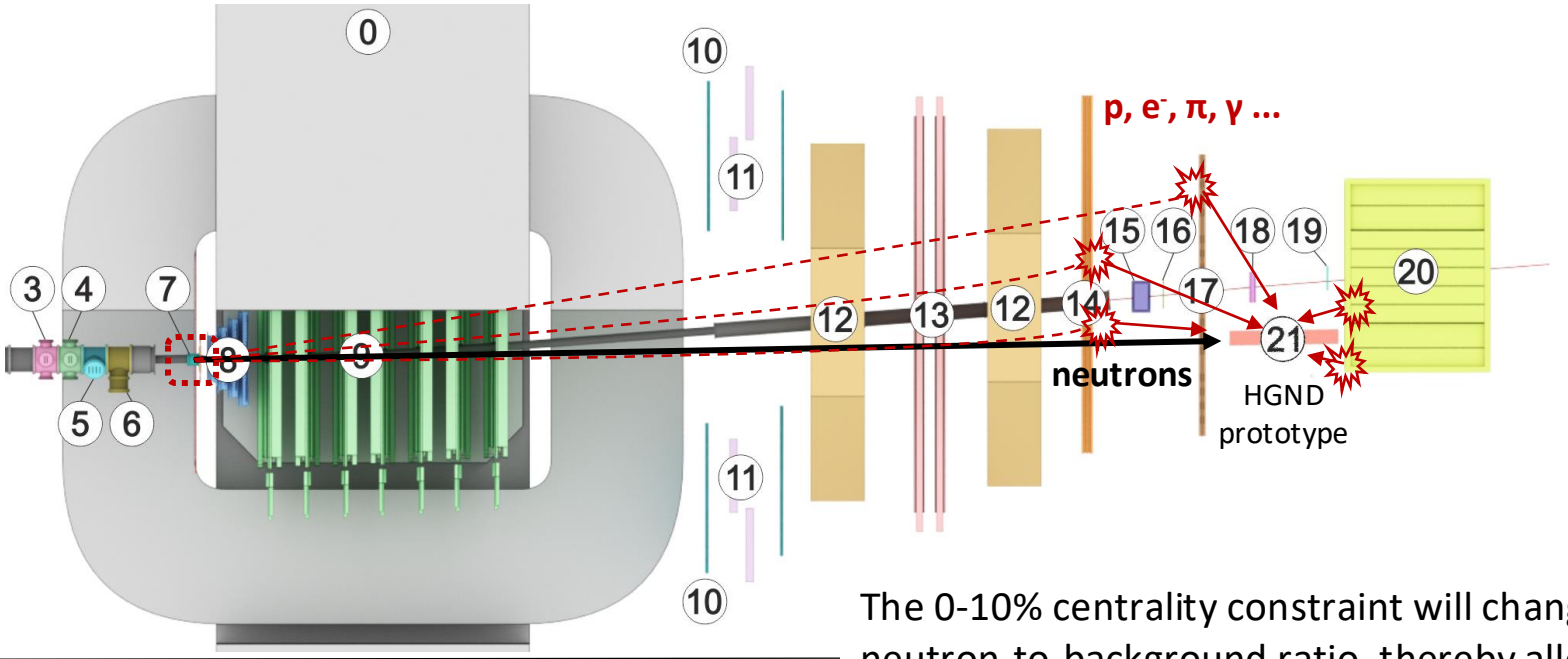
Using opposite selection, we analyze those events that we discard when analyzing neutrons.

The analysis shows that the distributions of reconstructed kinetic energy are in good agreement with the simulations, indicating a good description of the background and neutrons in the simulations.

Background validation from simulation

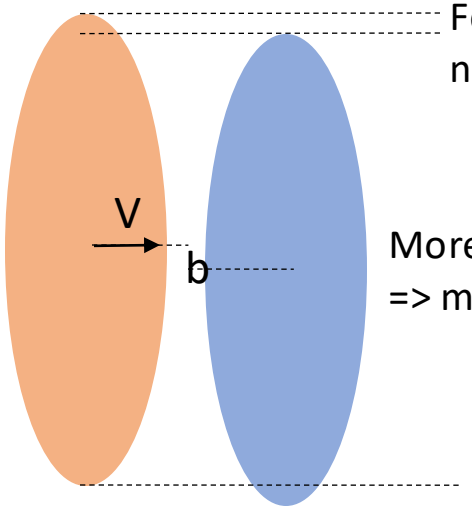
Semi-central collisions

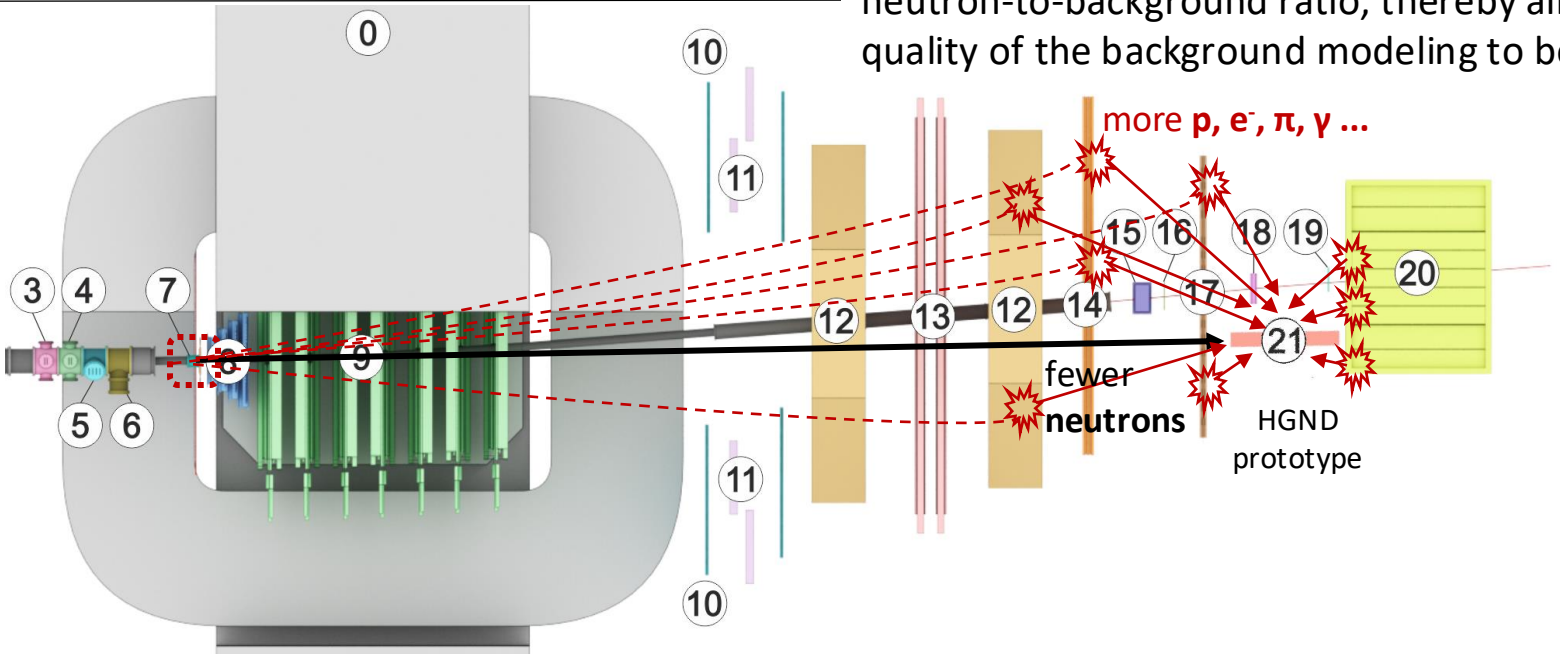




The 0-10% centrality constraint will change the neutron-to-background ratio, thereby allowing the quality of the background modeling to be verifie.

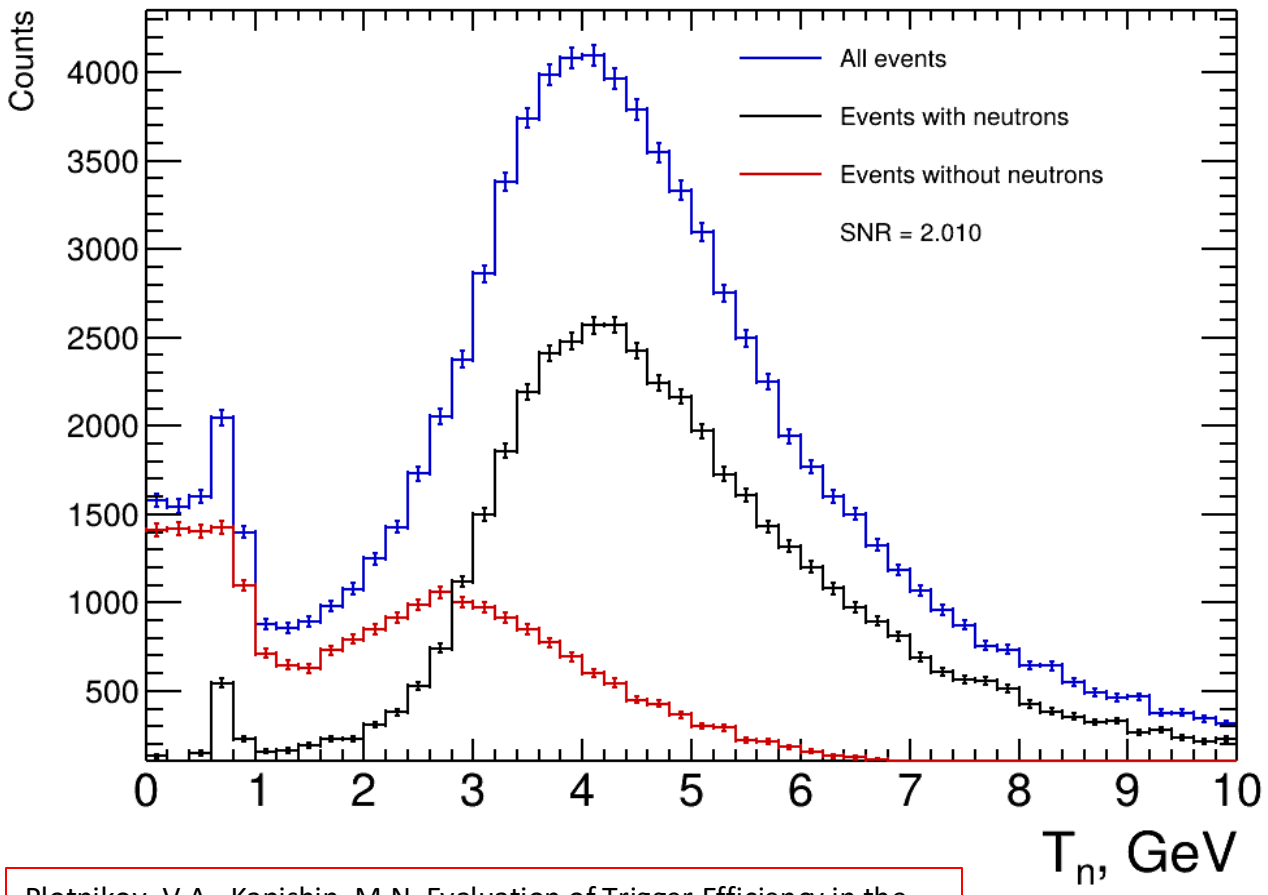
Most central collisions 0-10%





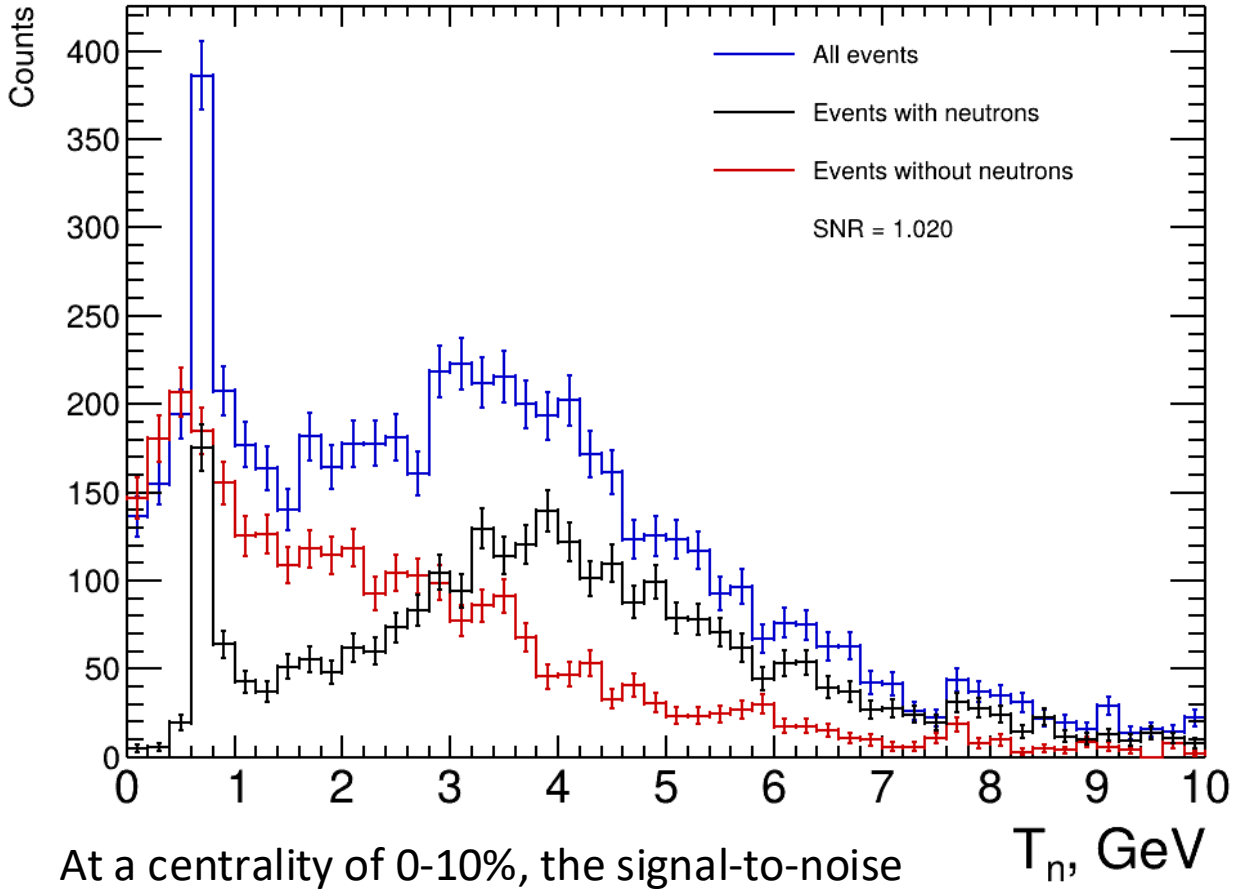
Background validation from simulation using the most central collisions

DCM-QGSM-SMM – CCT (with trigger eff. correction)



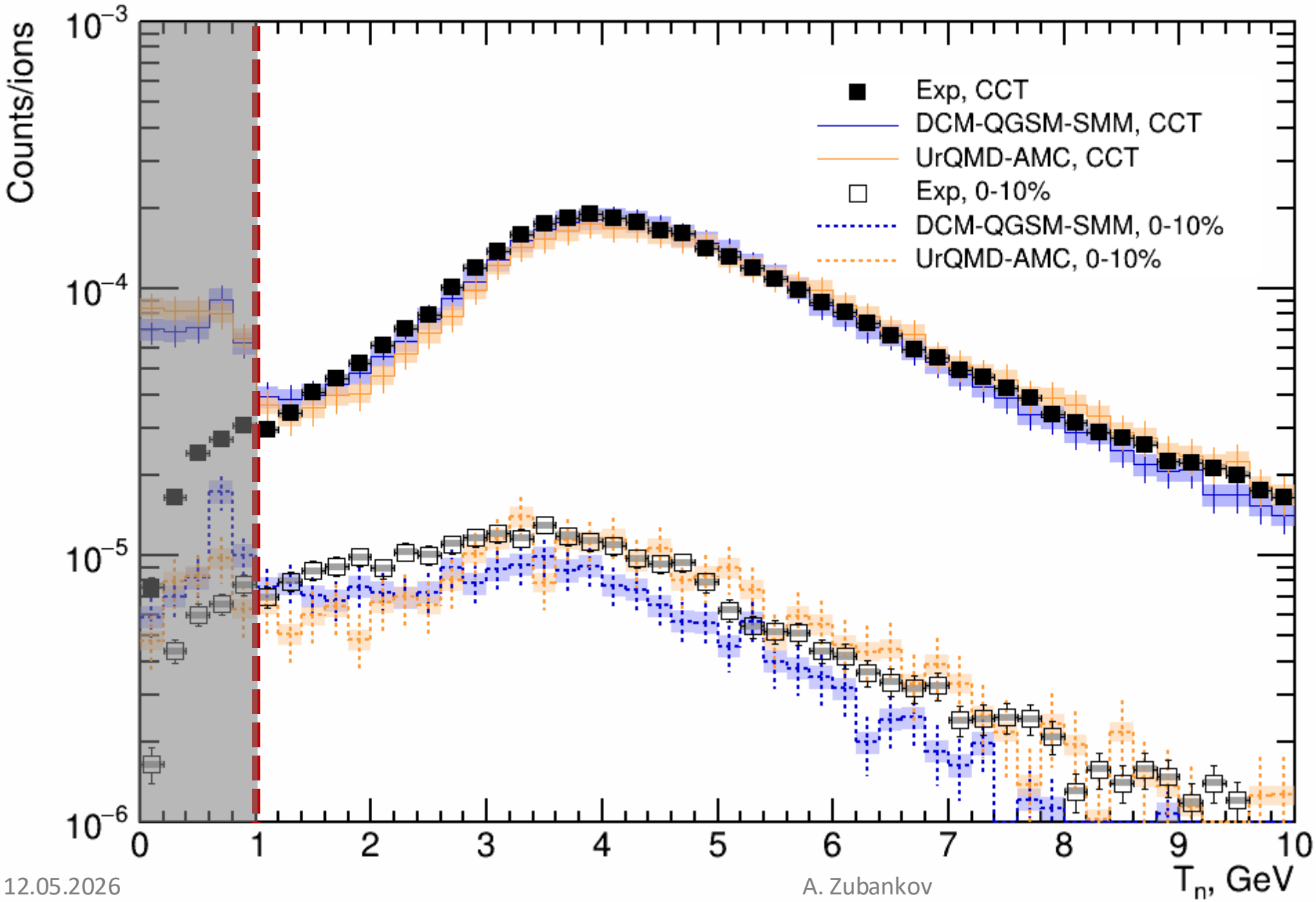
Plotnikov, V.A., Kapishin, M.N. Evaluation of Trigger Efficiency in the BM@N Experiment Session with a Beam of Xenon Ions with a Kinetic Energy of 3.8 AGeV. *Phys. Part. Nuclei Lett.* **22**, 1406–1415 (2025).

DCM-QGSM-SMM – 0-10%



At a centrality of 0-10%, the signal-to-noise ratio (neutrons to background) becomes almost 2 times smaller.

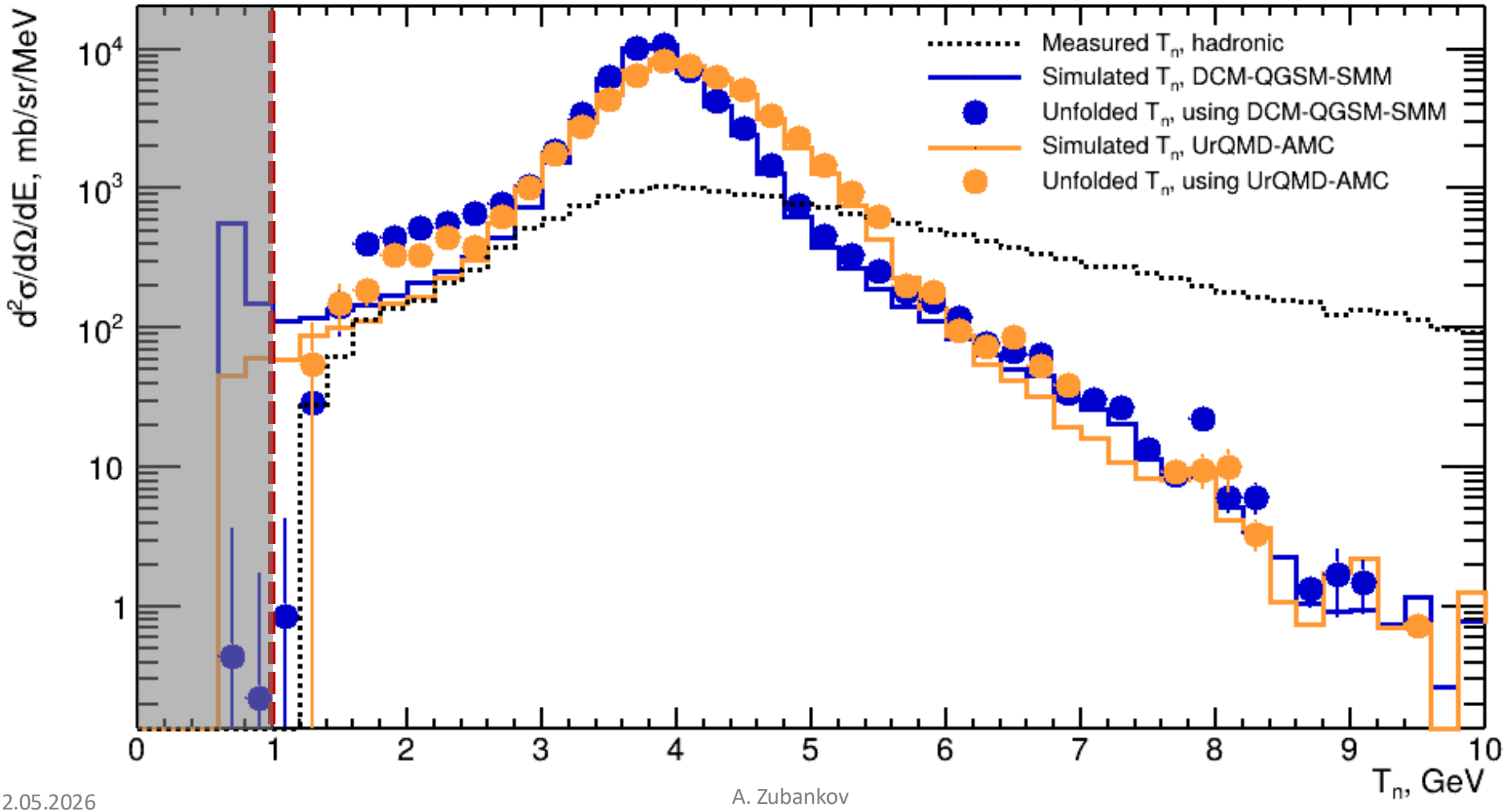
Background validation from simulation using the most central collisions



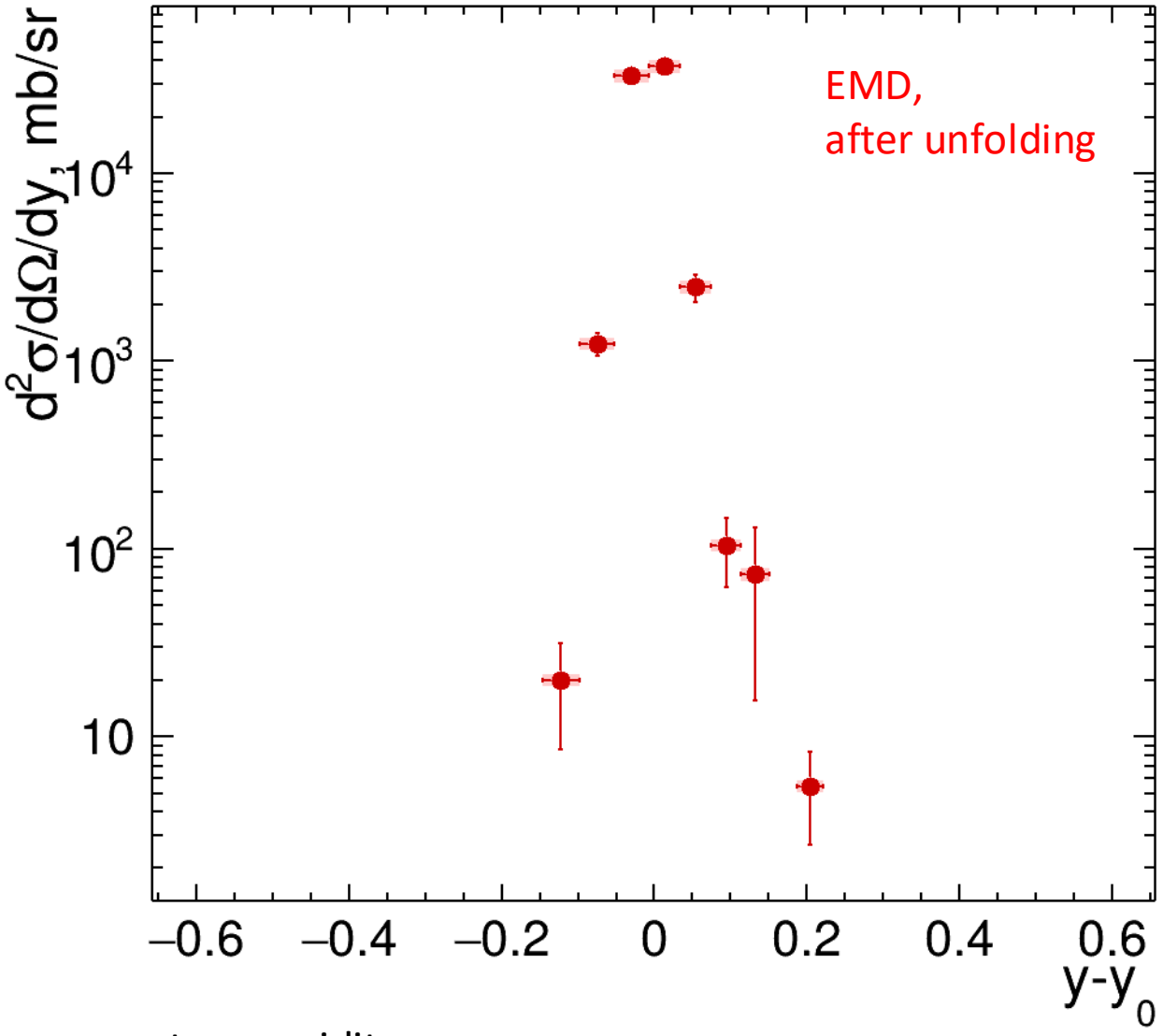
The analysis shows that the distributions of reconstructed kinetic energy are in good agreement with the simulations, indicating a good description of the background and neutrons in the simulations.

4. Measurements of differential cross section of forward neutron emission

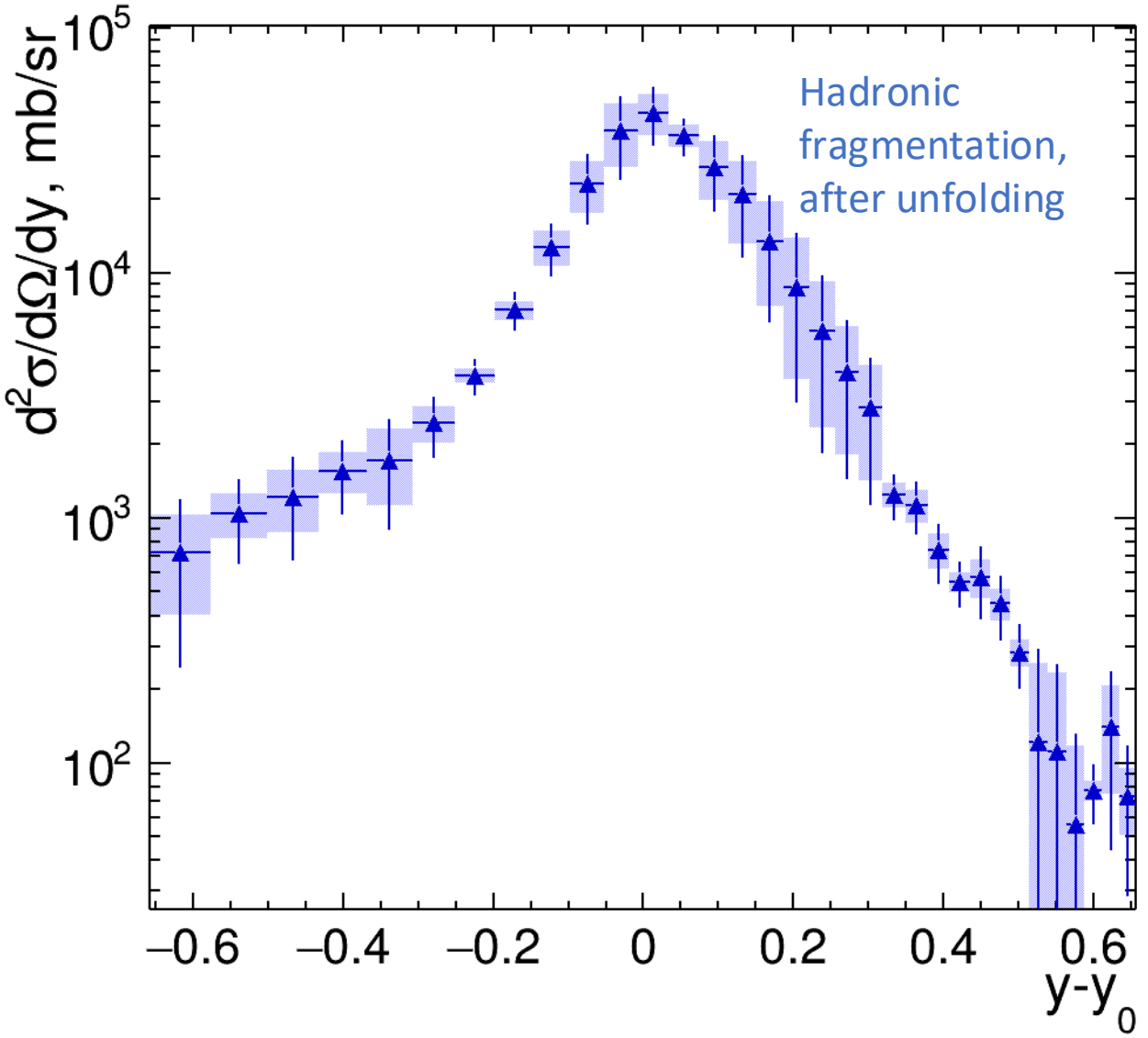
Unfolding using the response matrices from DCM-QGSM-SMM & UrQMD-AMC



Differential cross section of forward neutron emission



y – neutron rapidity
y_0 – beam rapidity

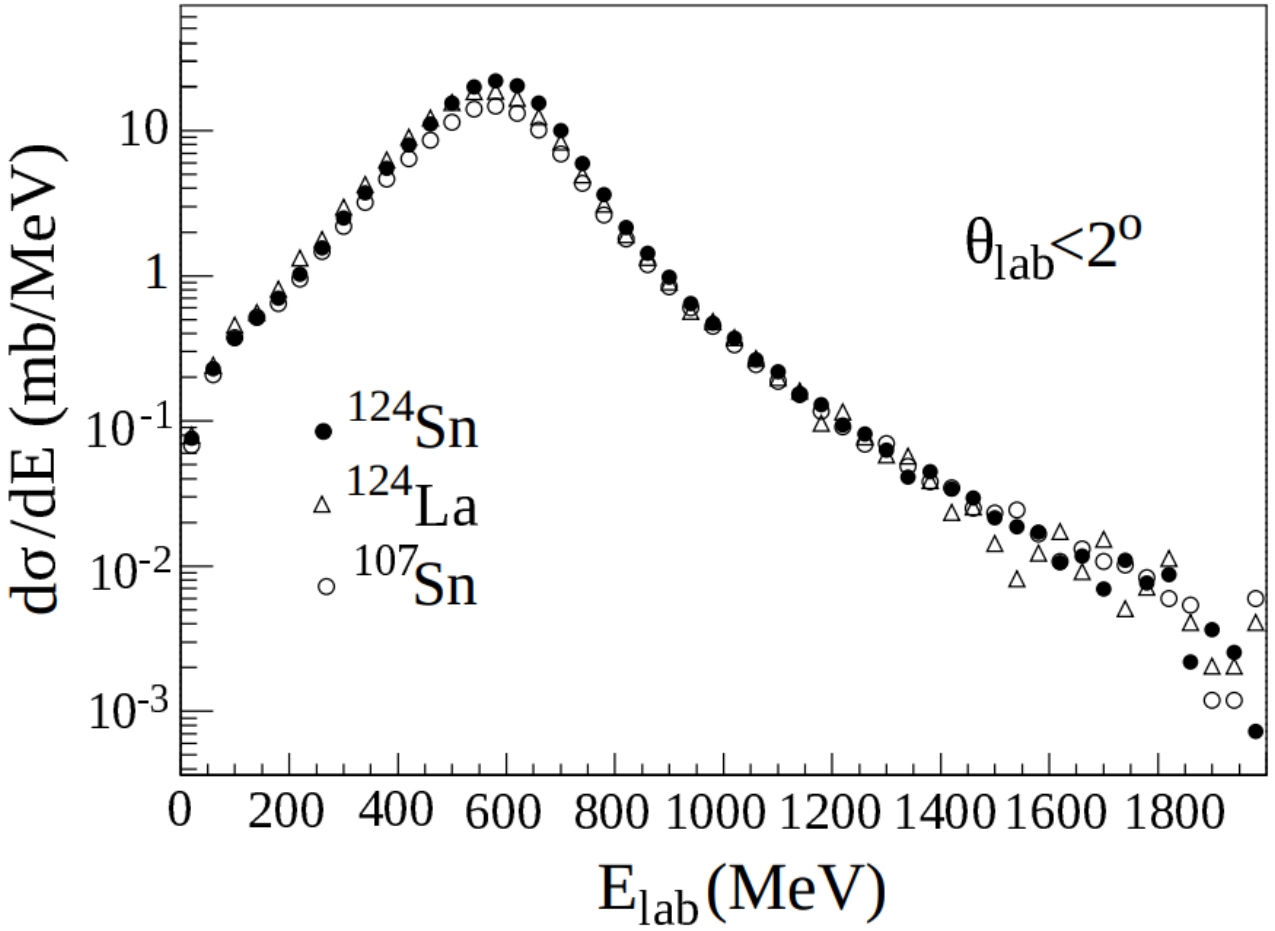


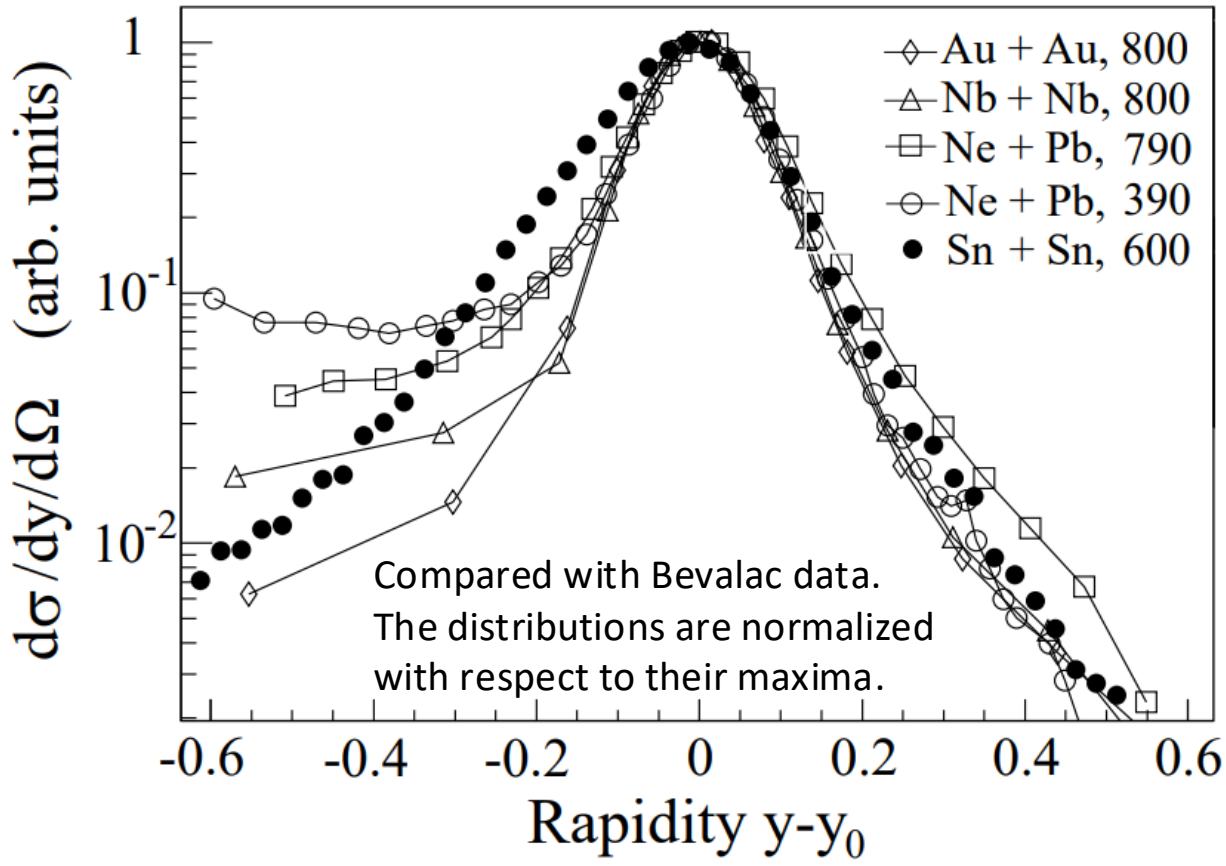
This difference between models was used as an additional source of systematic errors

5. Comparison with LAND ALADIN 600A MeV Sn+Sn data

600A MeV Sn+Sn measurements

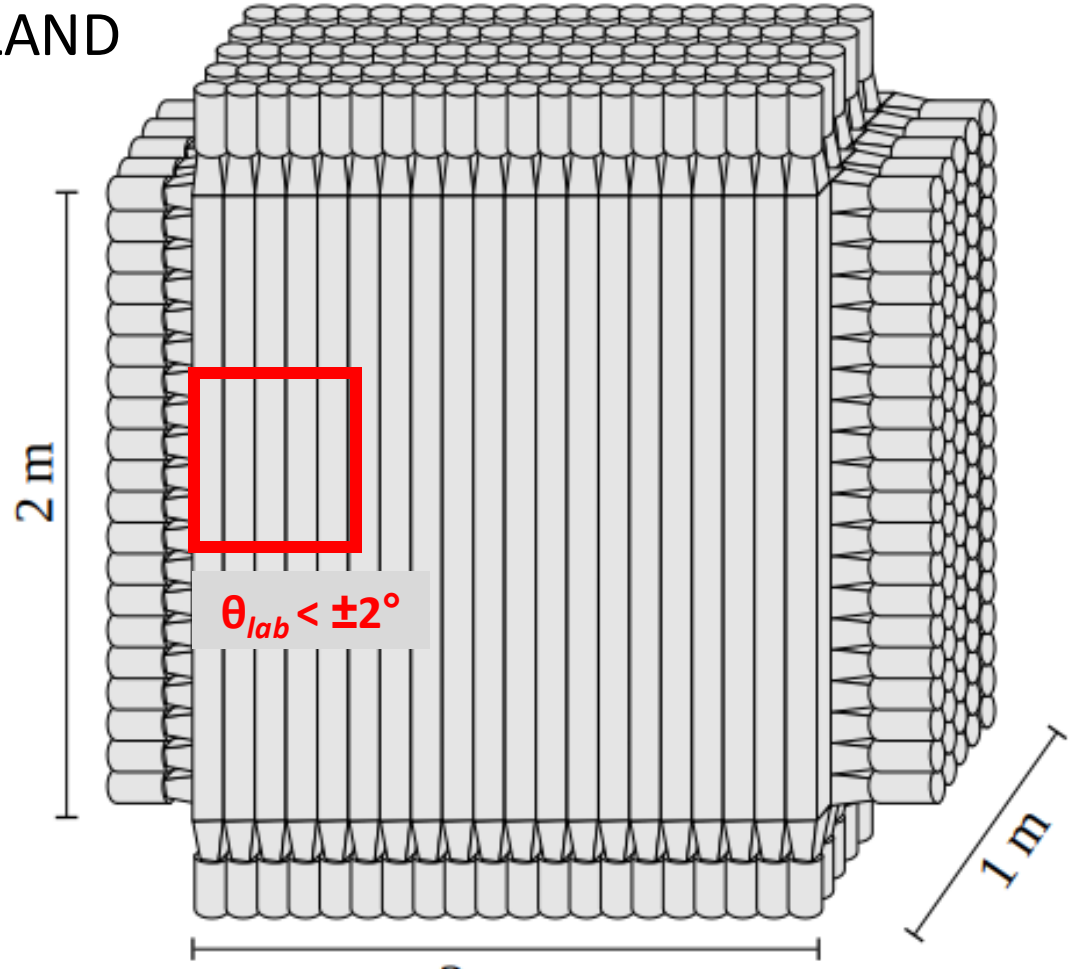
P. Pawłowski et al., Neutrons from projectile fragmentation at 600 MeV/nucleon, Phys. Rev. C **108**, 044610. https://doi.org/10.1103/PhysRevC.108.044610





LAND vs HGND prototype acceptance

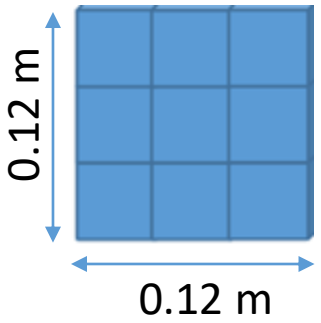
LAND



$\Omega_{LAND} \approx 3.86 \cdot 10^{-3}$ sr

LAND (2°): Maximum lab angle of emission of neutrons with a momentum in the projectile rest frame p'≤100 MeV/c and p'≤300 MeV/c is 4.69° and 13.8°, respectively.

HGND prototype



$\theta_{lab} <$ ±0.3°

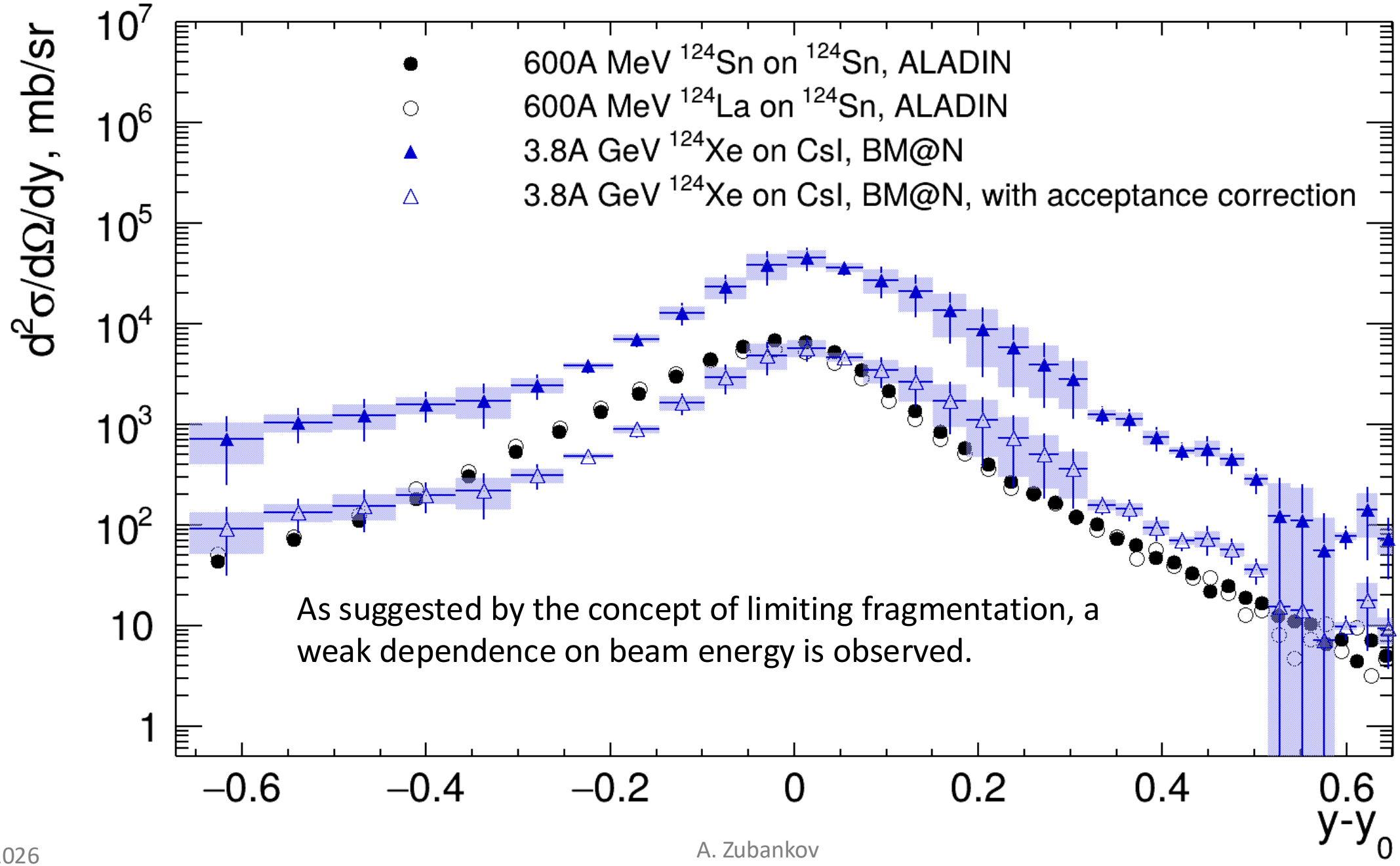
$\Omega_{HGND\ prototype} \approx 2.07 \cdot 10^{-4}$ sr

HGND prototype (0.3°): Maximum lab angle of emission of neutrons with a momentum in the projectile rest frame p'≤100 MeV/c and p'≤300 MeV/c is 1.23° and 3.7°, respectively.

The detector acceptances in both experiments are insufficient to cover the full distribution of neutrons.

~7.9 times difference in number of neutrons

Comparison with LAND 600A MeV Sn+Sn data



Conclusions

- The distributions of kinetic energy of neutrons from hadronic fragmentation and EMD of ^{124} Xe were measured.
- The distributions are in good agreement within the errors with simulations.
- The differential cross sections of forward neutron emission were measured.
- Taking into account the difference in acceptance, the differential cross sections are consistent with the data obtained by LAND at ALADIN in 600A MeV ^{124}Sn + ^{124}Sn collisions.

Analysis note: https://bmn.jinr.int/wp-content/uploads/2026/05/Note_forward_neutrons_HGND.pdf

Future plans

- Make the corrections that were proposed at the BERDS meeting.
- Conduct an analysis using the actual trigger efficiency obtained by D. Idrisov.
- Conduct background validation by extending tracks to the side surface of the HGND prototype.
- Prepare an extended version of the analysis note and article by autumn.

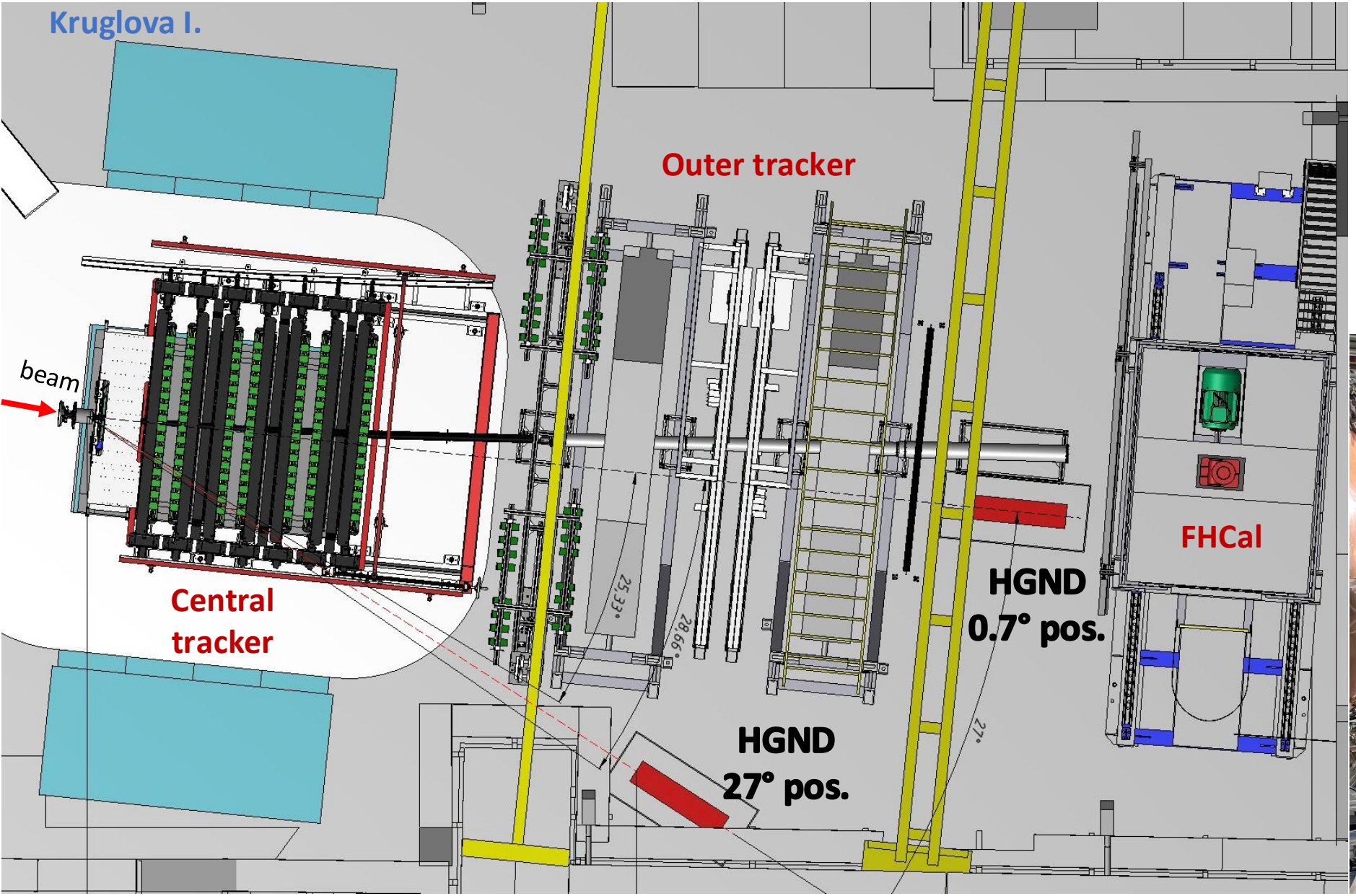
Analysis note: https://bmn.jinr.int/wp-content/uploads/2026/05/Note_forward_neutrons_HGND.pdf


Thank you for your attention!

Backup

HGND prototype

Прототип HGND в сеансе Xe+CsI@3.8A GeV на BM@N



Положение 0.7°:

Тестирование с известной энергией нейтронов (нейтроны-спектаторы) – 3.8 ГэВ.

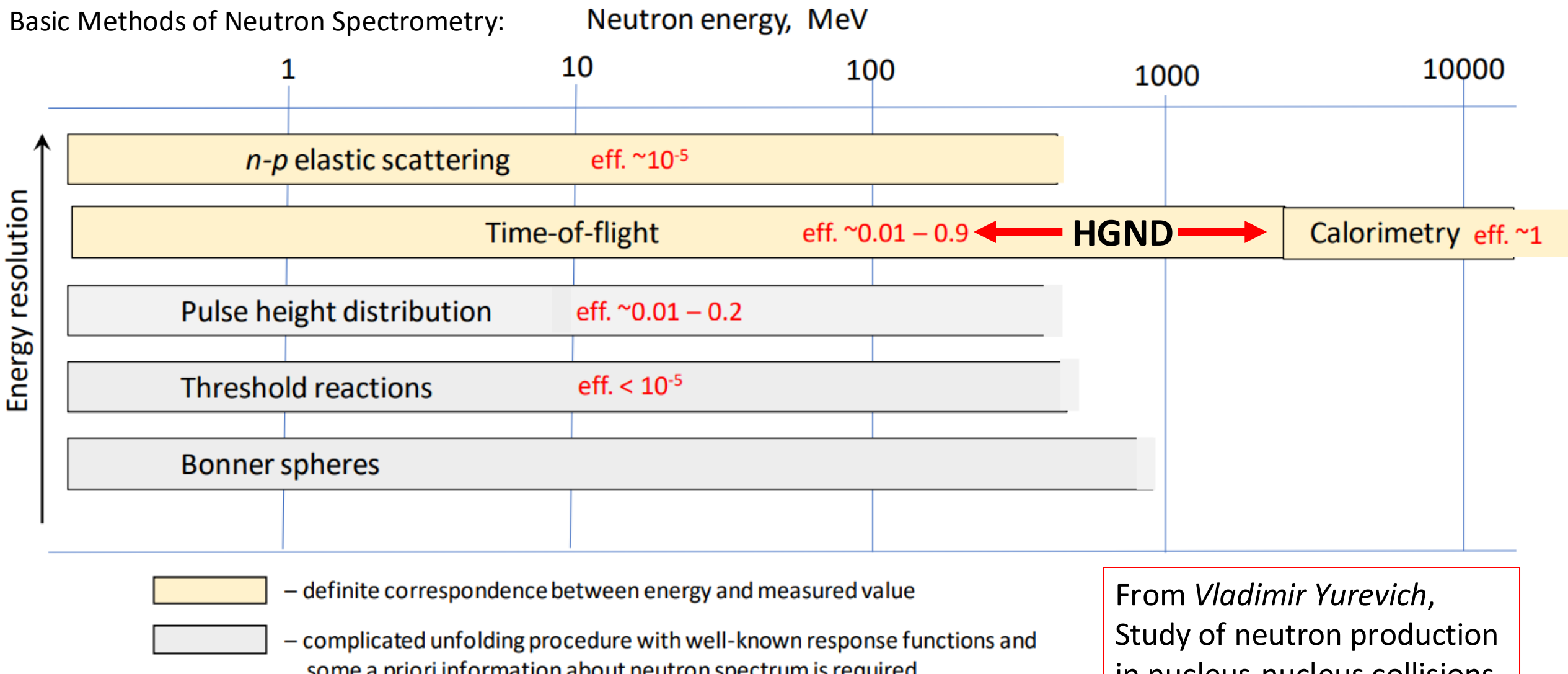
Положение 27°:

Измерения спектров нейтронов в области ~ midrapidity.



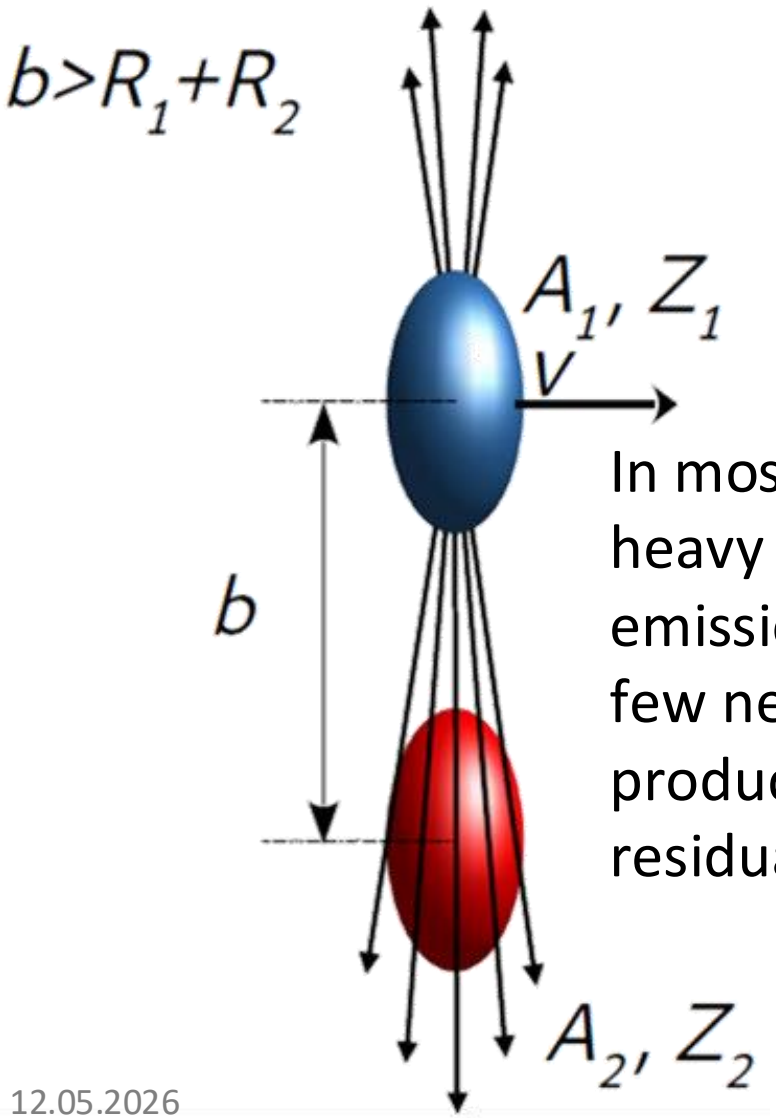
Introduction

Basic Methods of Neutron Spectrometry:



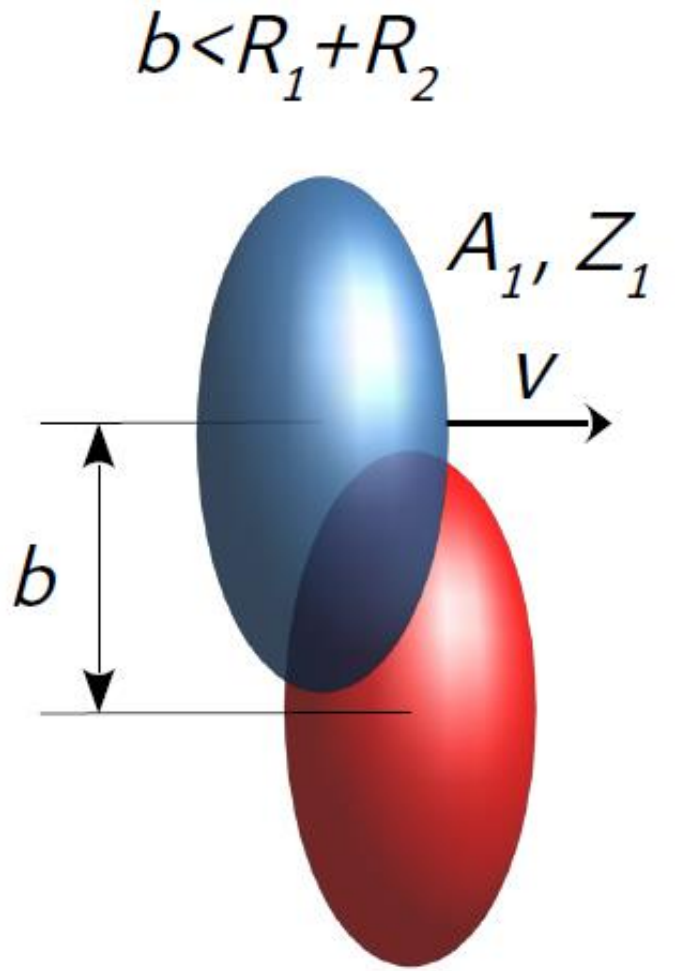
From *Vladimir Yurevich*, Study of neutron production in nucleus-nucleus collisions, BM@N collaboration meeting, 3–8 Oct. 2021

Electromagnetic dissociation EMD:



In most cases, EMD of a heavy nucleus results in the emission of a single or just few neutrons with the production of a single residual nucleus

Hadronic interactions:



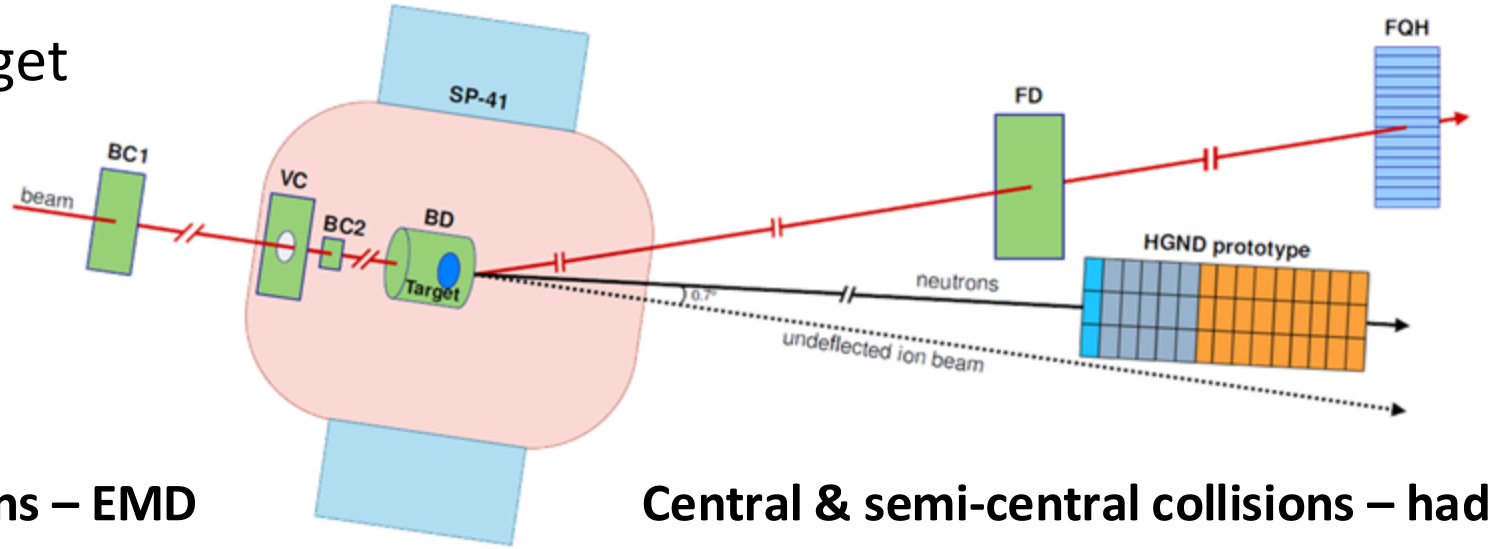
Multiple production of spectator neutrons

Analyzed runs

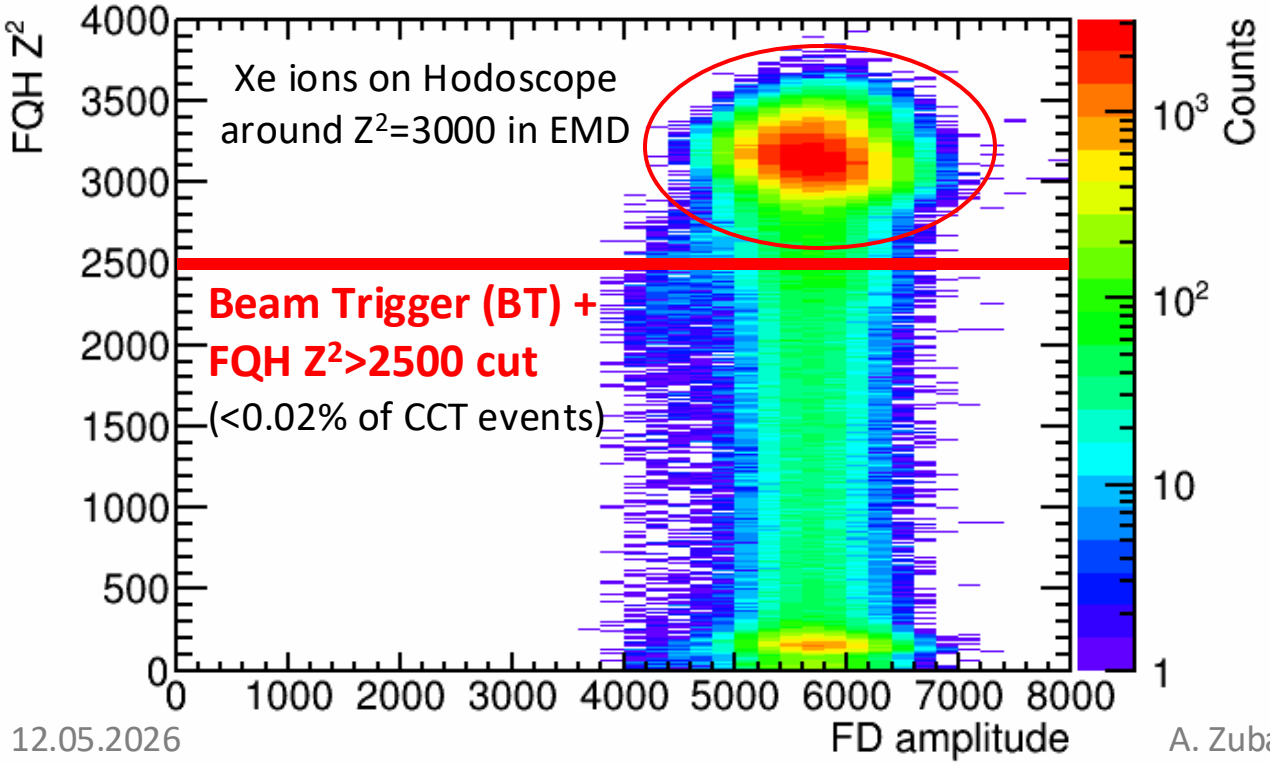
Interaction	Run	BT prescale	Target	N_{bitBT}	N_{ev}	N_n
Hadronic	8299, 8300	1999	CsI 2%	20286	522672	164872
Hadronic	8225	1999	CsI 1%	3416	46752	14183
Hadronic	8285, 8291, 8296	1999	empty	12006	2789	893
EMD	8281, 8284	1	CsI 2%	877084	694206	2266
EMD	8282, 8283	1	empty	141782	139717	160

Selection of EMD and hadronic interactions events

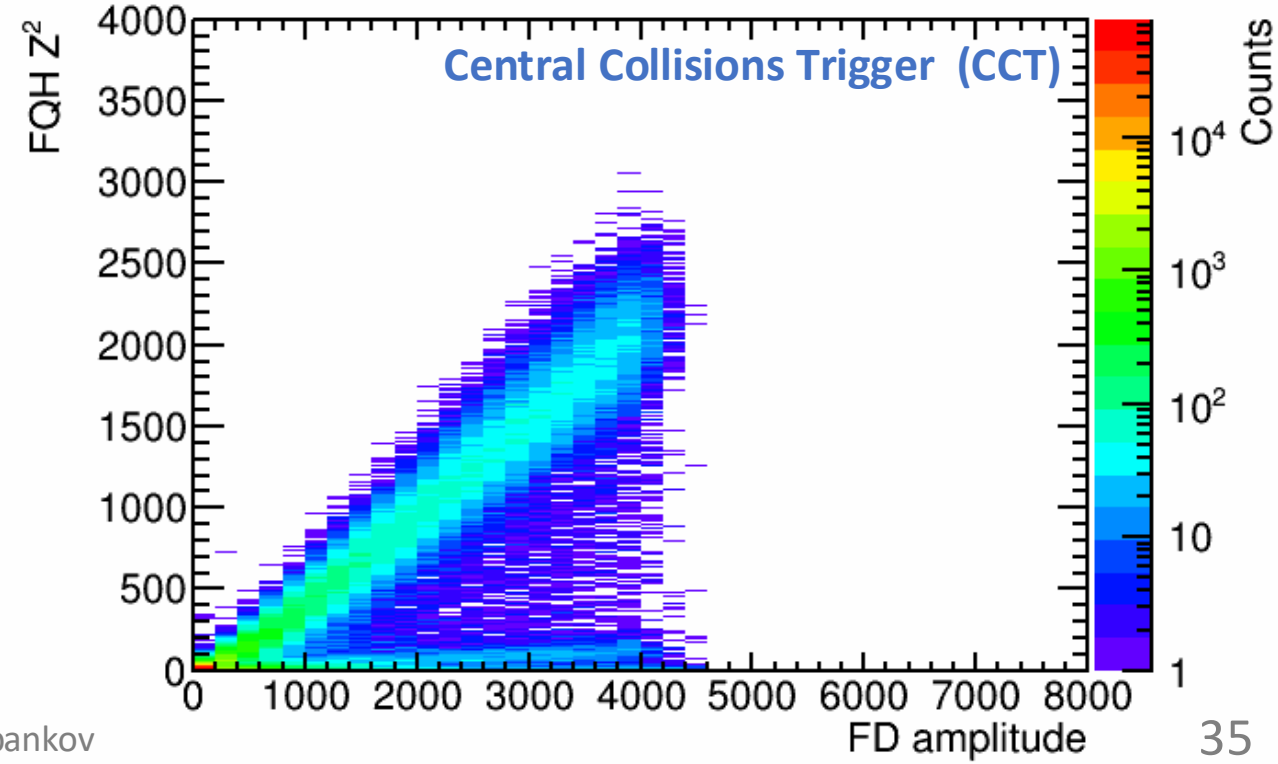
Only single Xe ion in target



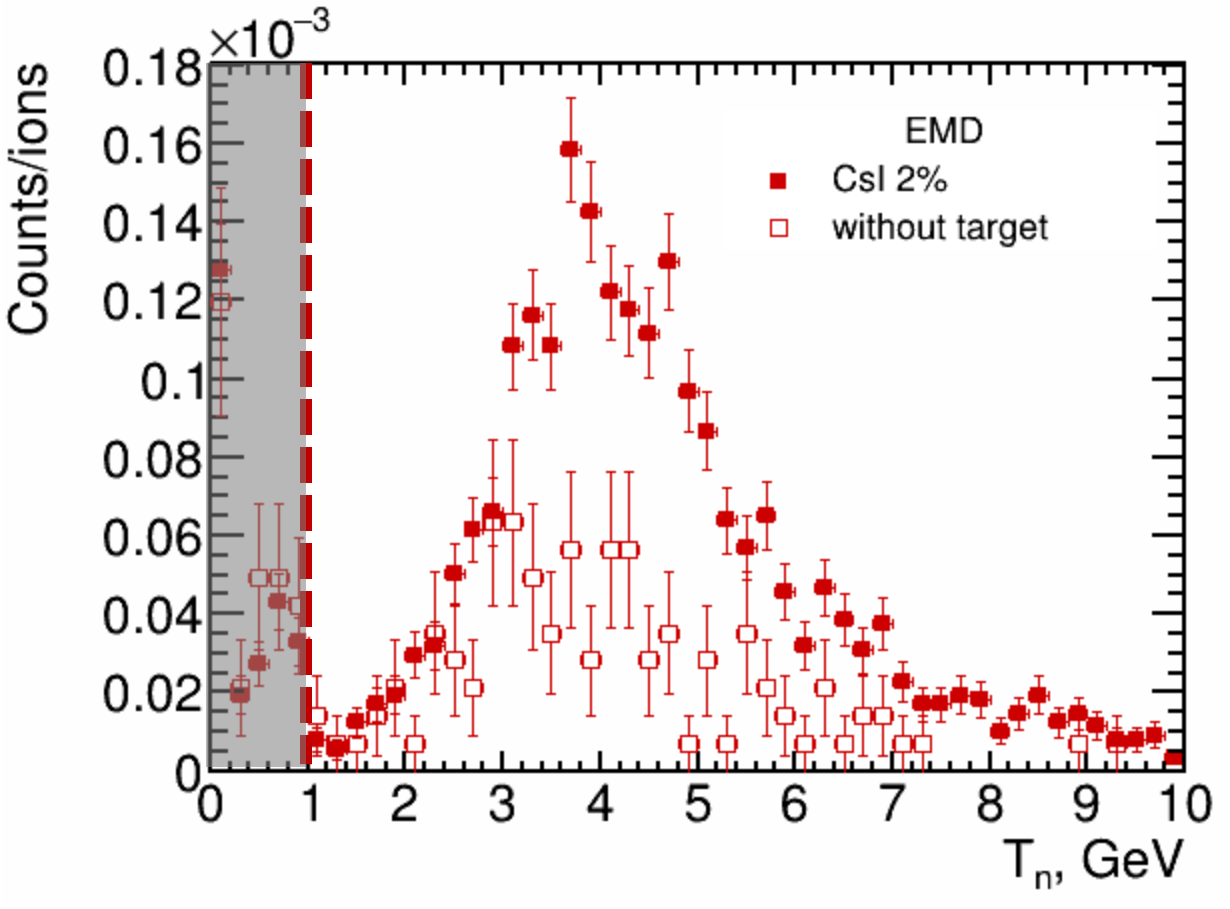
Ultra-peripheral collisions – EMD

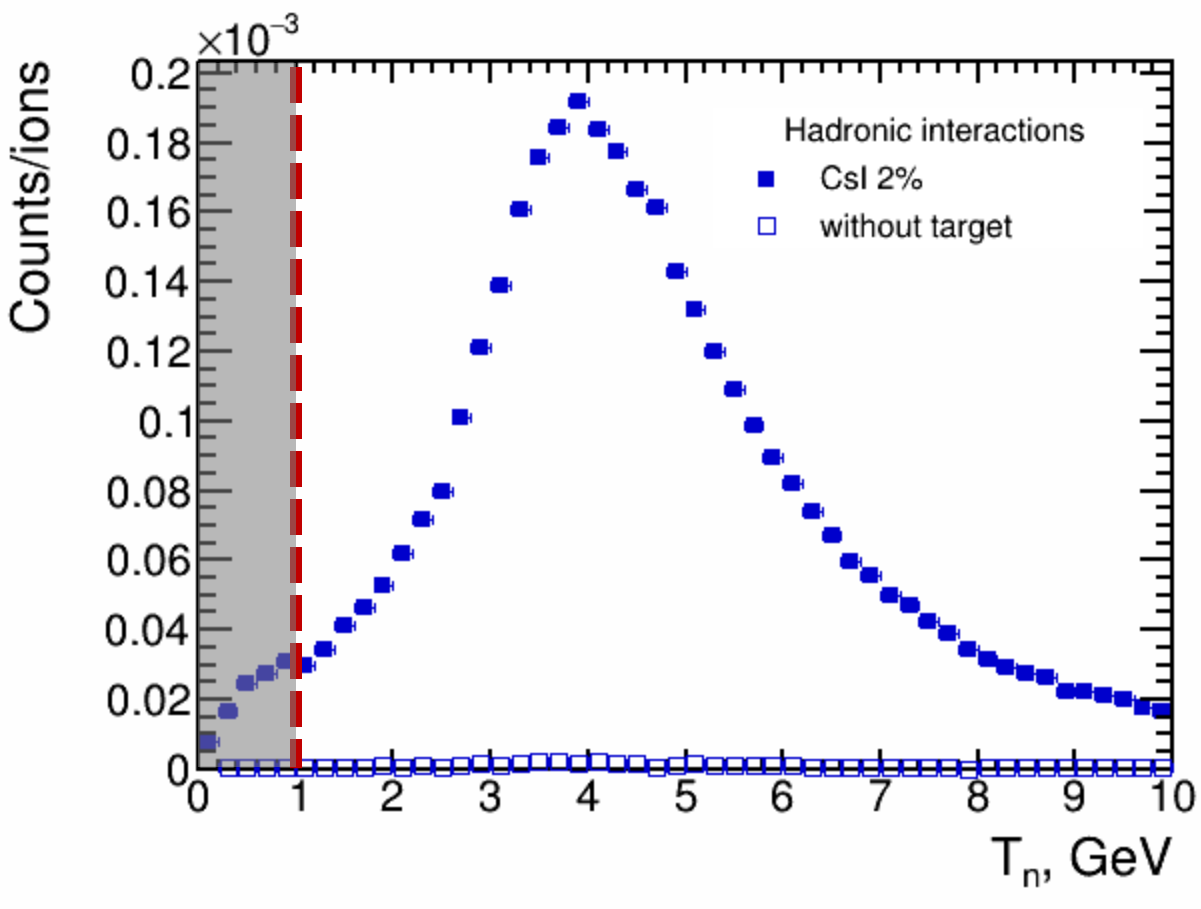


Central & semi-central collisions – hadronic interactions



Reconstructed neutron spectra

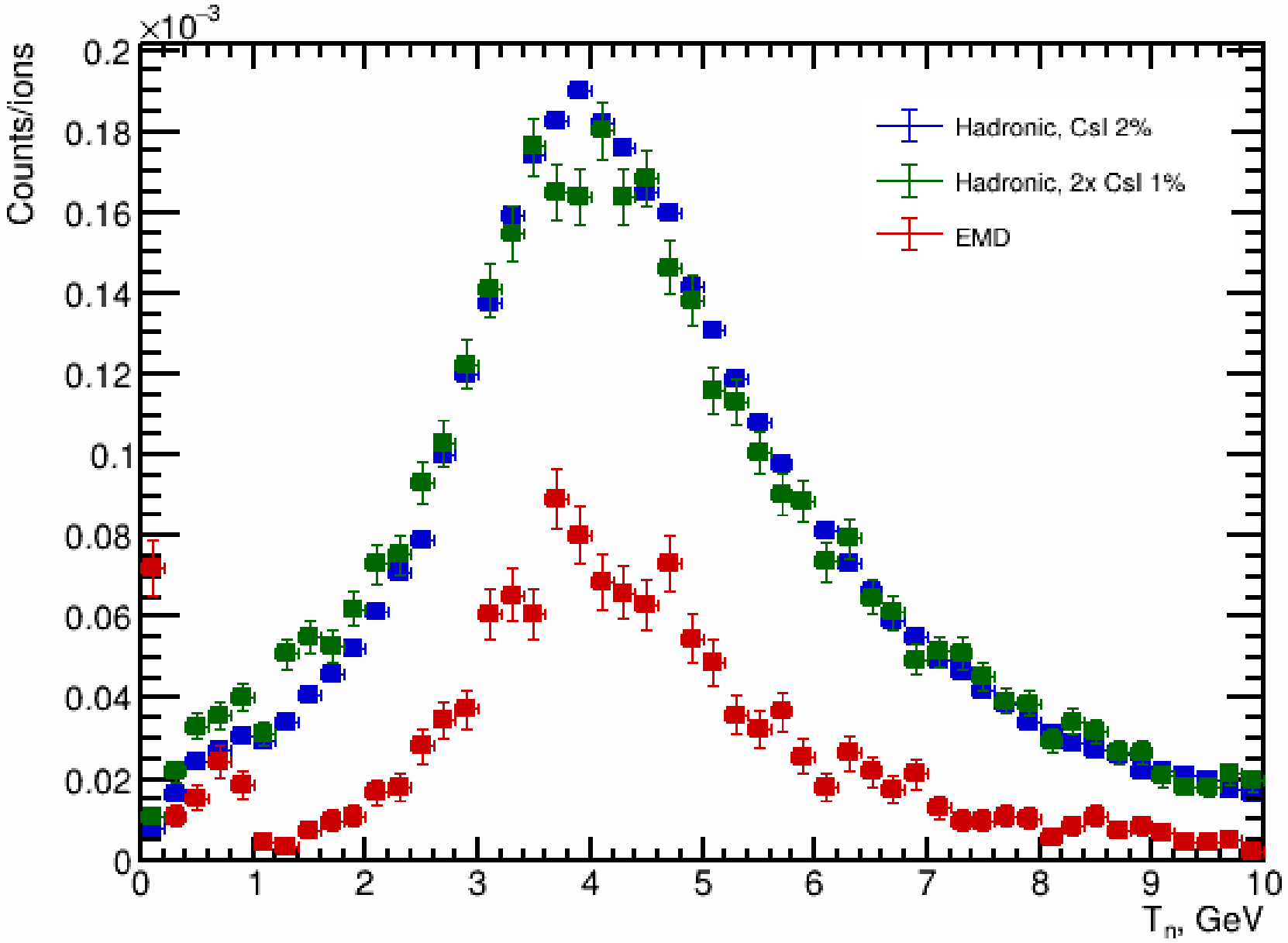




Reconstructed spectra were obtained both for runs with CsI 2% target and without it to estimate fraction of out of target interactions.

Empty target spectra were subtracted from target spectra.

Comparison with thinner target



Corrected spectra after subtracting empty target spectra

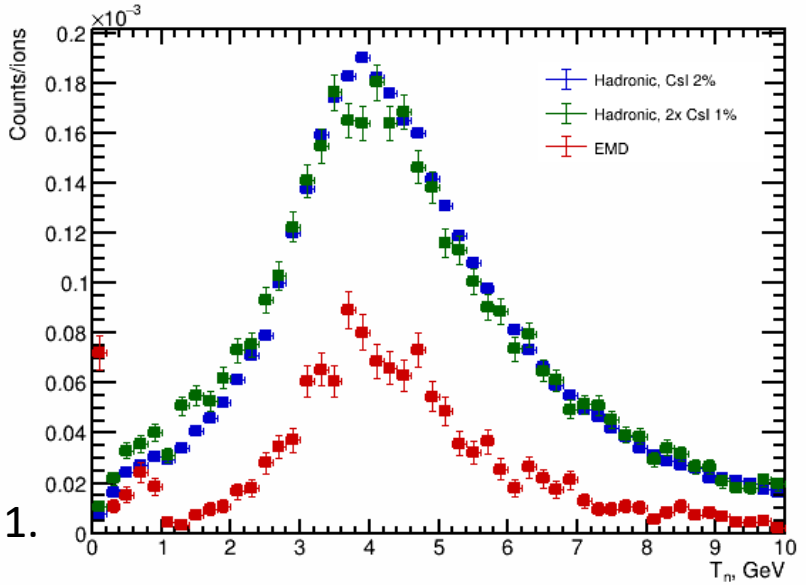
Measurements with 1% and 2% target are consistent

Sources of systematics

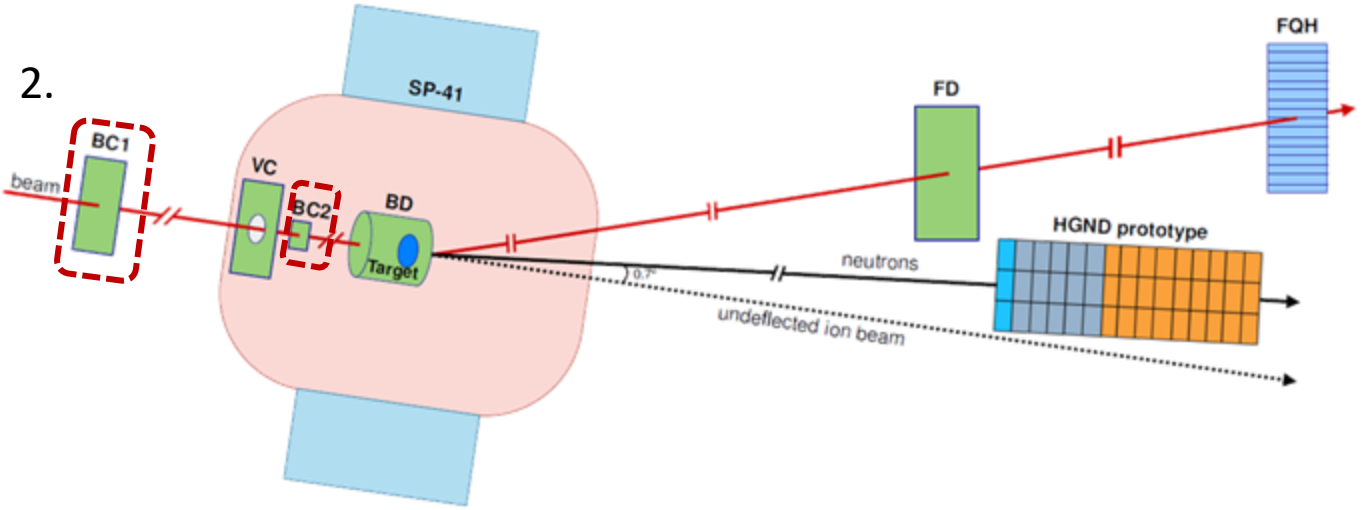
The sources of systematics in obtaining the number of neutrons:

1. The number of incident ions with CsI 2% or CsI 1% targets.
2. Start trigger time obtained using BC1 or BC2.
3. Unevenness of the number of neutrons on HGND prototype surface – using only the central module or all 9 mudules.
4. Uncertainty in the number of neutrons estimated with or without photon rejection.

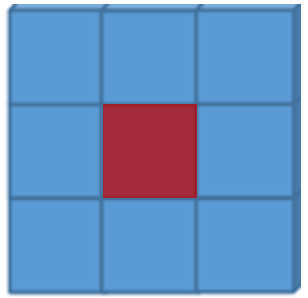
1.



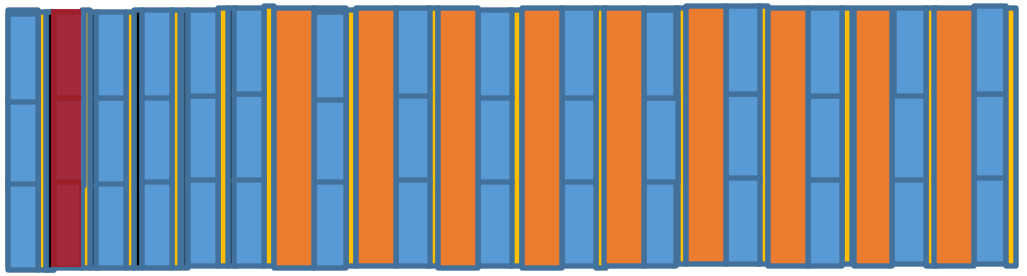
2.



3.



4.

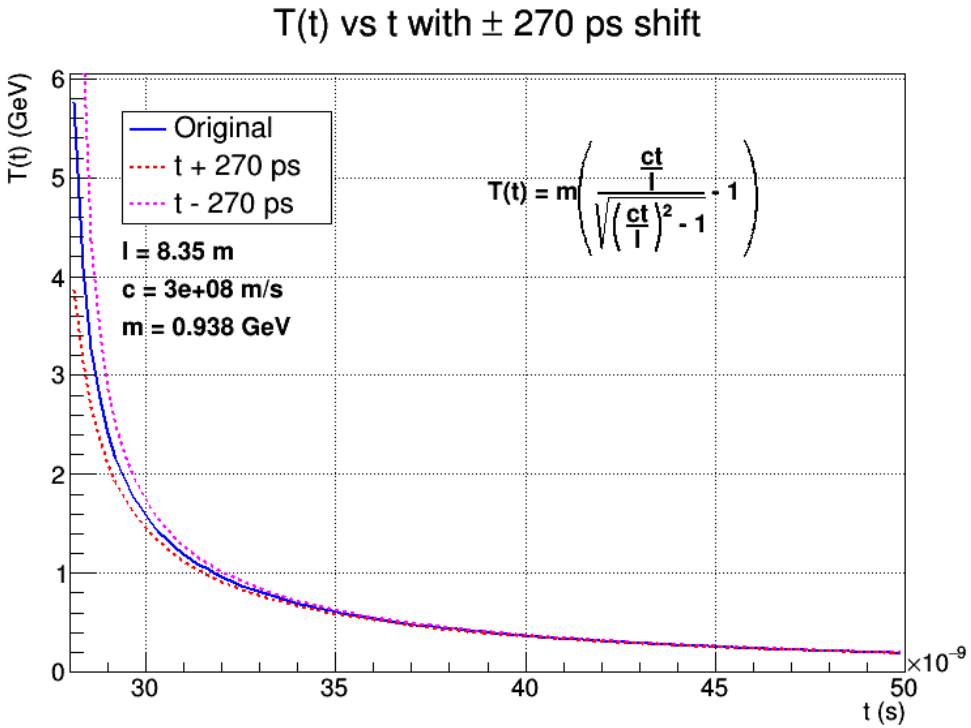


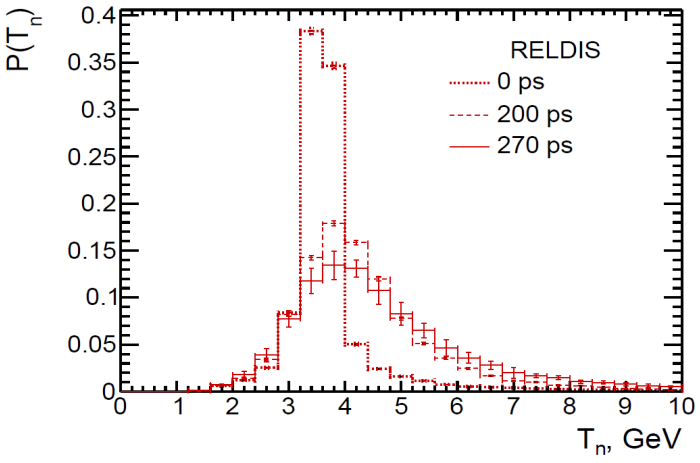
Sources of systematics

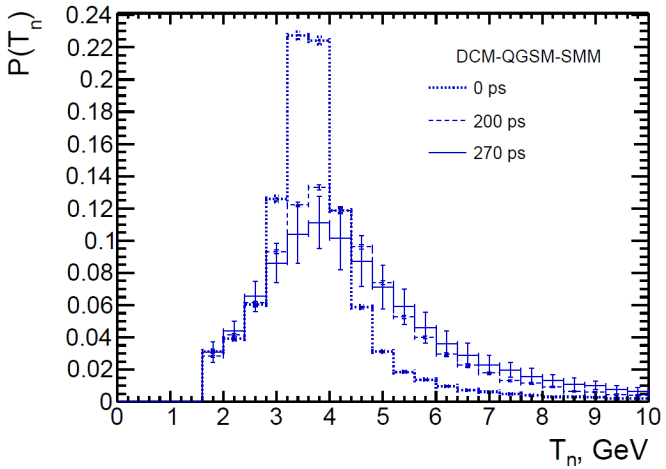
$$\delta_{syst} = \sqrt{\delta_{n/ions}{}^2 + \delta_{tr.time}{}^2 + \delta_{modules}{}^2 + \delta_{\gamma-rejection}{}^2}$$

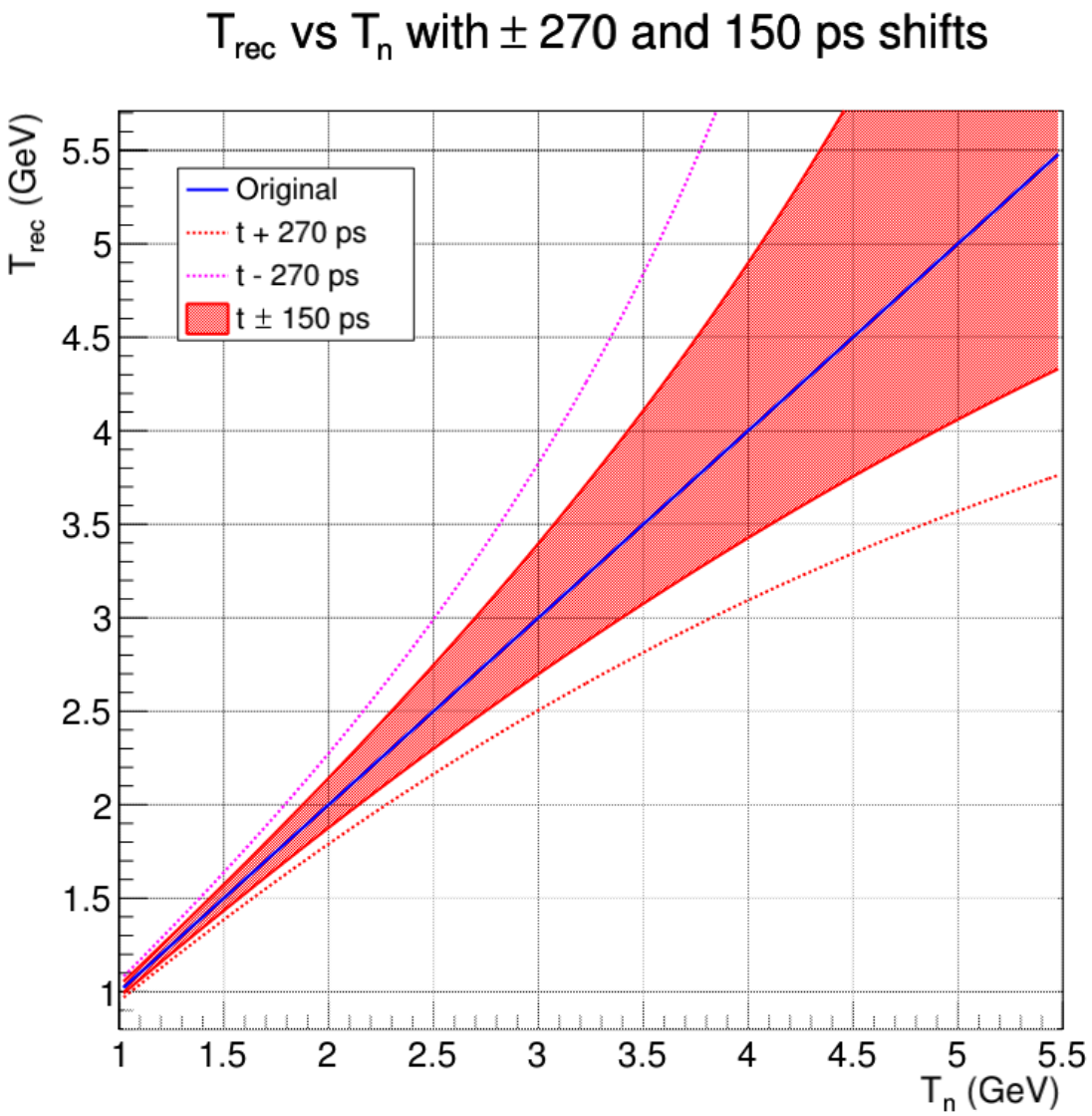
Source of systematics	EMD systematics RELDIS	Hadronic systematics	
		DCM-QGSM-SMM	UrQMD-AMC
$\delta_{n/ions}$	-	0.62%	
$\delta_{tr.time}$	0.09%	2.93%	
$\delta_{modules}$	7.47%	6.74%	4.39%
$\delta_{\gamma\text{-rejection}}$	0.66%	6.20%	6.77%
Total δ_{syst}	7.50%	9.64%	8.61%

Impact of time resolution

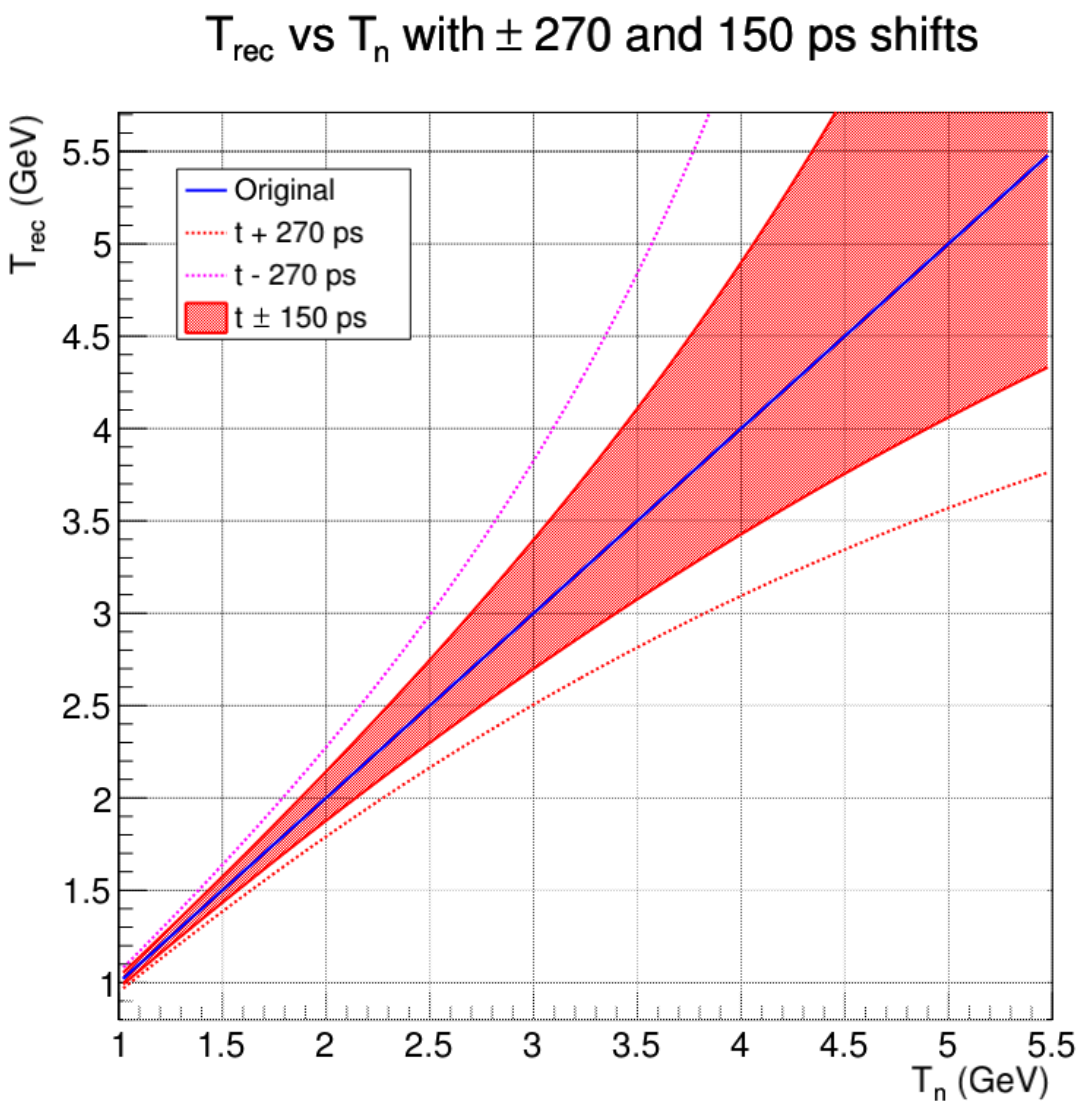


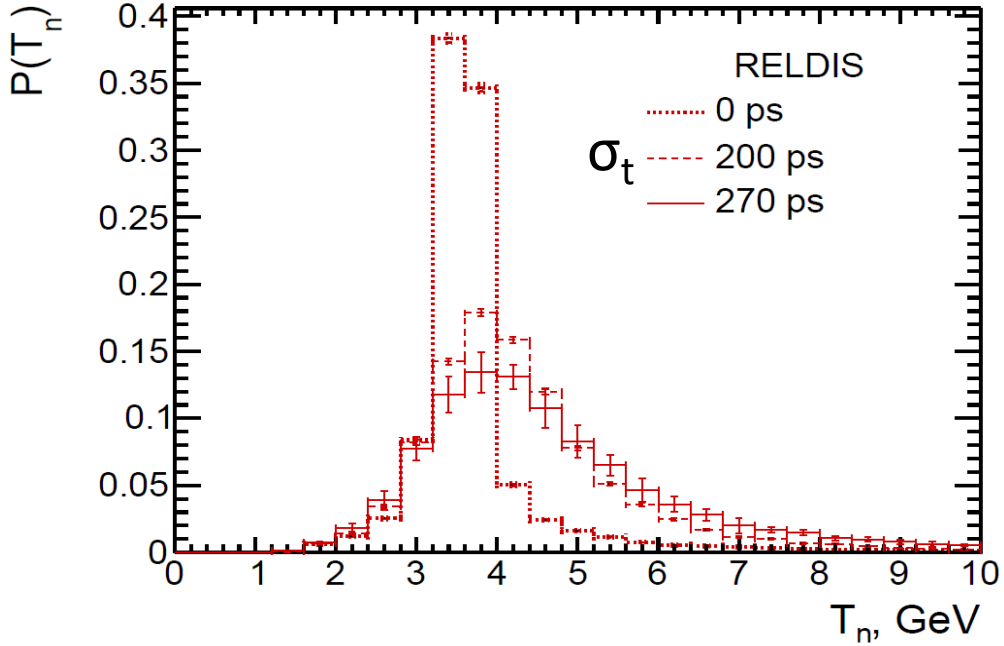


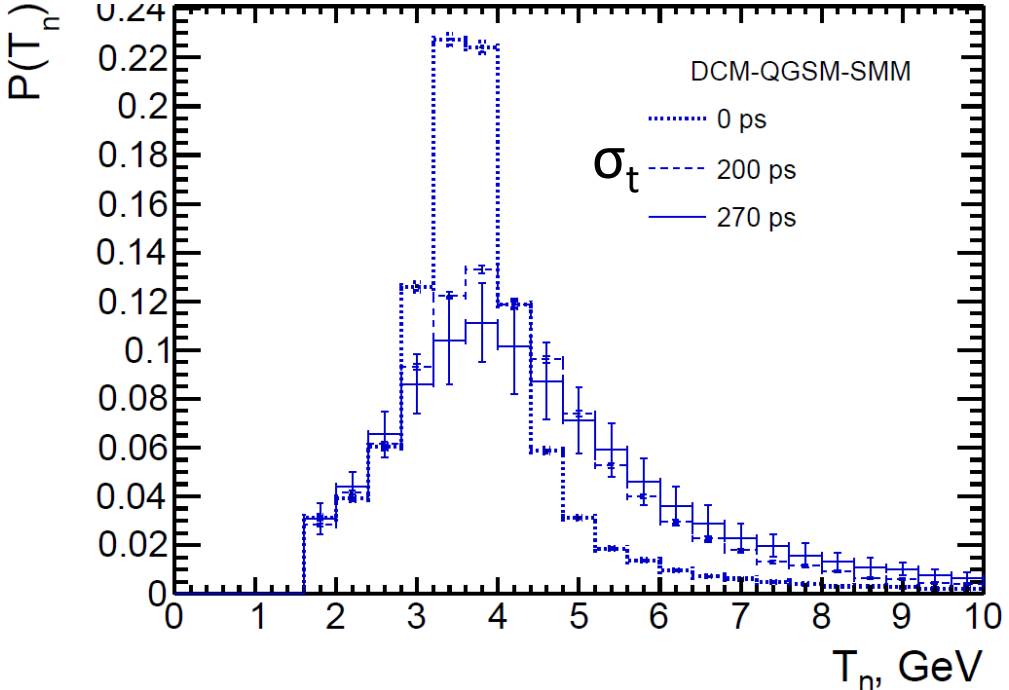




Влияние временного разрешения на спектр нейтронов

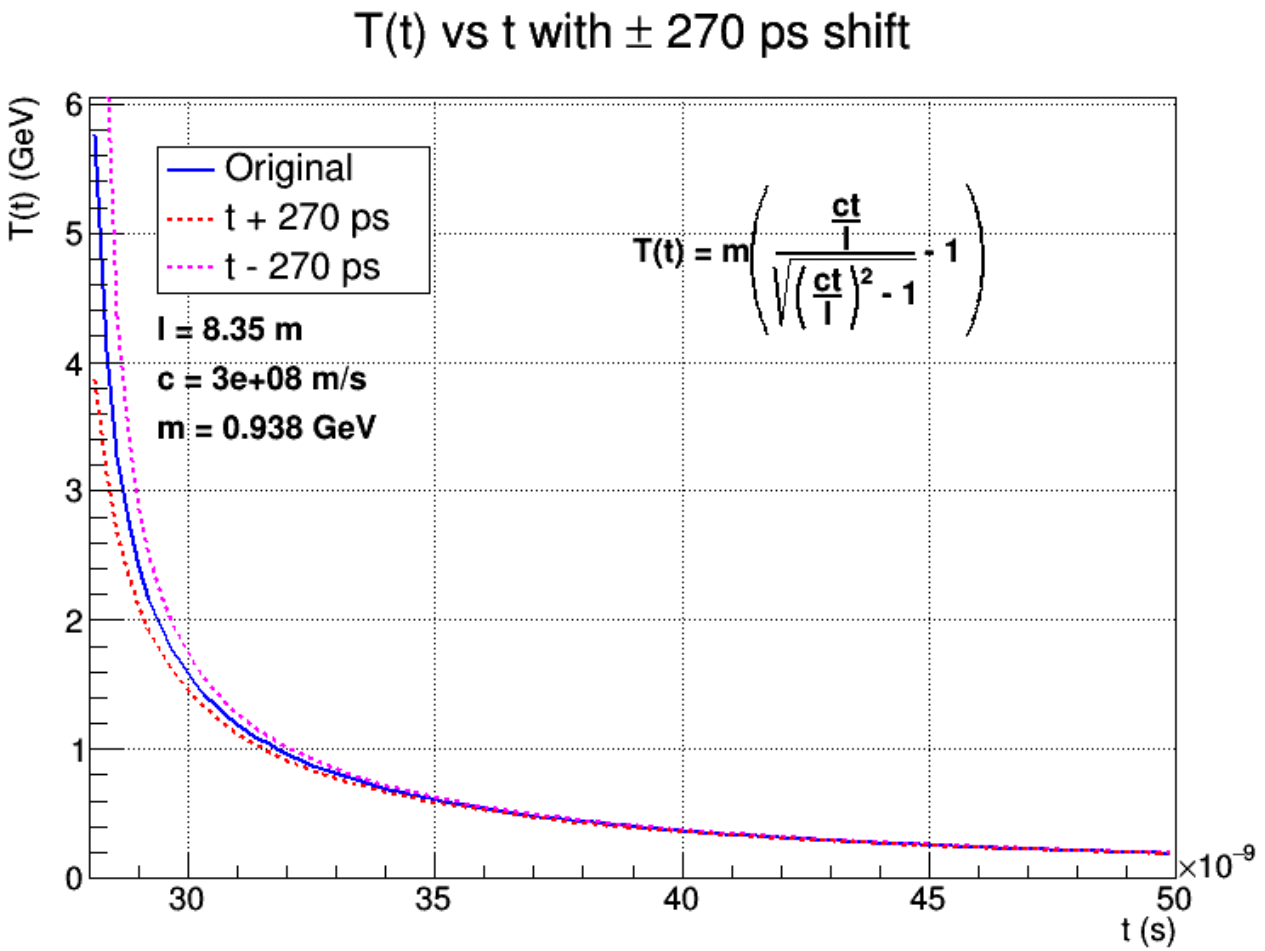


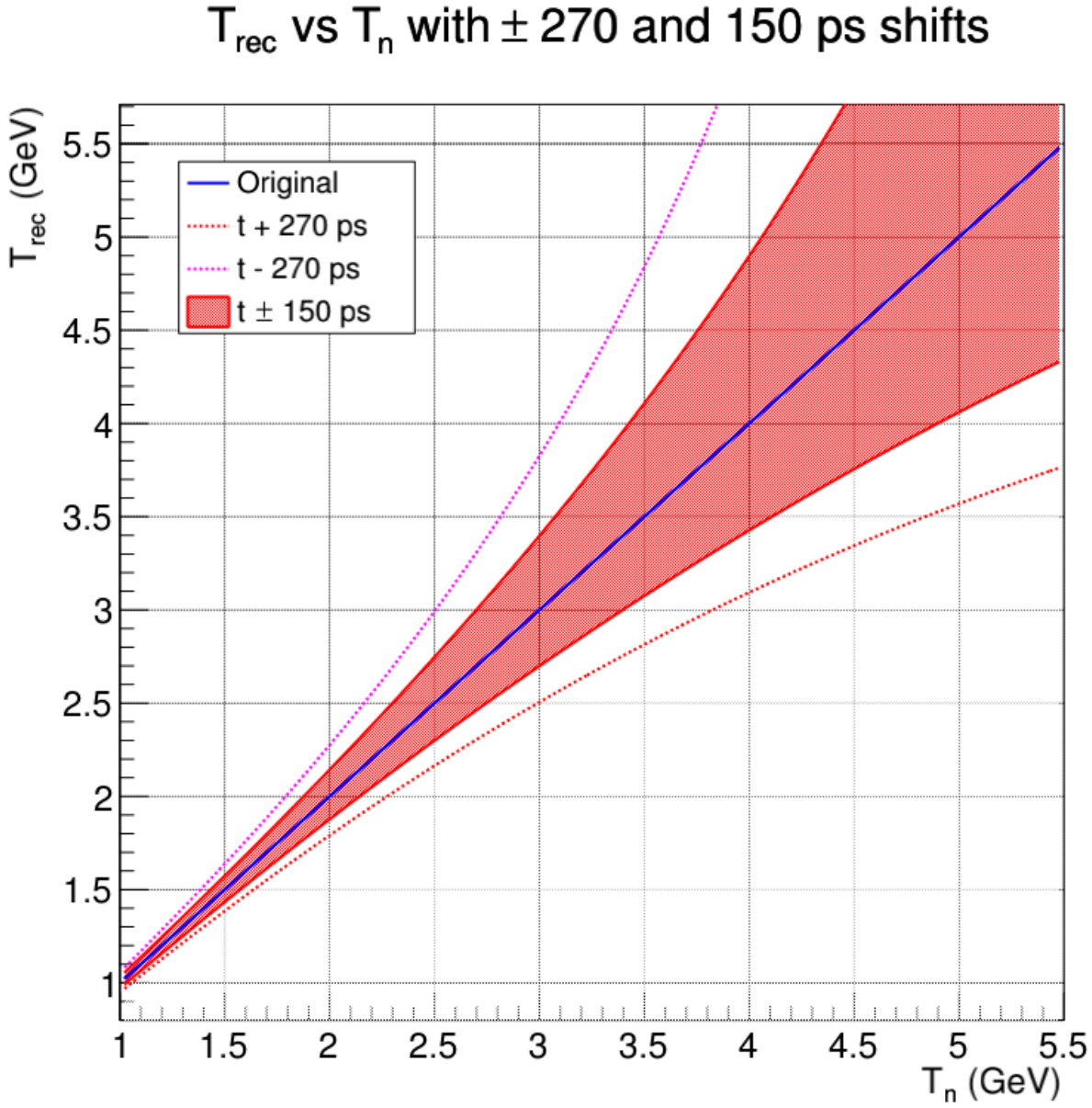




Спектры размазываются в сторону высоких энергий из-за временного разрешения ~270 ps.

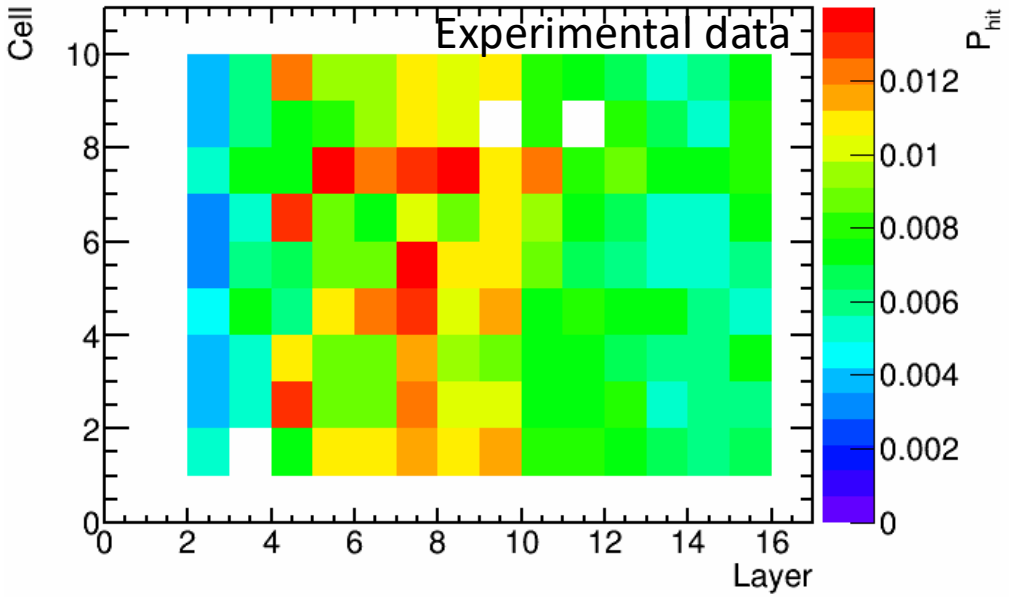
Time resolution

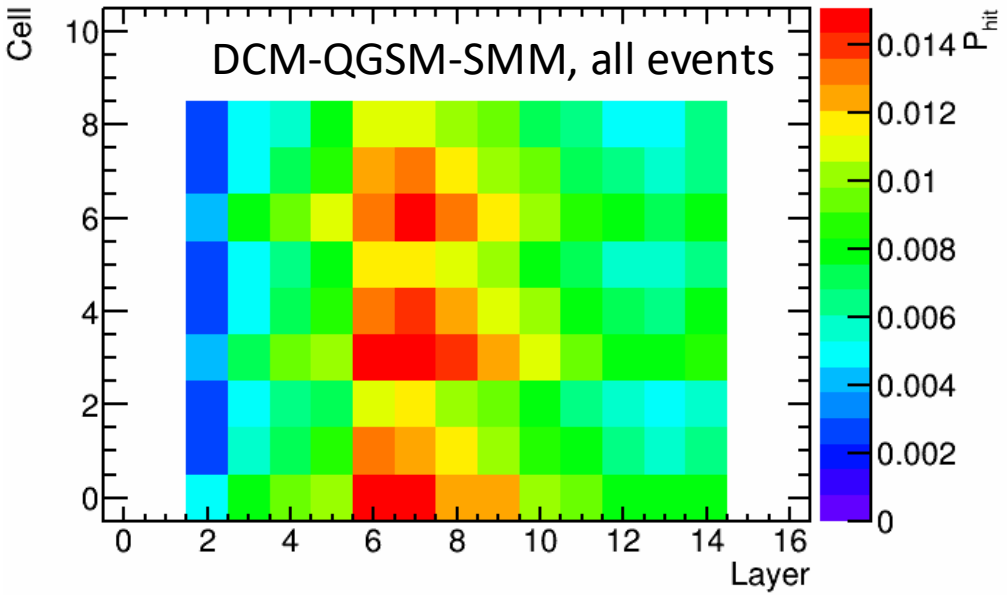


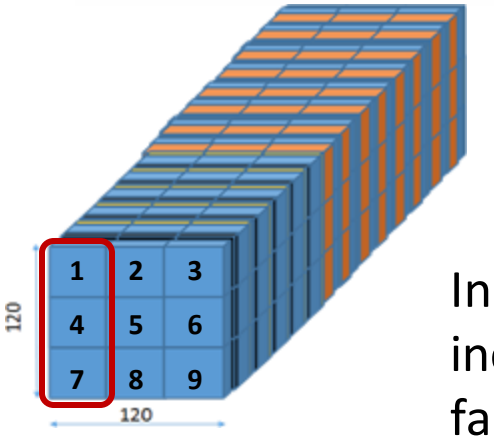


Background source

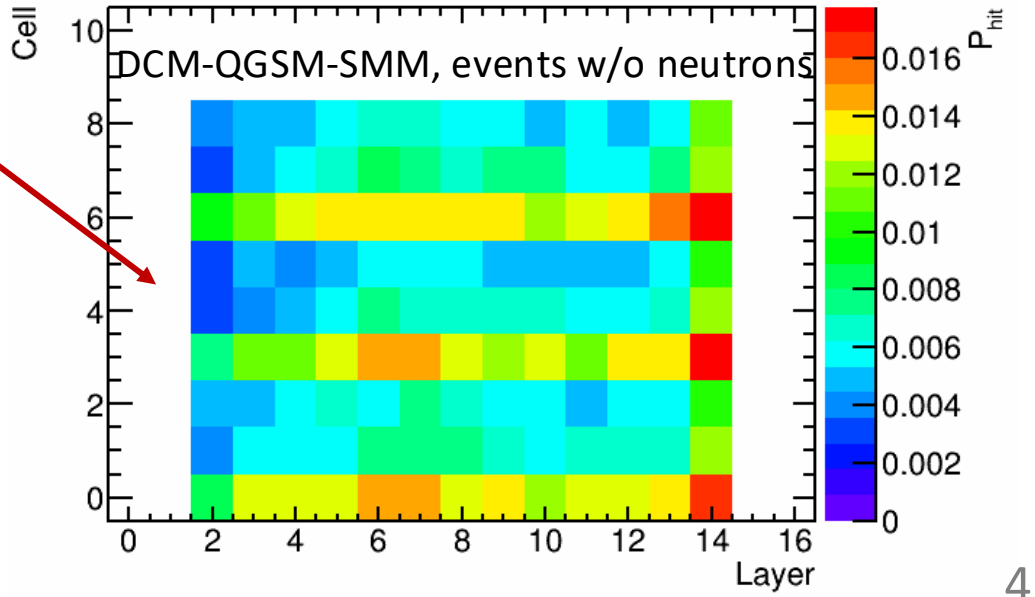
Cells for which the T_n is reconstructed





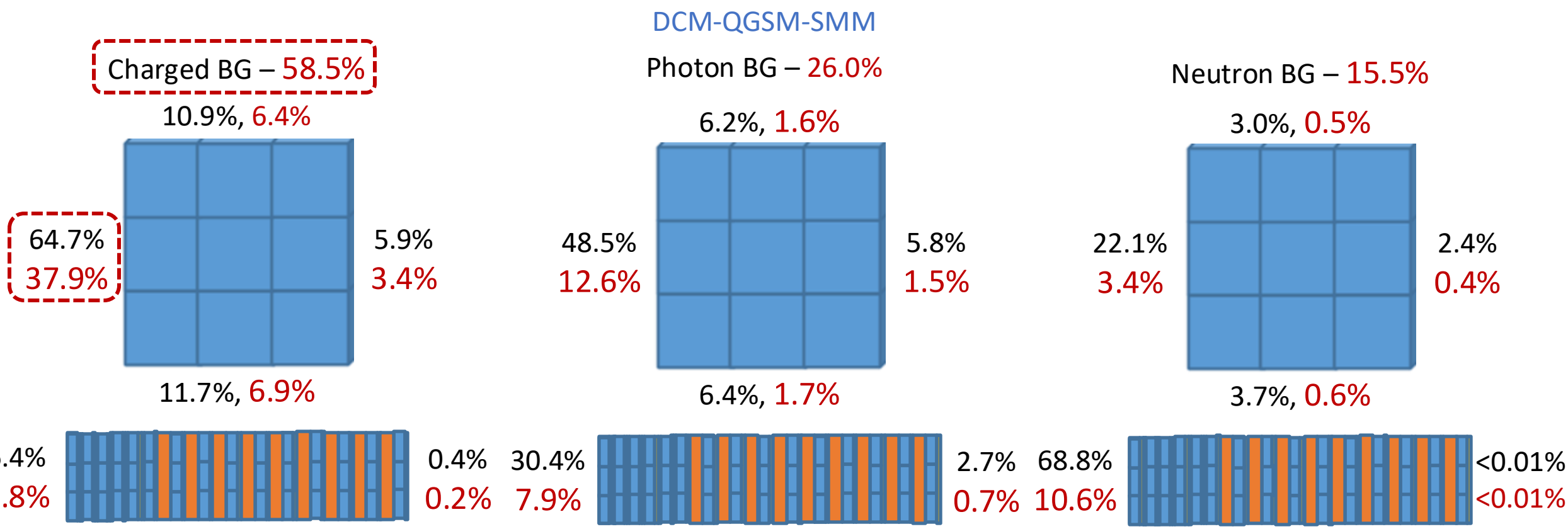


BG that passes the neutron selection criteria and cannot be obtained by analysis of existing data



In the events where neutrons were not incident on the HGND prototype but were falsely identified as neutrons, the cells closest to the beam are most often triggered

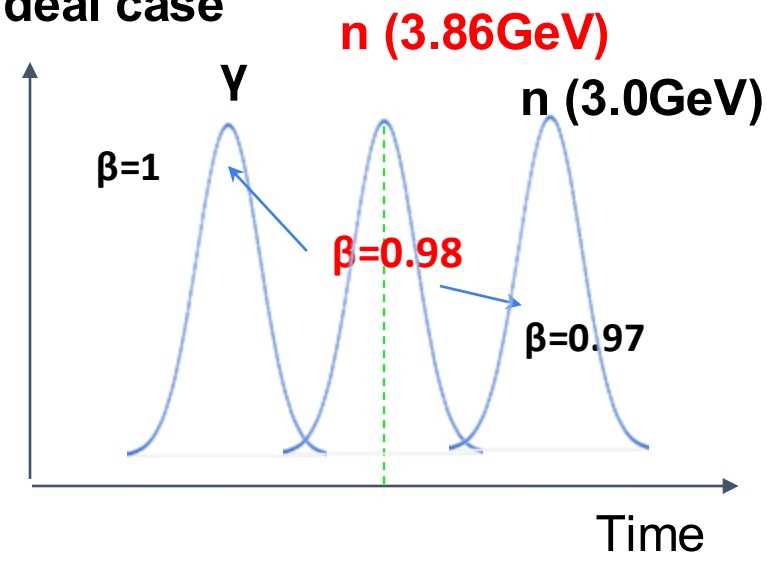
Sources of background in events without primary neutrons



- The main source of the background is the background from charged particles – 58.5%.
- The main direction of the background is the side closest to the beam – 53.9%.
- Only 0.02% of the background from charged particles on the side surface of HGND prototype closest to the beam is the background from the primary charged particles

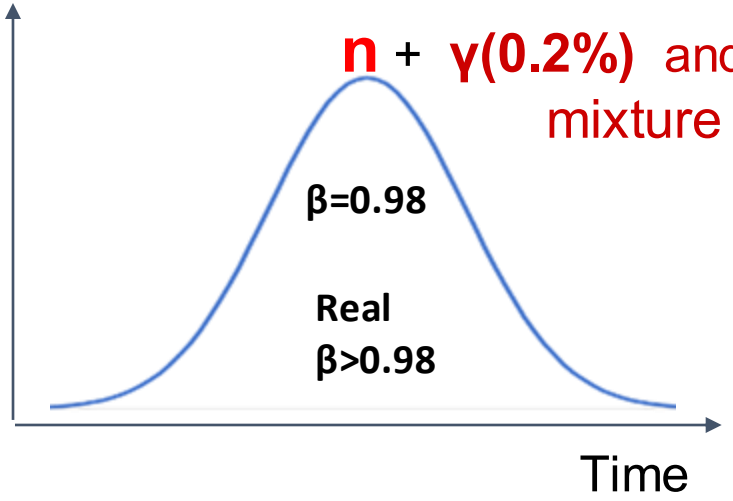
HGND calibration

Ideal case

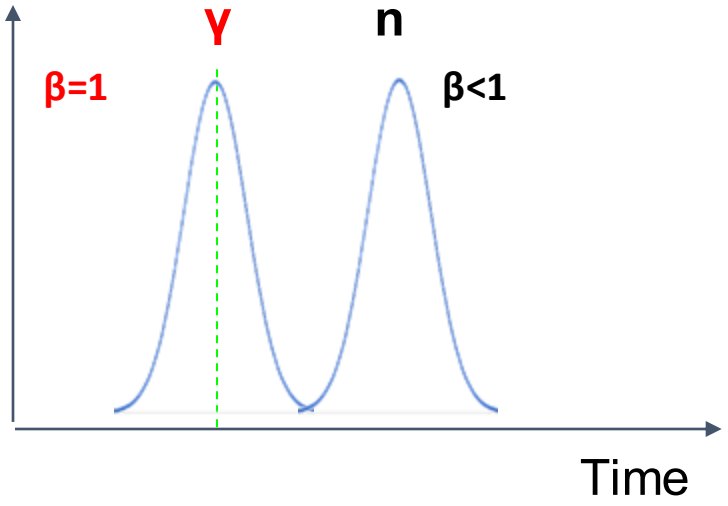


Calibration on neutrons

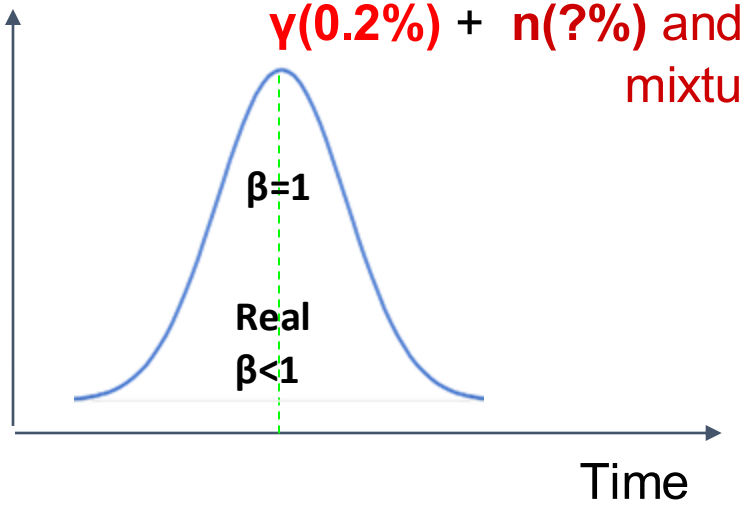
Real data



Calibration on neutrons

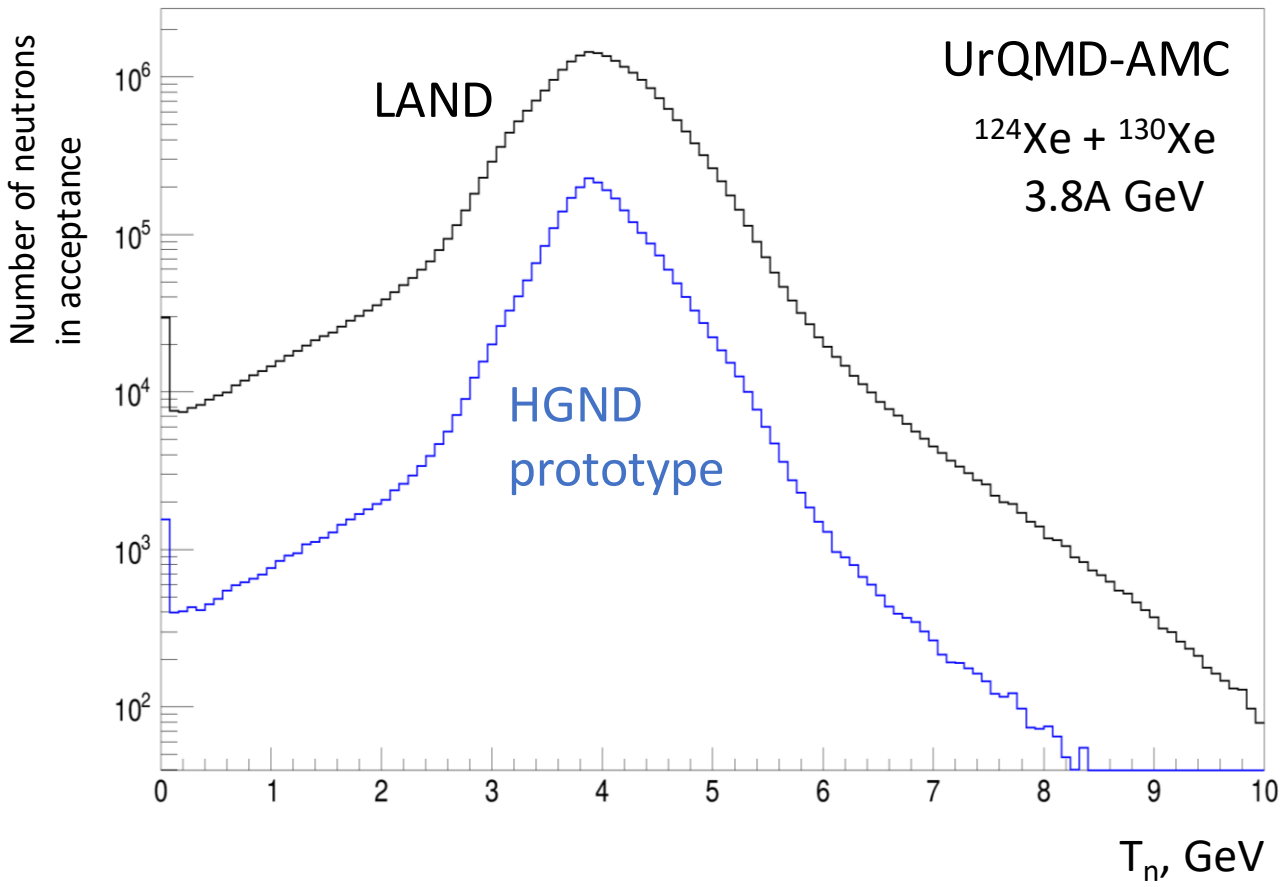


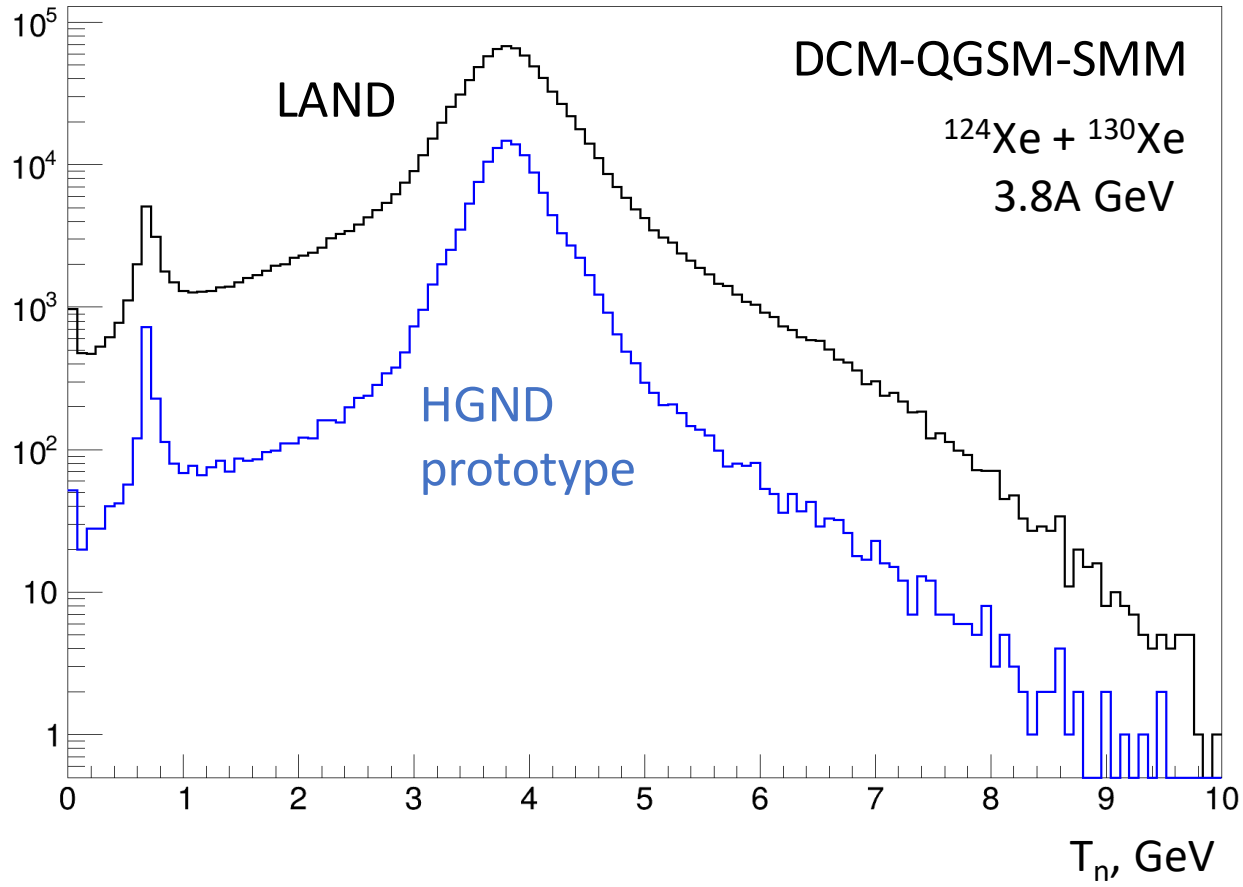
Calibration on photons



Calibration on photons is possible up to 8 layer

LAND vs HGND prototype acceptance



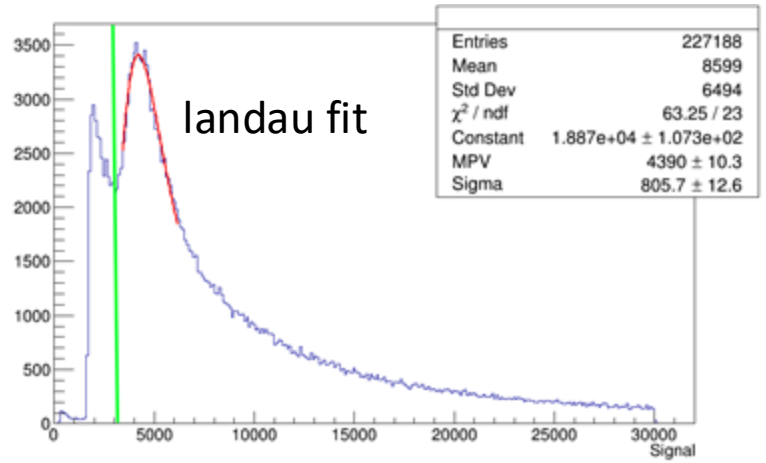


~7.9 times difference

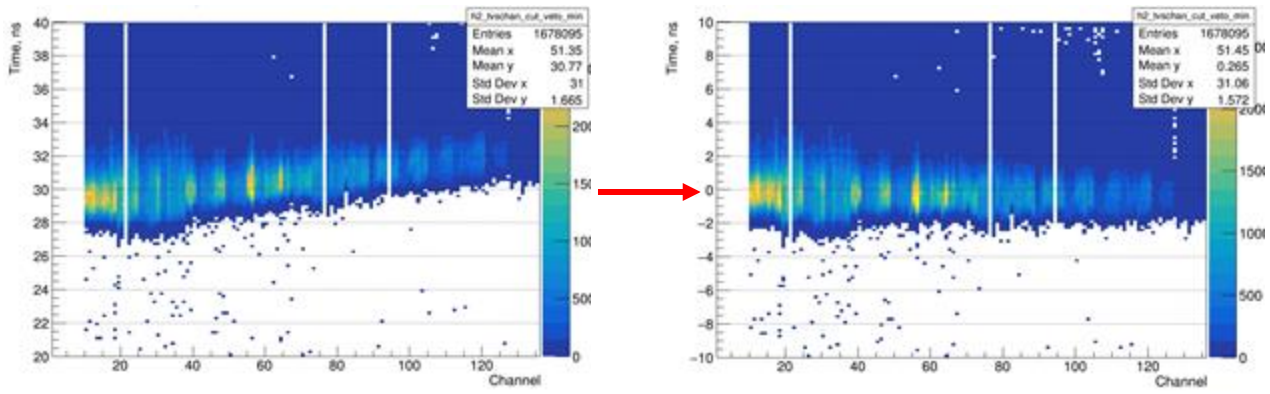
HGND calibration

1. Amplitude normalization

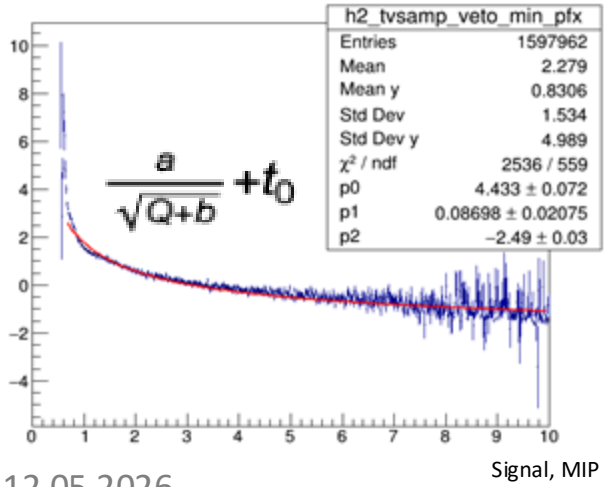
$$Ampl = Ampl \cdot \frac{1}{MPV}$$



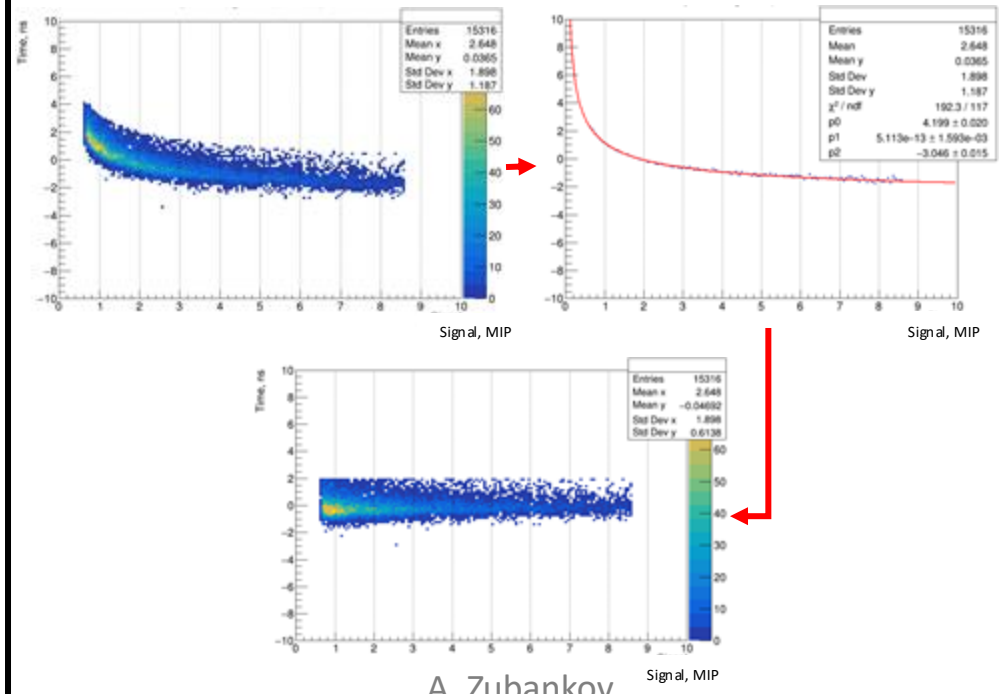
2. Time shift for all channels by the average fit value



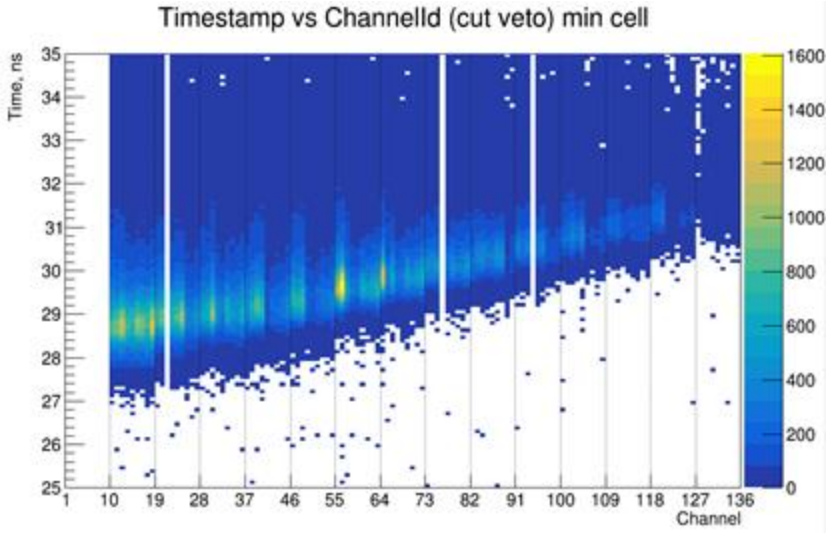
3. Determination of parameters of the approximating function for all channels & time limit



4. Time-amplitude correction

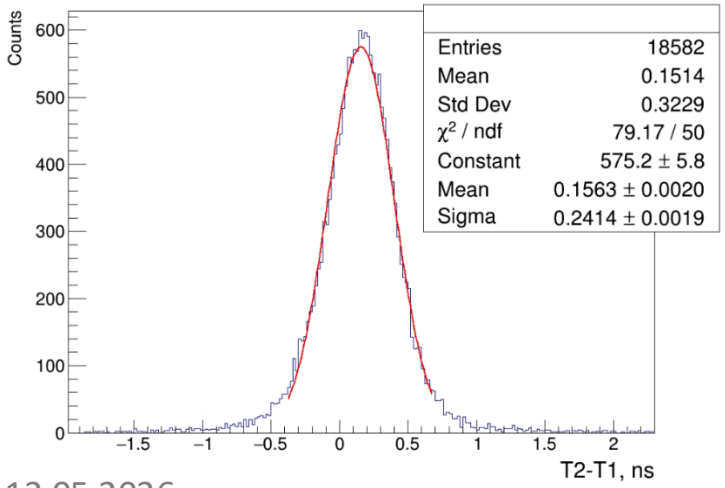


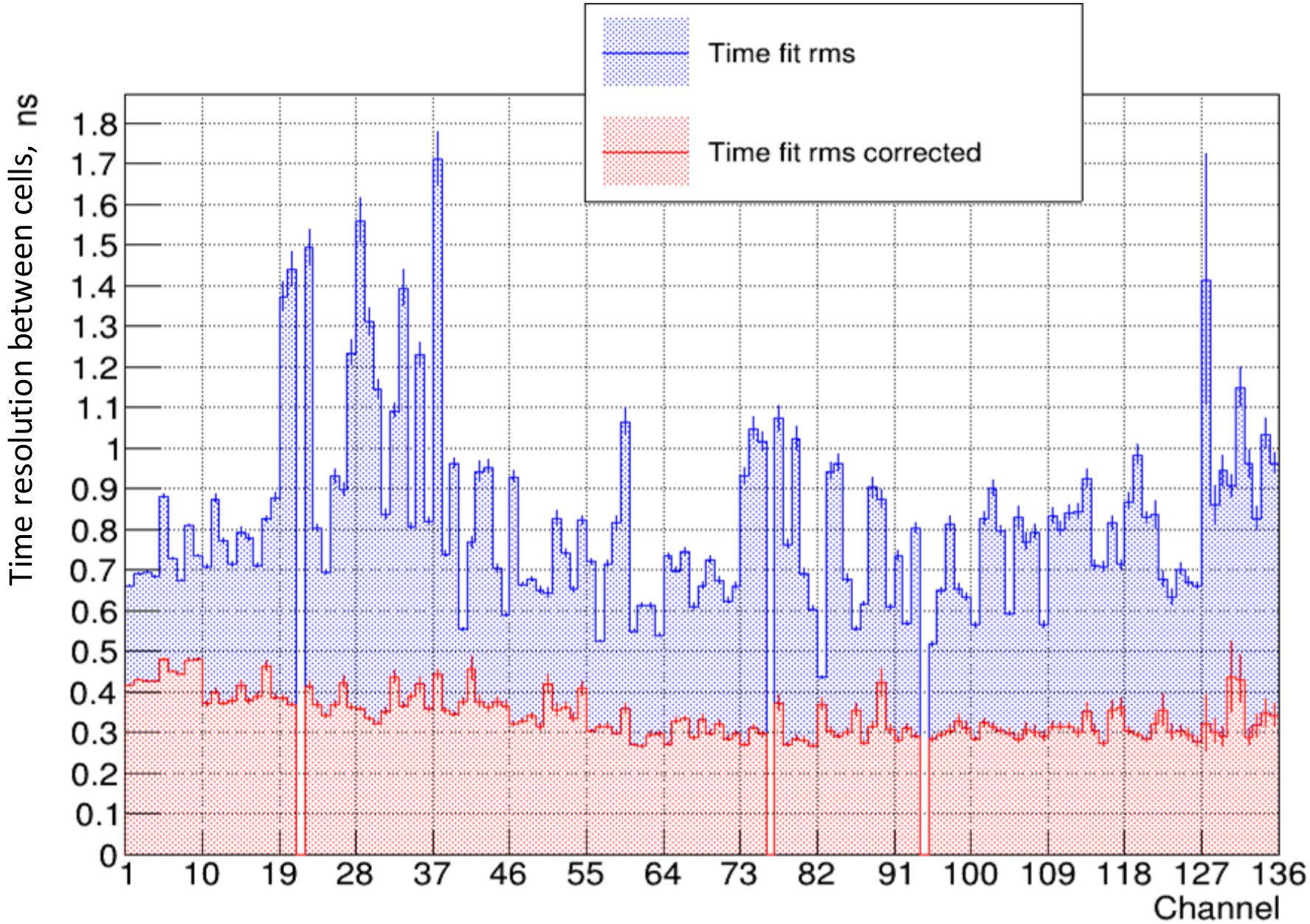
5. Time shift



HGND calibration

Time-amplitude correction of signals made it possible to get rid of the dependence of time on signal amplitude, which improved the time resolution by ~2.4 times.

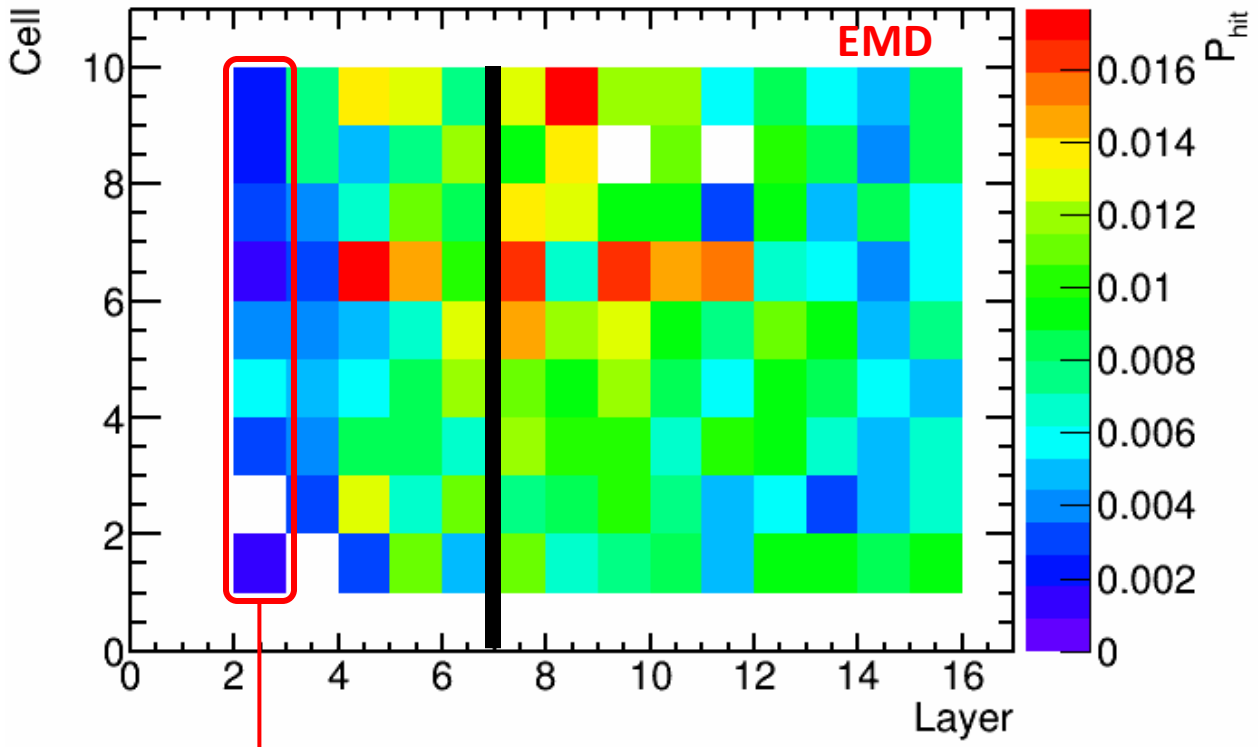


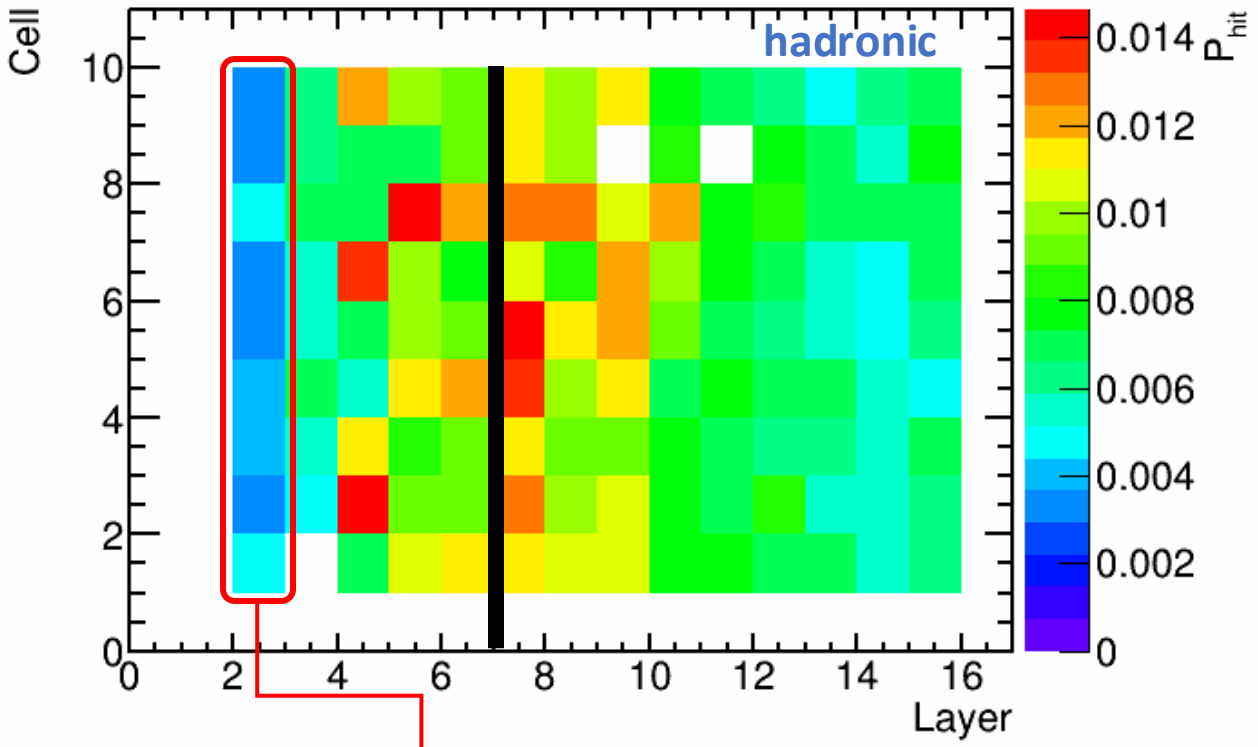


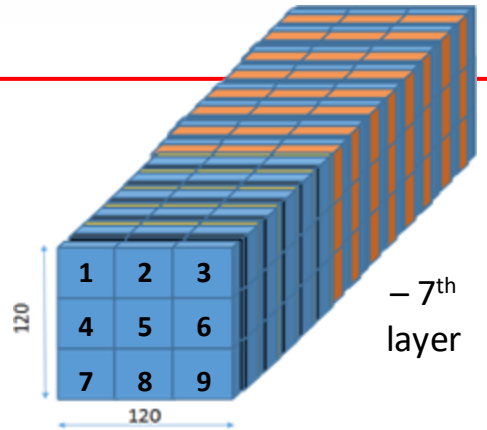
Fastest cells for EMD vs hadronic interactions

Comparison of hadronic interactions (CCT2) with electromagnetic dissociation (BT)

Run 8281 (BT) vs 8300 (CCT2) 3.8 AGeV





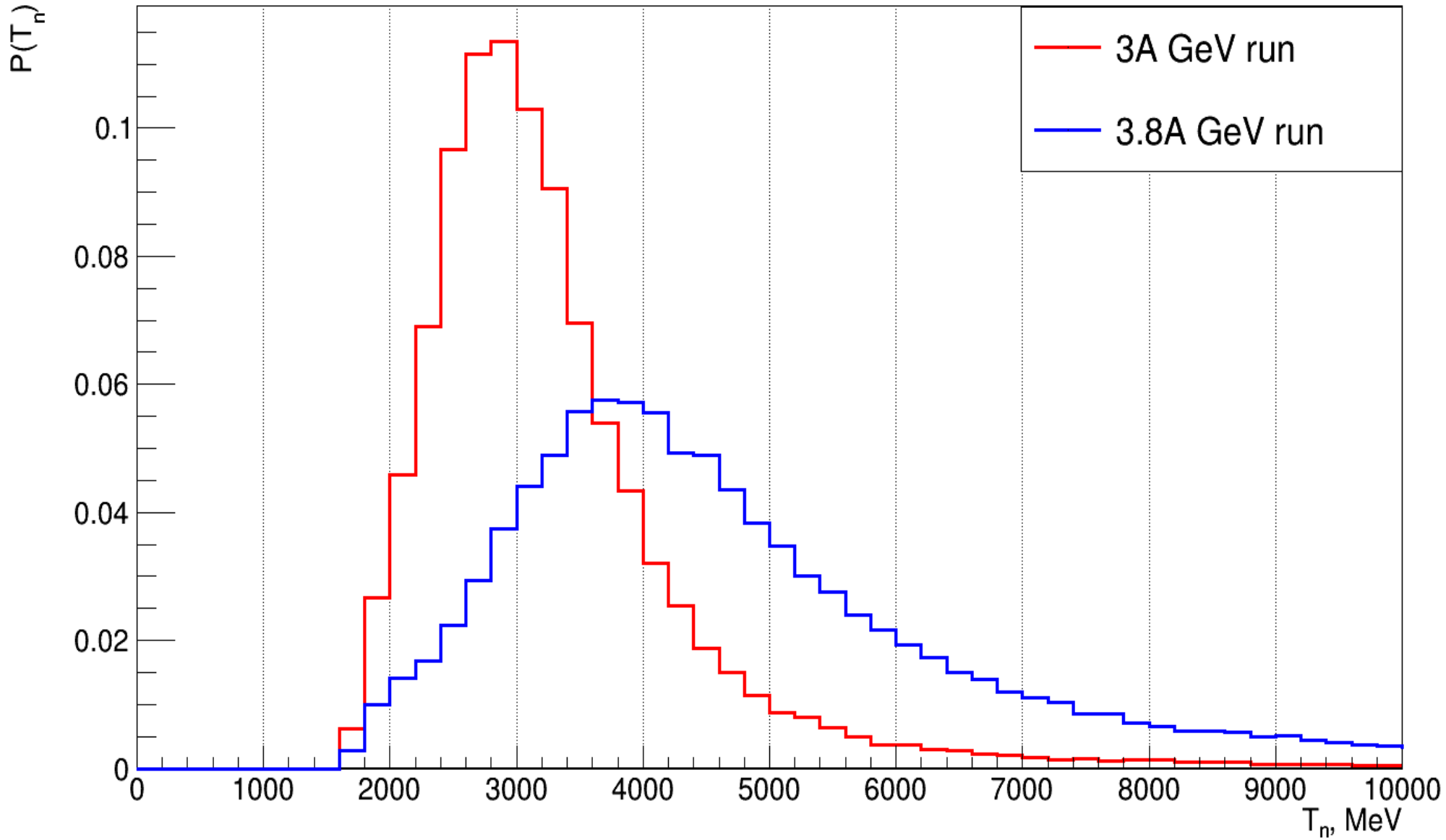


– 7th layer

γ-quanta cut – no hits in 1-2 layers in module => 1.55 X_0 or 0.11 λ_{int}

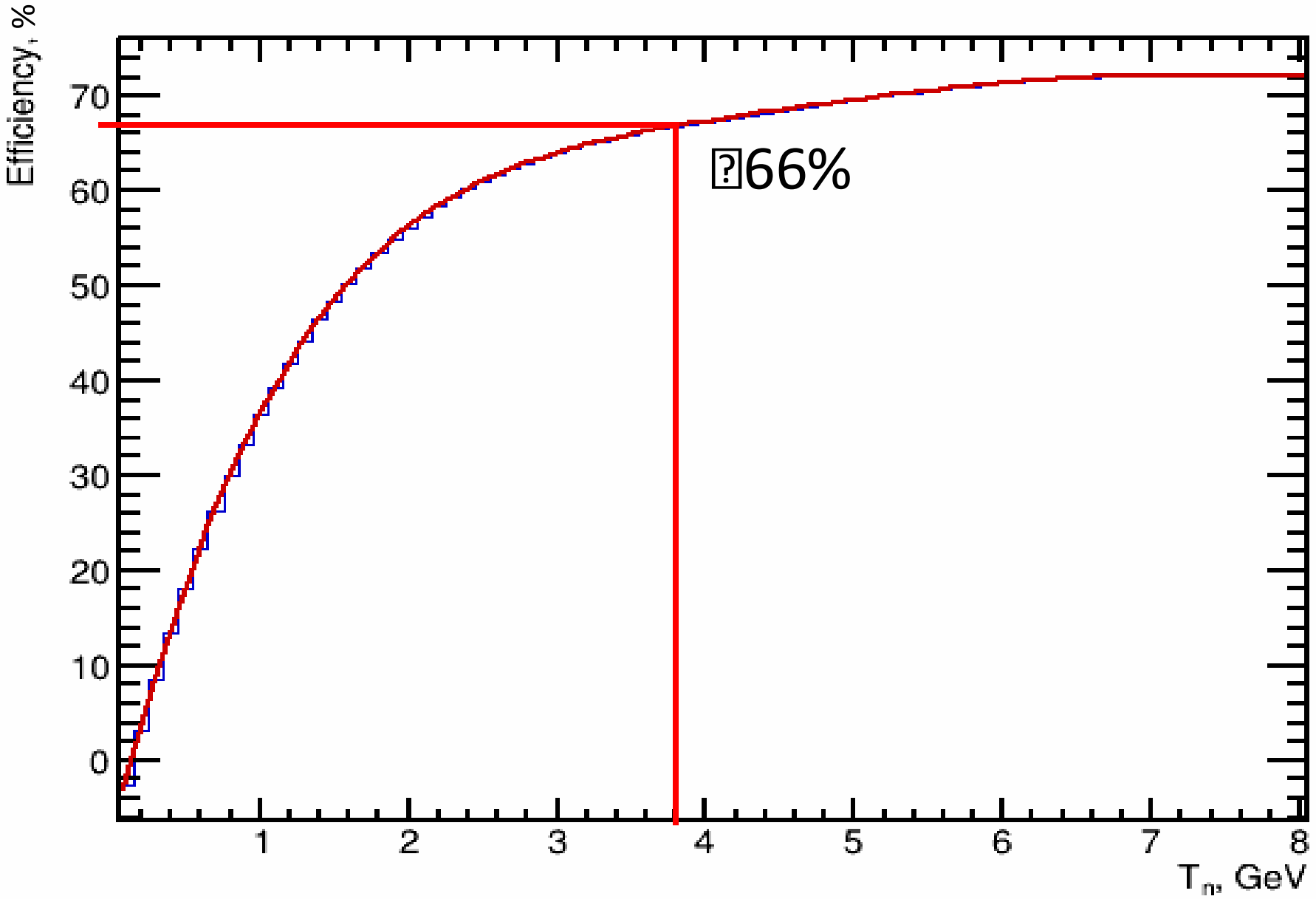
Most of the neutrons are deposited after the 7th layer for both EMD and nuclear interaction

Reconstructed neutrons



Reconstructed neutron spectra for both 3A GeV and 3.8A GeV runs are in correct positions.

Efficiency of HGND prototype

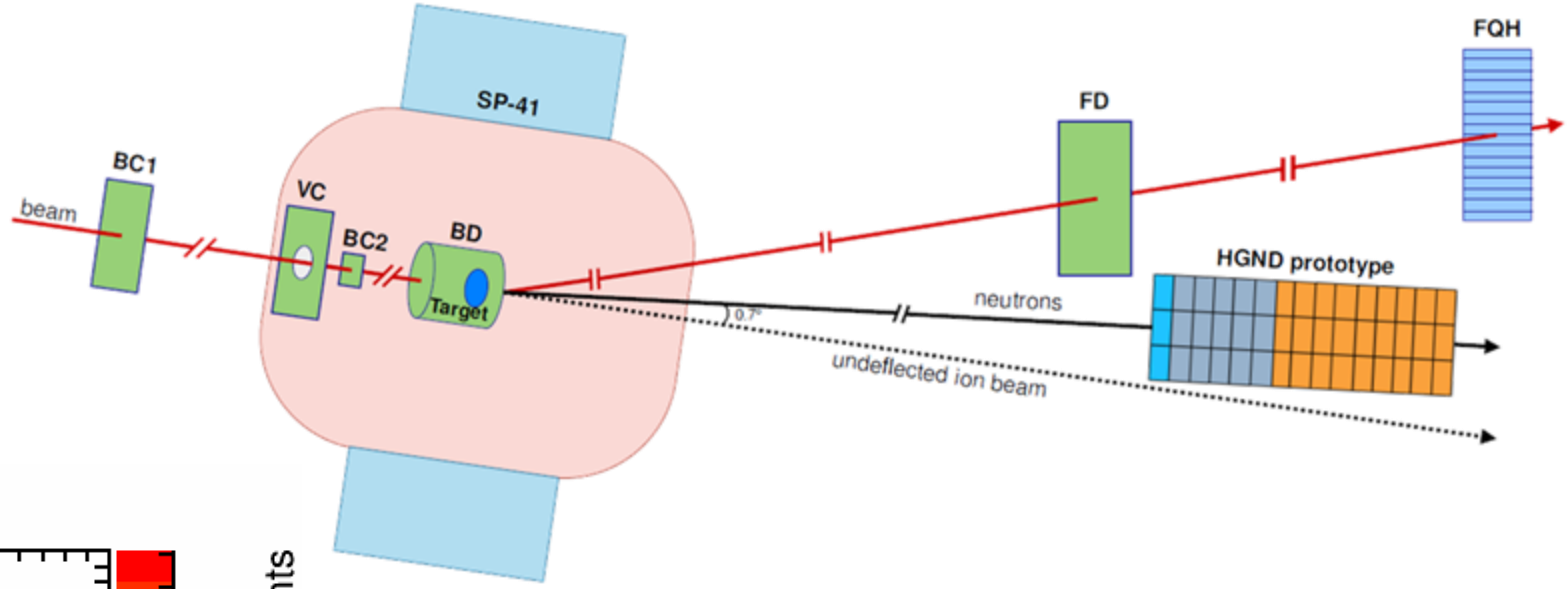


Geant4 simulation:

Particle source, only neutrons

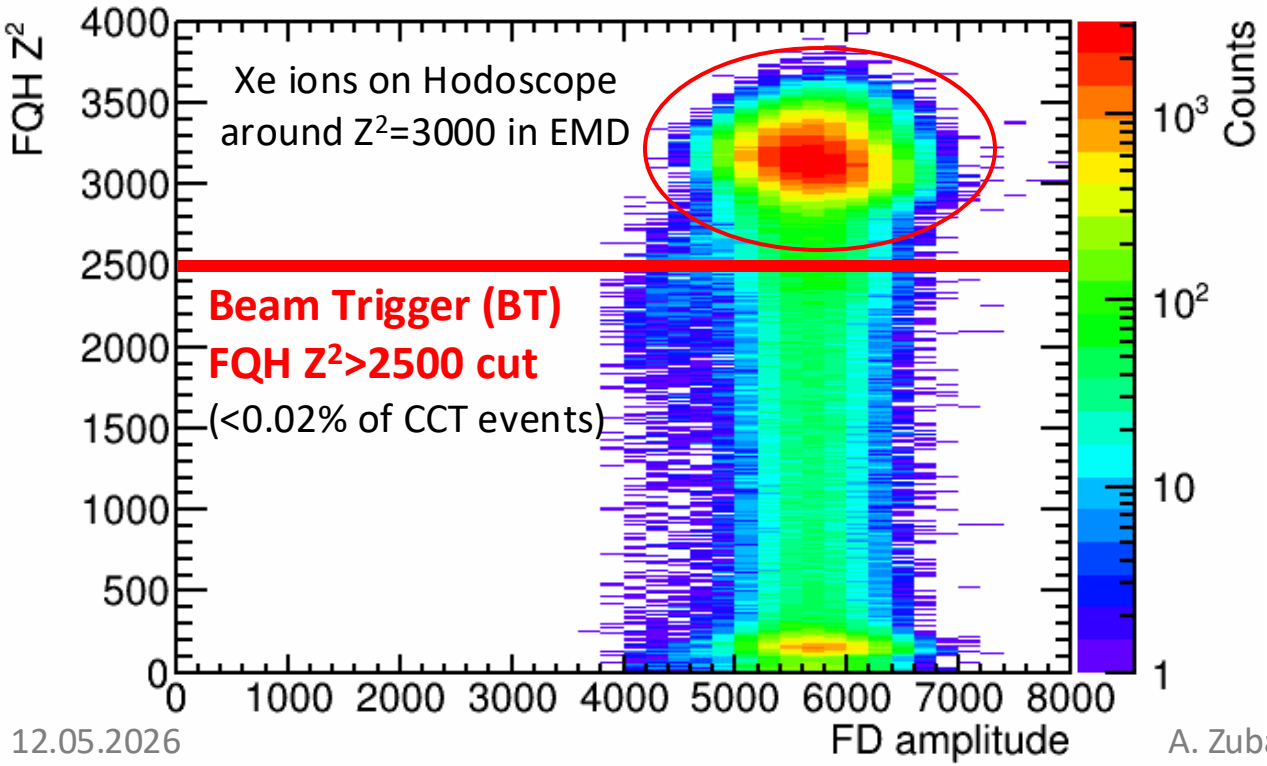
- VETO-cut
- γ-cut
- ToF cut

Selection of EMD events in measurements

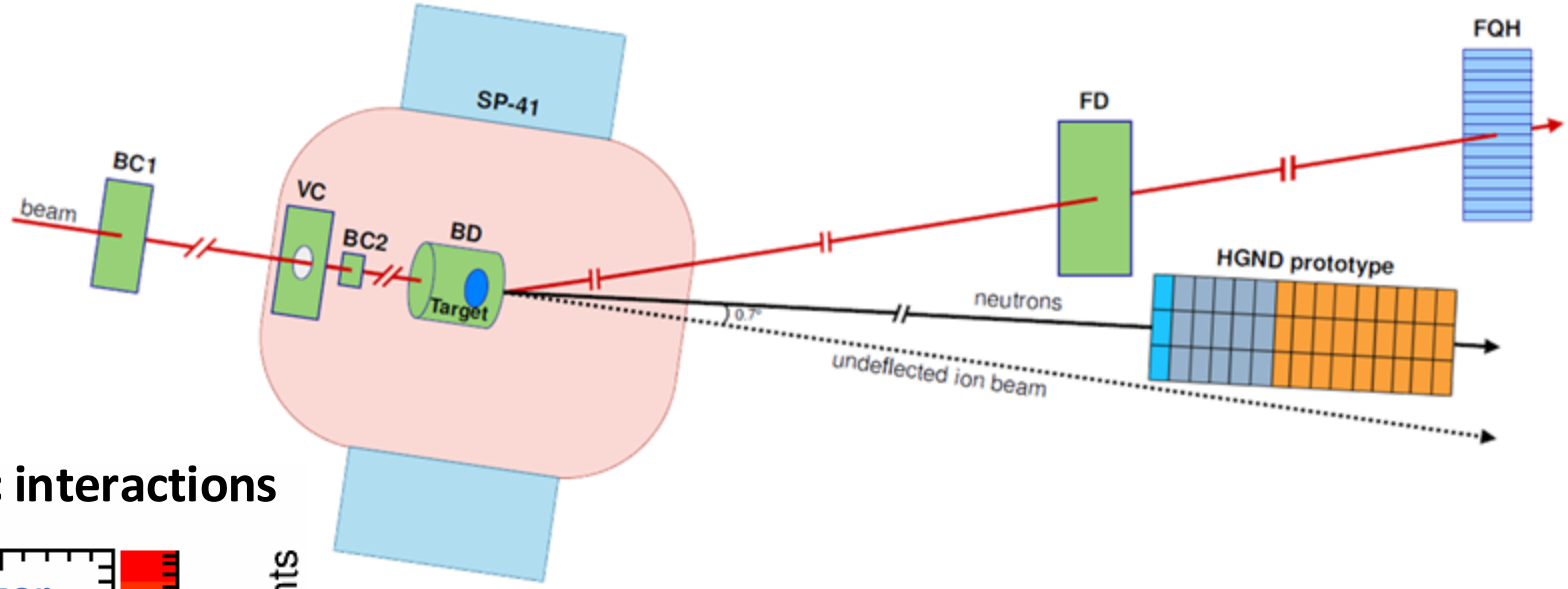


Only single Xe ion in target

Ultra-peripheral collisions – EMD

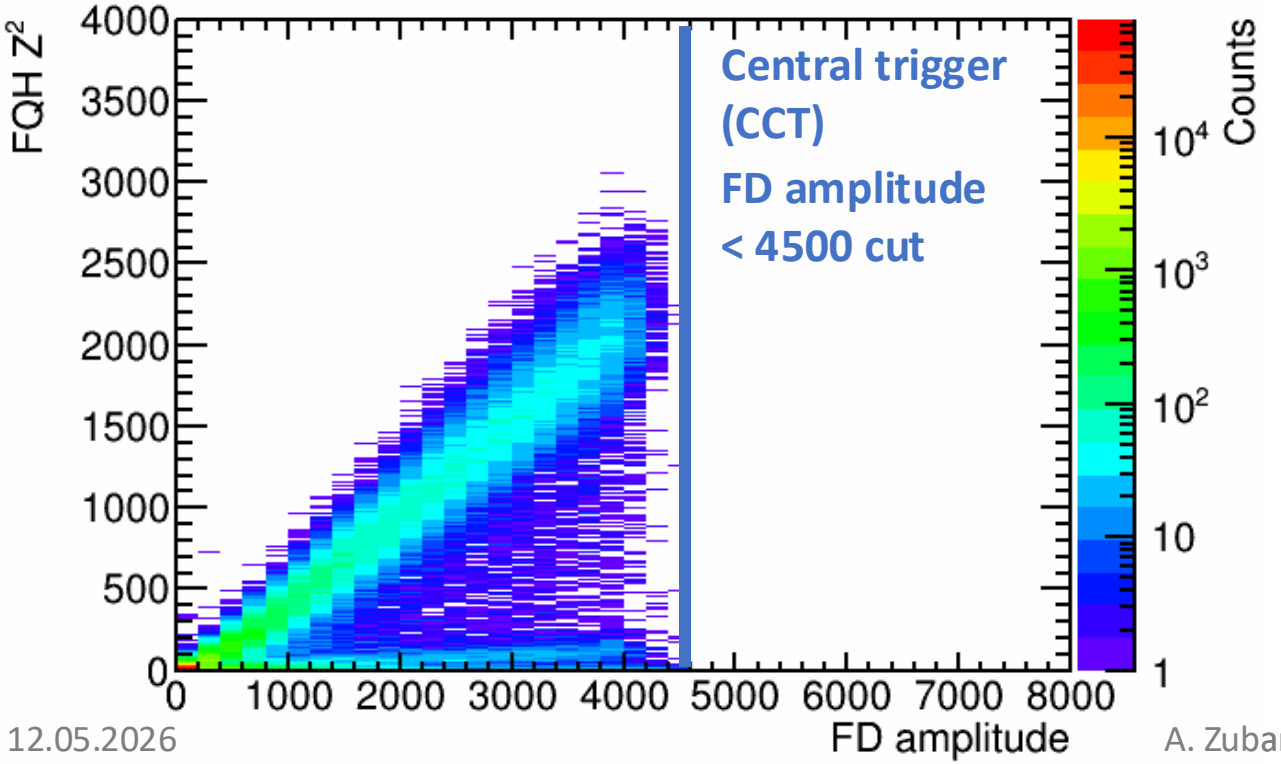


Selection of hadronic fragmentation events in measurements



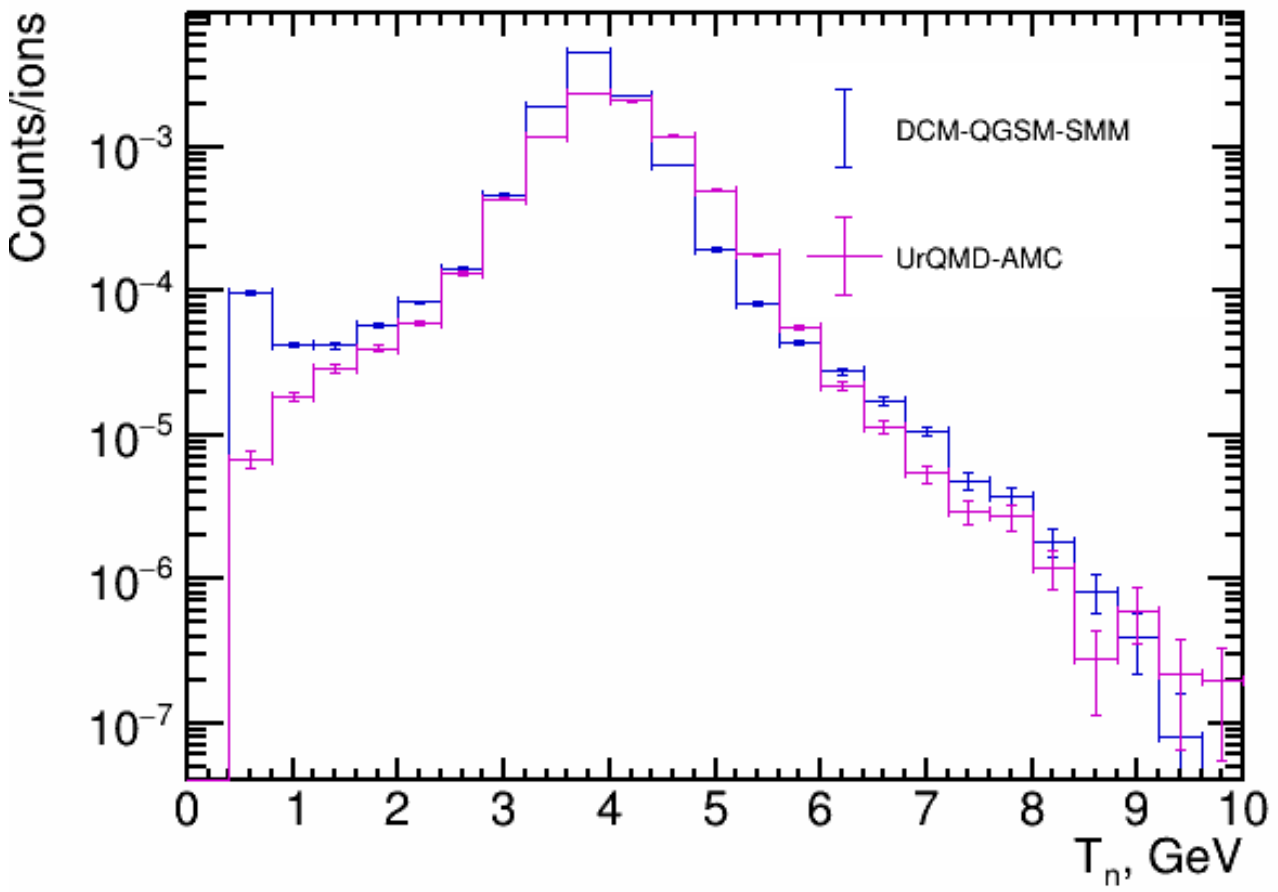
Only single Xe ion in target

Central & semi-central collisions – hadronic interactions

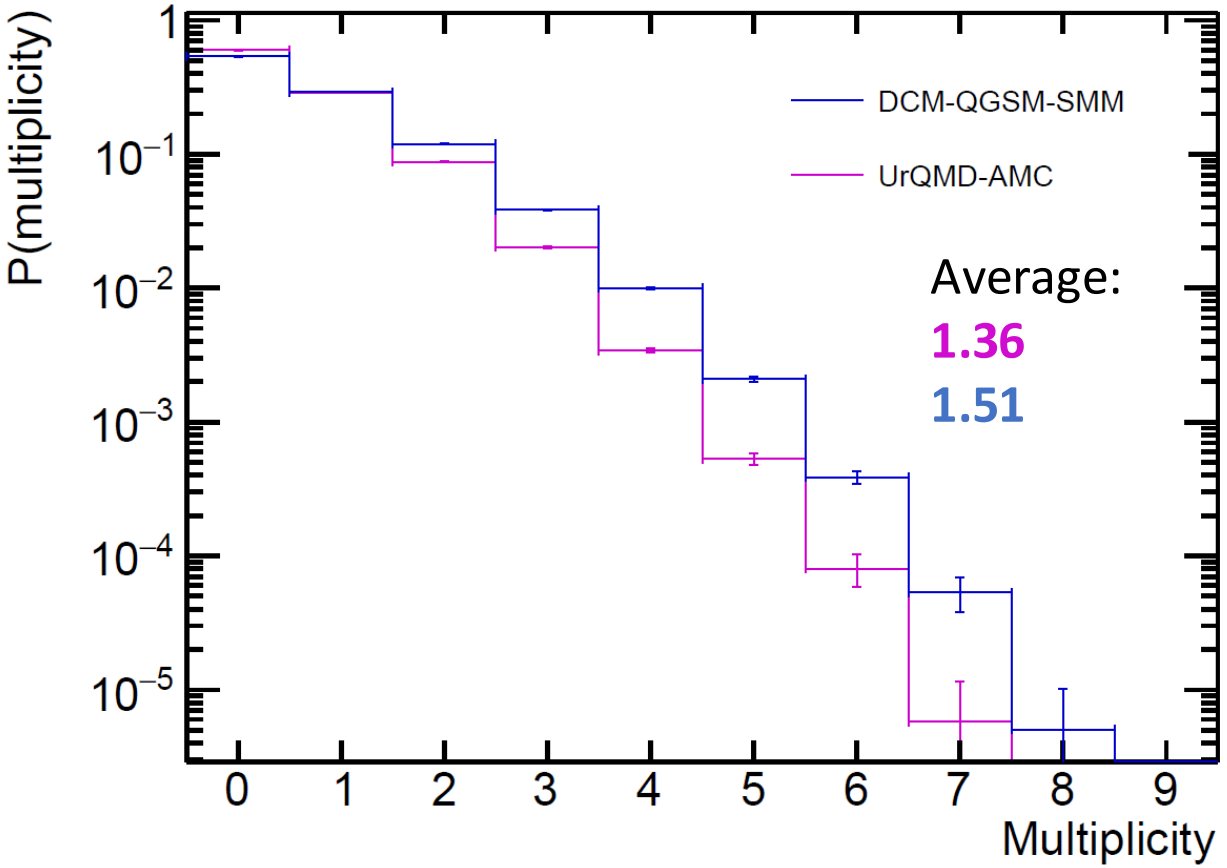


Spectator neutrons in acceptance of the HGND prototype

Neutron kinetic energy in acceptance of the HGND prototype



Neutron multiplicity in acceptance of the HGND prototype



Trigger efficiency correction from experimental data was applied for all histograms.

HGND prototype efficiency

$$\Omega_n = \frac{N_{hit}}{N_{gen}} \qquad \varepsilon_n = \frac{N_{rec}}{N_{hit}}$$

Model	Ω_n, %	ε_n, %	Ω_n x ε_n, %
RELDIS	34.21 ± 0.25	60.06 ± 0.44	20.55 ± 0.21
DCM-QGSM-SMM	3.87 ± 0.02	37.33 ± 0.17	1.45 ± 0.01
UrQMD-AMC	2.63 ± 0.01	45.09 ± 0.25	1.19 ± 0.01

Cross-section estimation using different models

$$\sigma = \frac{N_{ev} \cdot \langle N_n \rangle}{N_{ions}} \cdot \frac{A}{d \cdot N_A \cdot \rho} \cdot \left(\Omega_n \times \varepsilon_n\right)$$

$d = 0.175\,cm$

$N_A = 6.02 \cdot 10^{23}\,mol^{-1}$

$\rho = 4.53\,g/cm^3$

	RELDIS	DCM-QGSM-SMM	UrQMD-AMC
$Y = N_{ev}/N_{ions}$, $neutrons/ion$	$(1.49 \pm 0.12) \cdot 10^{-3}$	$(3.78 \pm 0.02) \cdot 10^{-3}$	
$N_{ev} \cdot \langle N_n \rangle / N_{ions} \cdot (\Omega_n \times \varepsilon_n)$	$(6.92 \pm 0.57_{stat} \pm 0.17_{syst}) \cdot 10^{-3}$	$(16.31 \pm 0.10_{stat} \pm 1.31_{syst}) \cdot 10^{-3}$	$(17.98 \pm 0.13_{stat} \pm 0.60_{syst}) \cdot 10^{-3}$
σ^{exp}	$1.88 \pm 0.16_{stat} \pm 0.05_{syst}$ b	$4.44 \pm 0.03_{stat} \pm 0.36_{syst}$ b	$4.90 \pm 0.03_{stat} \pm 0.16_{syst}$ b
σ^{sim}	1.89±0.02 b	4.76±0.01 b	4.89±0.01 b

Preliminary estimations are in good agreement within the errors with the modeling predictions.

Approach to cross-section estimation

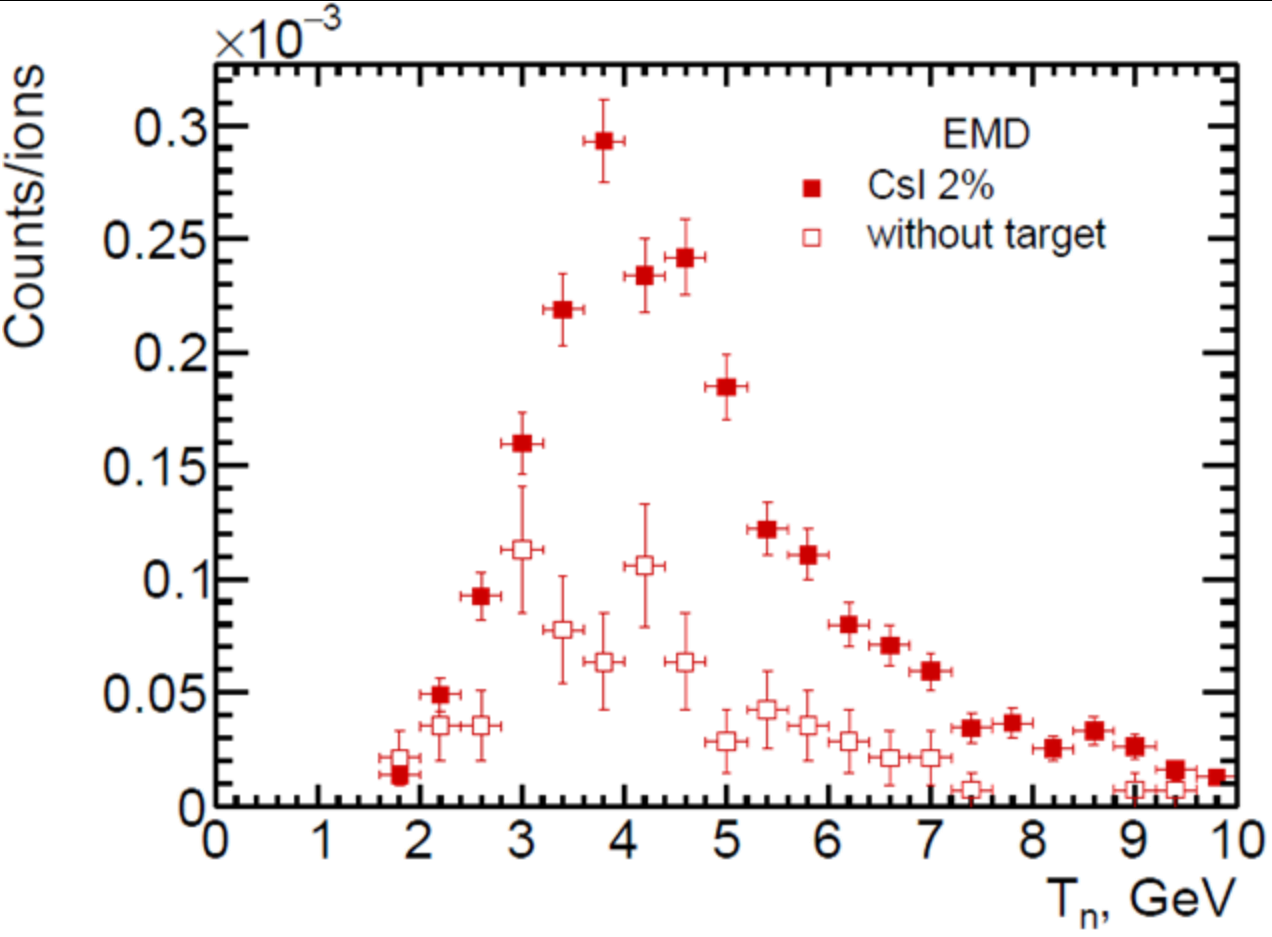
$$d = 0.175\ cm$$
$$N_A = 6.02 \cdot 10^{23} mol^{-1}$$
$$\rho = 4.53\ g/cm^3$$

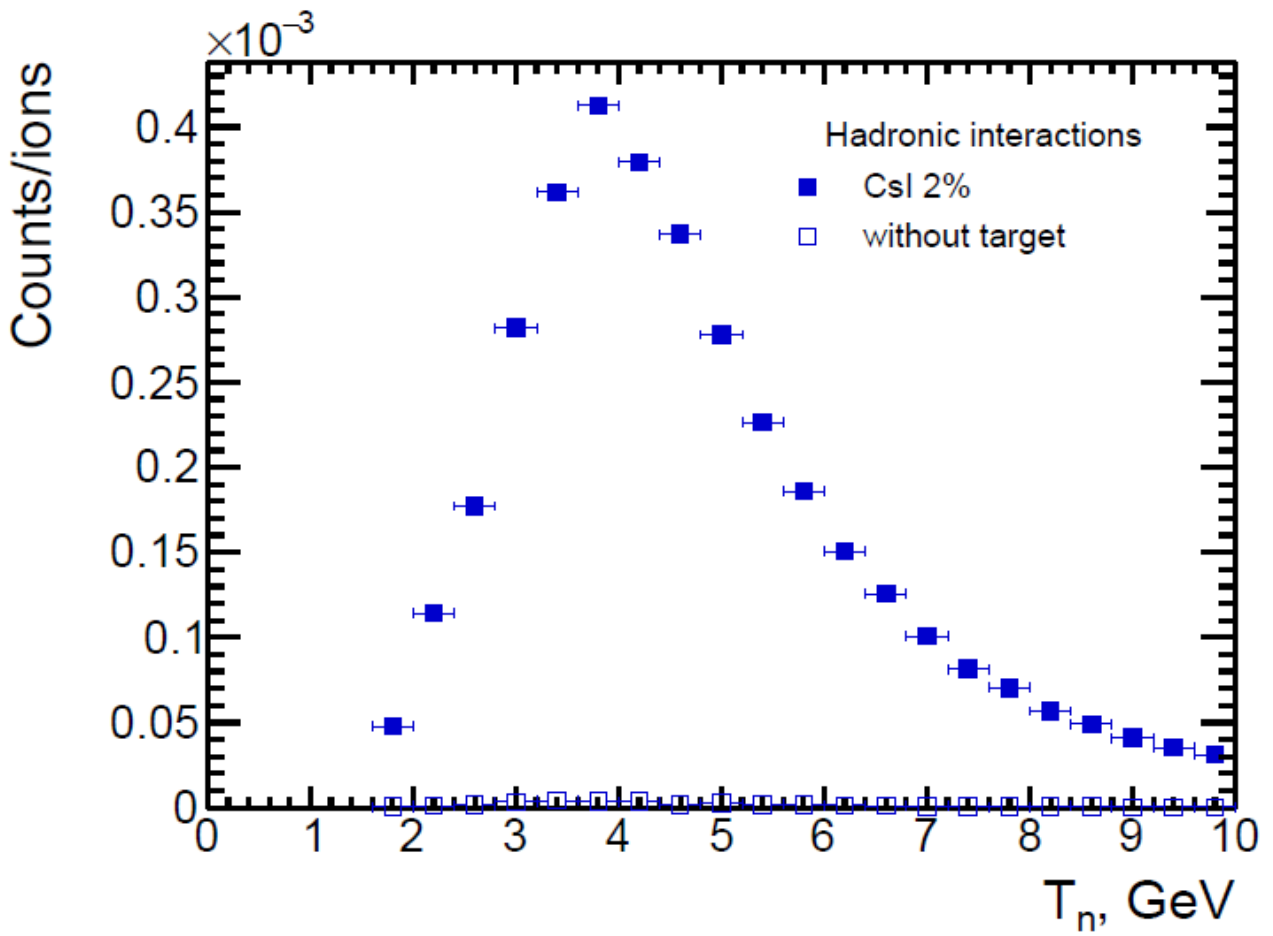
$$\sigma = \frac{N_{ev}}{N_{ions}} \cdot \frac{A}{d \cdot N_A \cdot \rho} \cdot \langle N_n \rangle \cdot (\Omega_n \times \varepsilon_n) = Y_{corr} \cdot \frac{A}{d \cdot N_A \cdot \rho}$$

	RELDIS	DCM-QGSM-SMM	UrQMD-AMC
σ_{exp}, b	$1.88 \pm 0.16_{stat} \pm 0.05_{syst}$	$4.44 \pm 0.03_{stat} \pm 0.36_{syst}$ b	$4.90 \pm 0.03_{stat} \pm 0.16_{syst}$ b
σ_{sim}, b	1.89±0.02 b	4.76±0.01 b	4.89±0.01 b

Estimations are in good agreement within the errors with the modeling predictions.

Reconstructed spectra for EMD and hadronic interactions

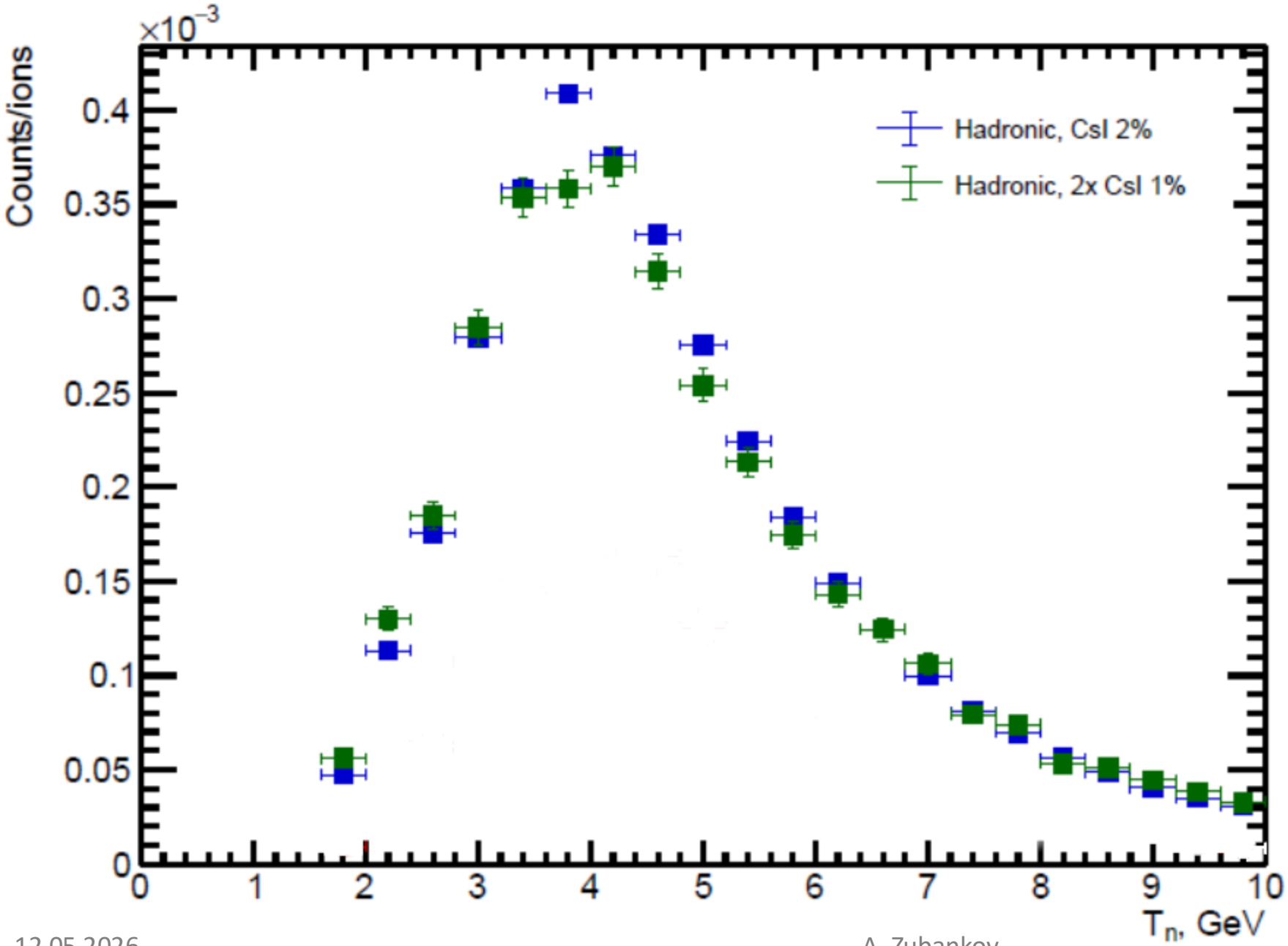




Reconstructed spectra were obtained both for runs with CsI 2% target and without it to estimate fraction of out of target interactions.

Empty target spectra were subtracted from target spectra.

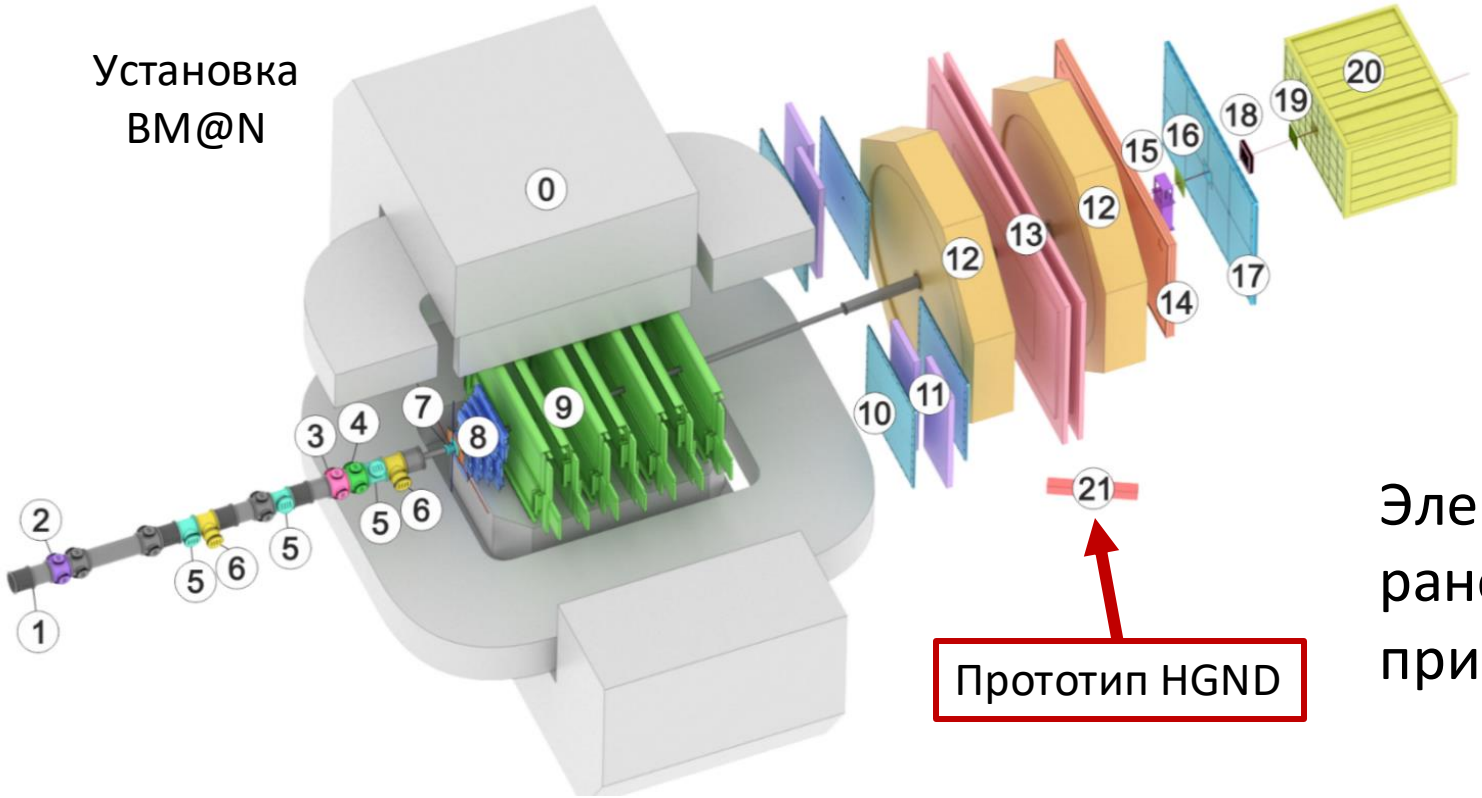
Comparison with thinner target



Corrected spectra after subtracting empty target spectra

Measurements with 1% and 2% target are consistent

Прототип HGND



Для проверки концепции полномасштабного HGND был протестирован **прототип HGND** в реакции ^{124}Xe+CsI при энергии пучка 3.8A ГэВ в эксперименте BM@N.

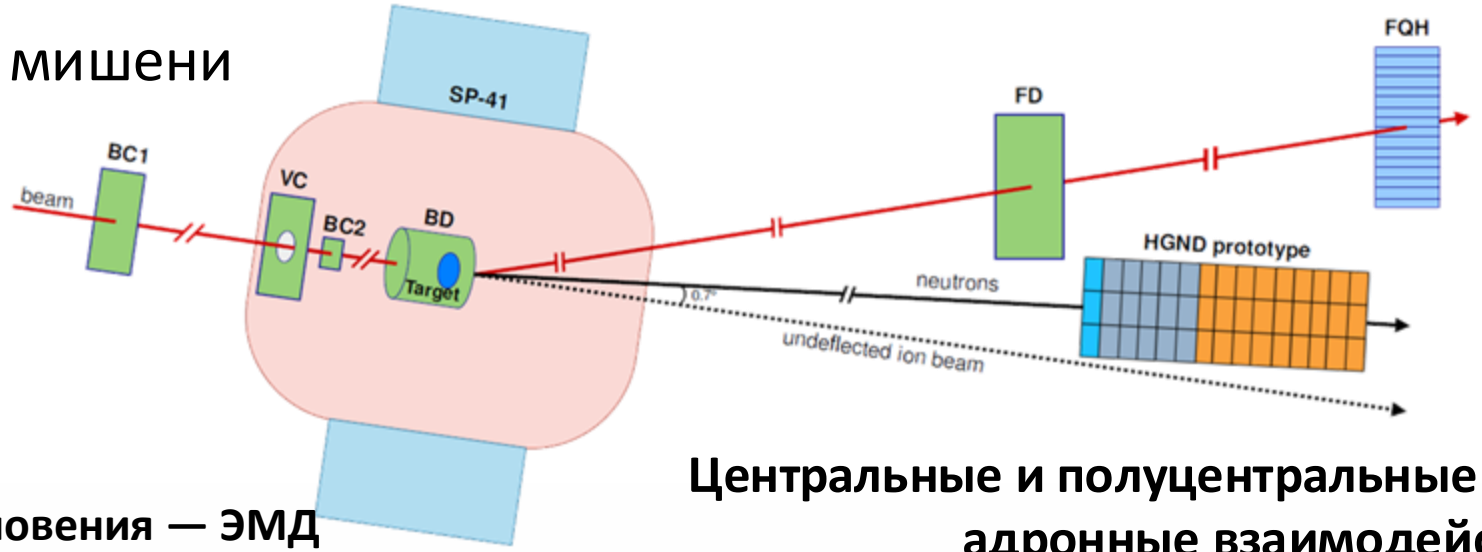
Электромагнитная диссоциация (ЭМД) ранее не изучалась в столкновениях Xe при энергиях 2–4A ГэВ.

Прототип HGND может быть использован для изучения нейтронов из ультрапериферических столкновений и нейтронов-спектаторов на пучках из Нуклотрона.

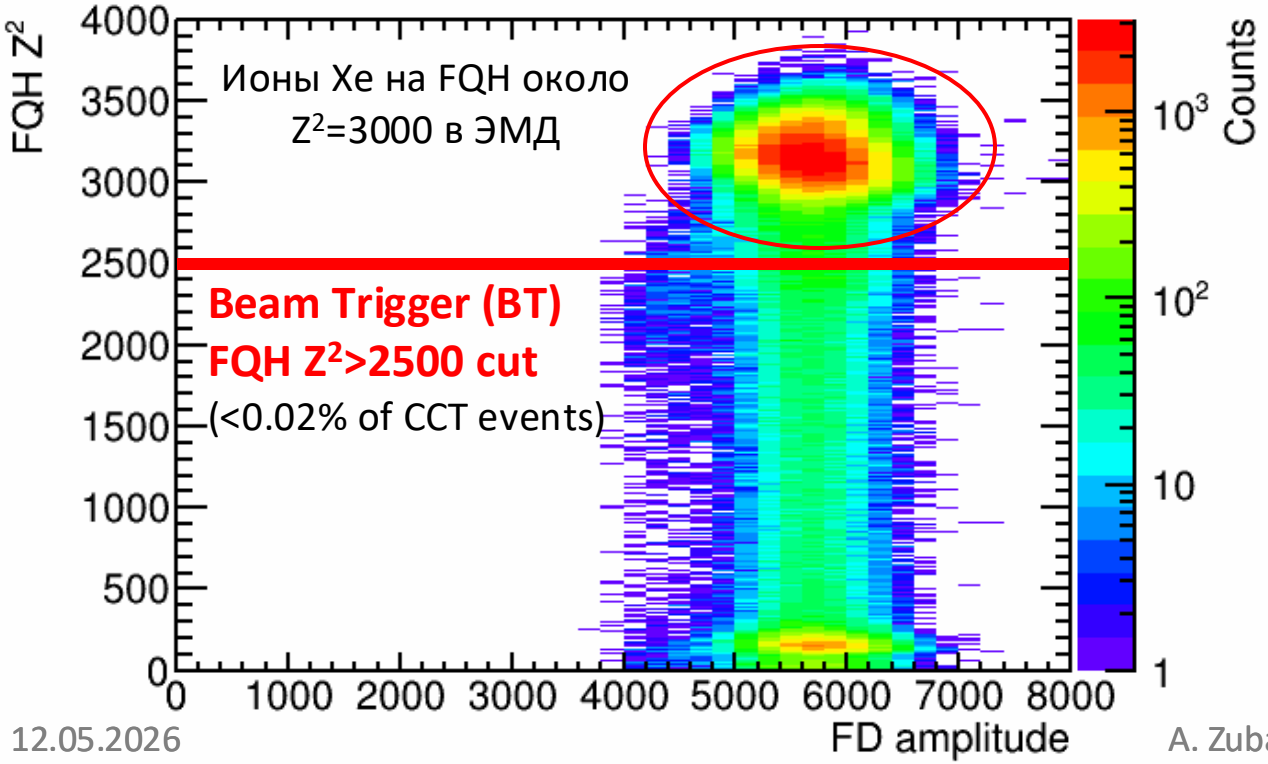
Измерены **выходы нейтронов** с помощью прототипа HGND с модельно-оцененной эффективностью для центральных и полуцентральных столкновений, а также для ЭМД ^{124}Xe.

Отбор событий ЭМД и адронных взаимодействий

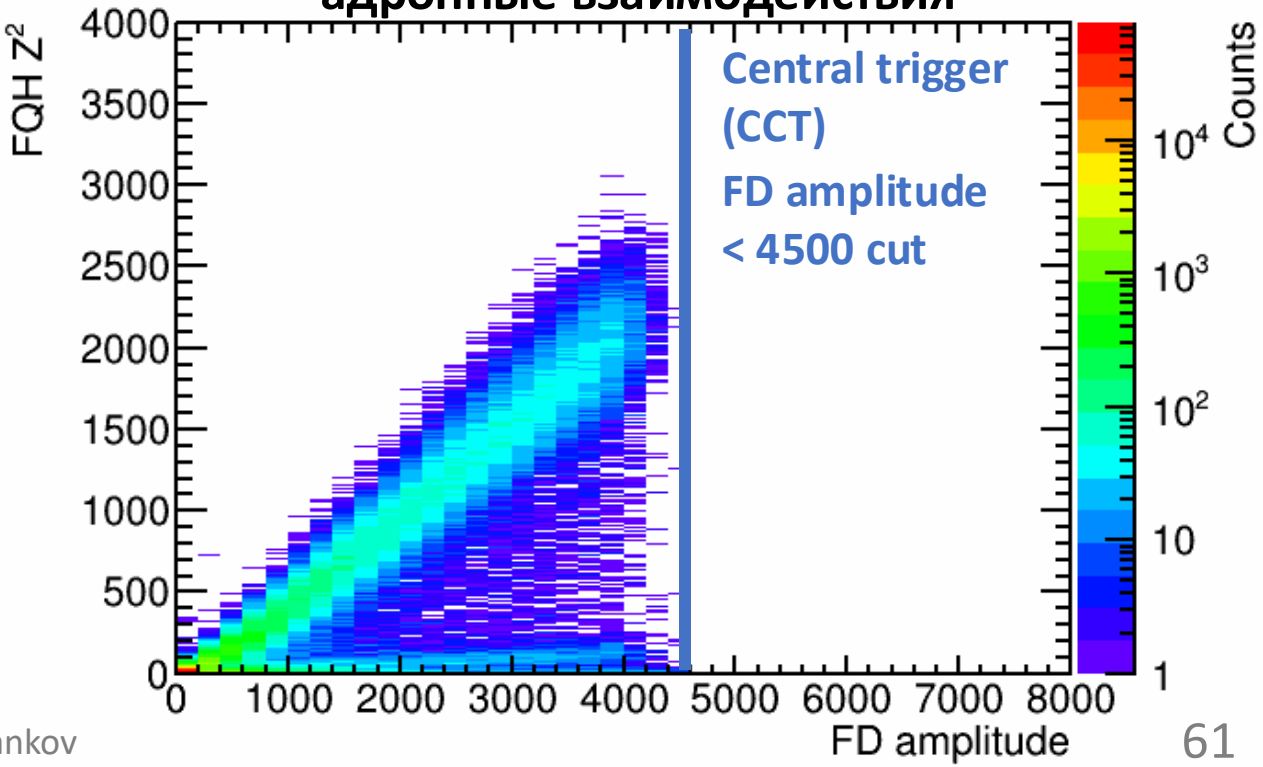
Только один ион Xe на мишени



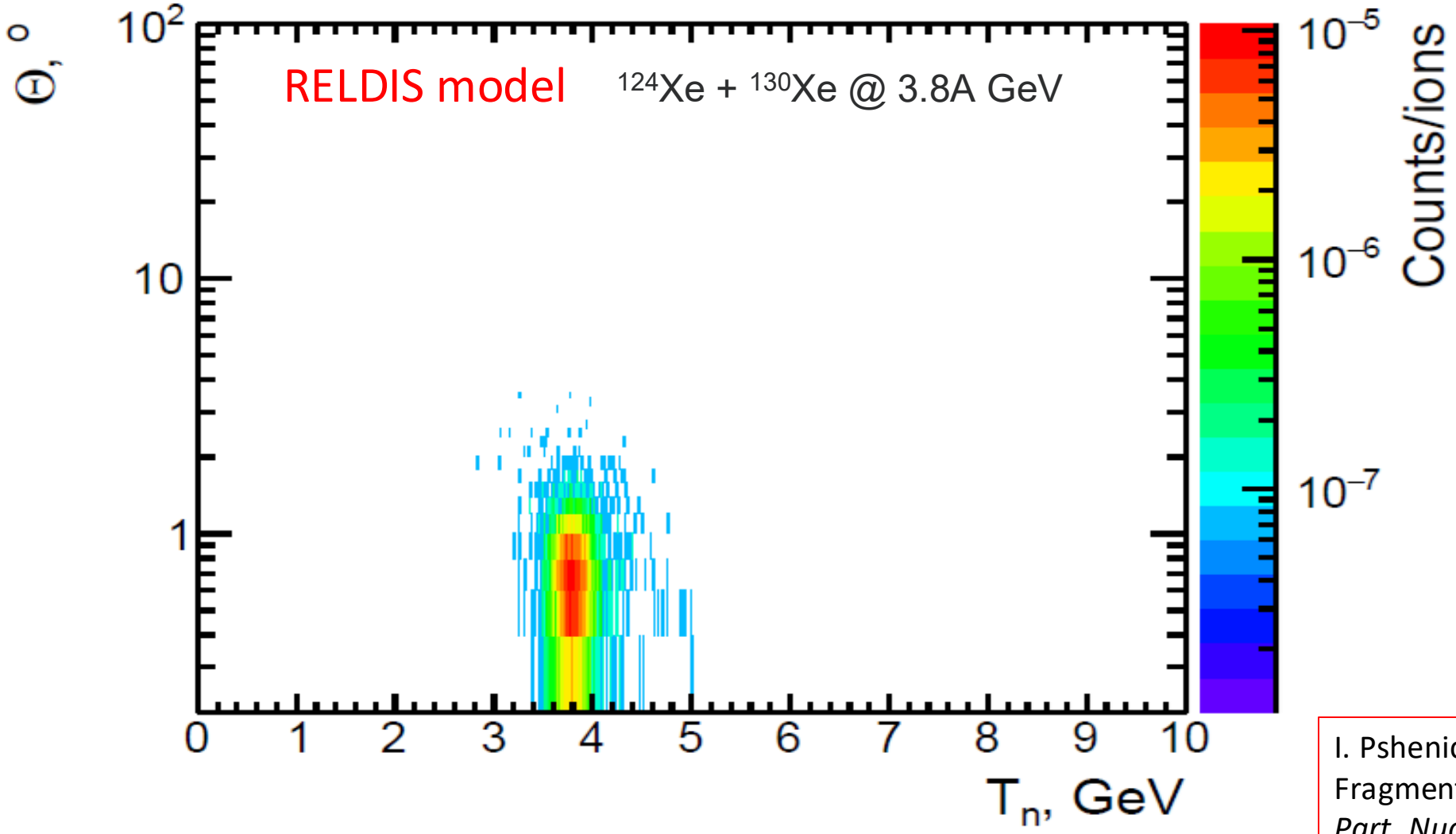
Ультраперифирические столкновения — ЭМД



Центральные и полуцентральные столкновения — адронные взаимодействия



Симуляция ЭМД с помощью RELDIS



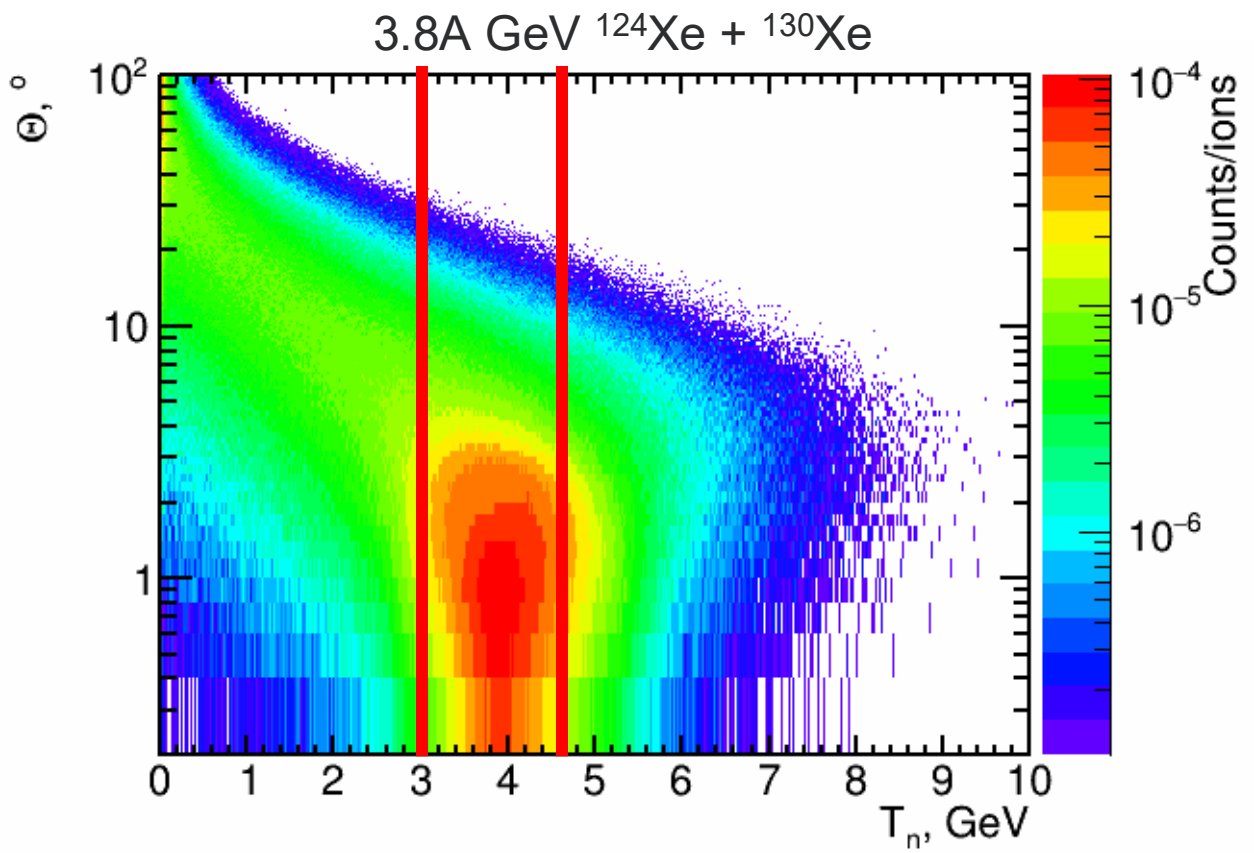
I. Pshenichnov, Electromagnetic Excitation and Fragmentation of Ultrarelativistic Nuclei. *Phys. Part. Nucl.* **2011**, 42 (2), 215-250.

Средняя множественность нейтронов– **1.05**

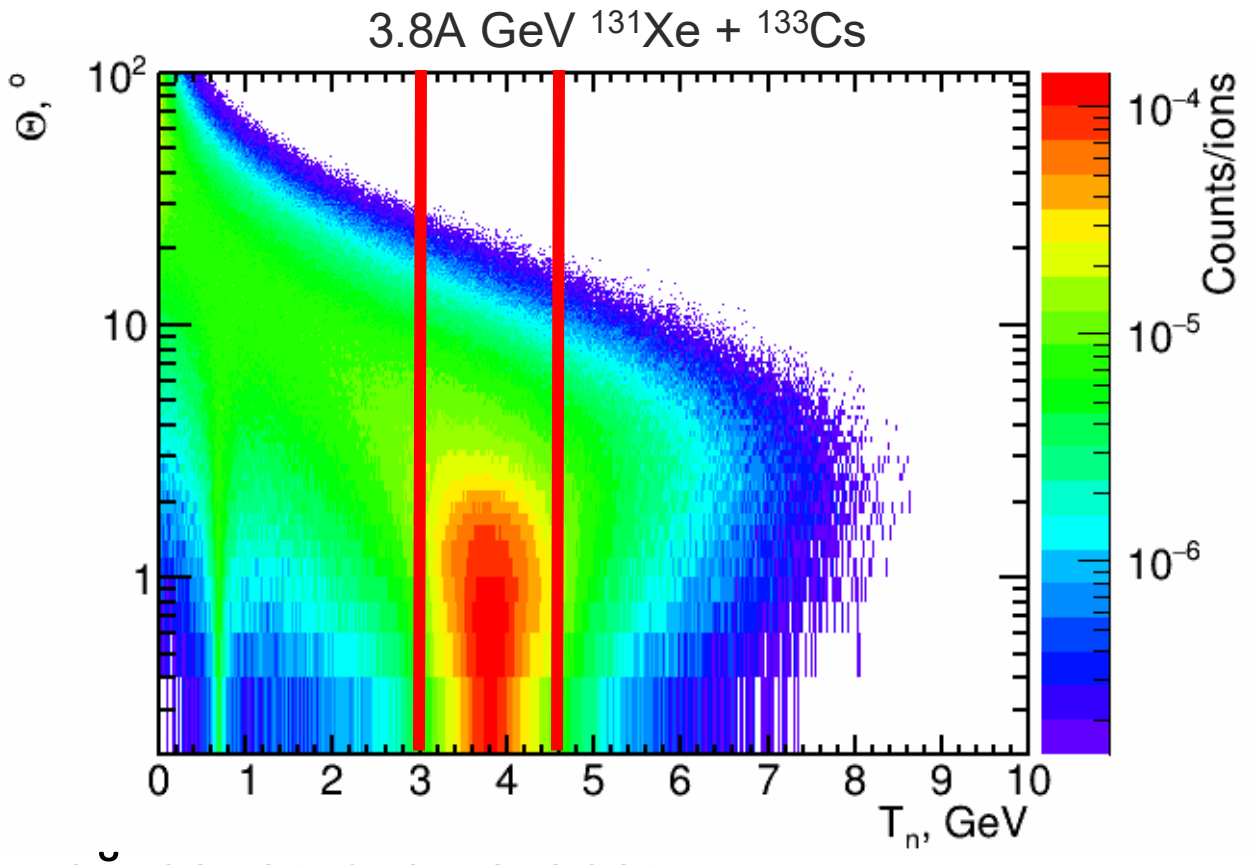
Средняя множественность нейтронов в акцептансе прототипа HGND – **1.02**

UrQMD-AMC vs DCM-QGSM-SMM

UrQMD-AMC (in Cascade mode)



DCM-QGSM-SMM



Средняя множественность нейтронов-спектаторов:

17.70 **16.01**

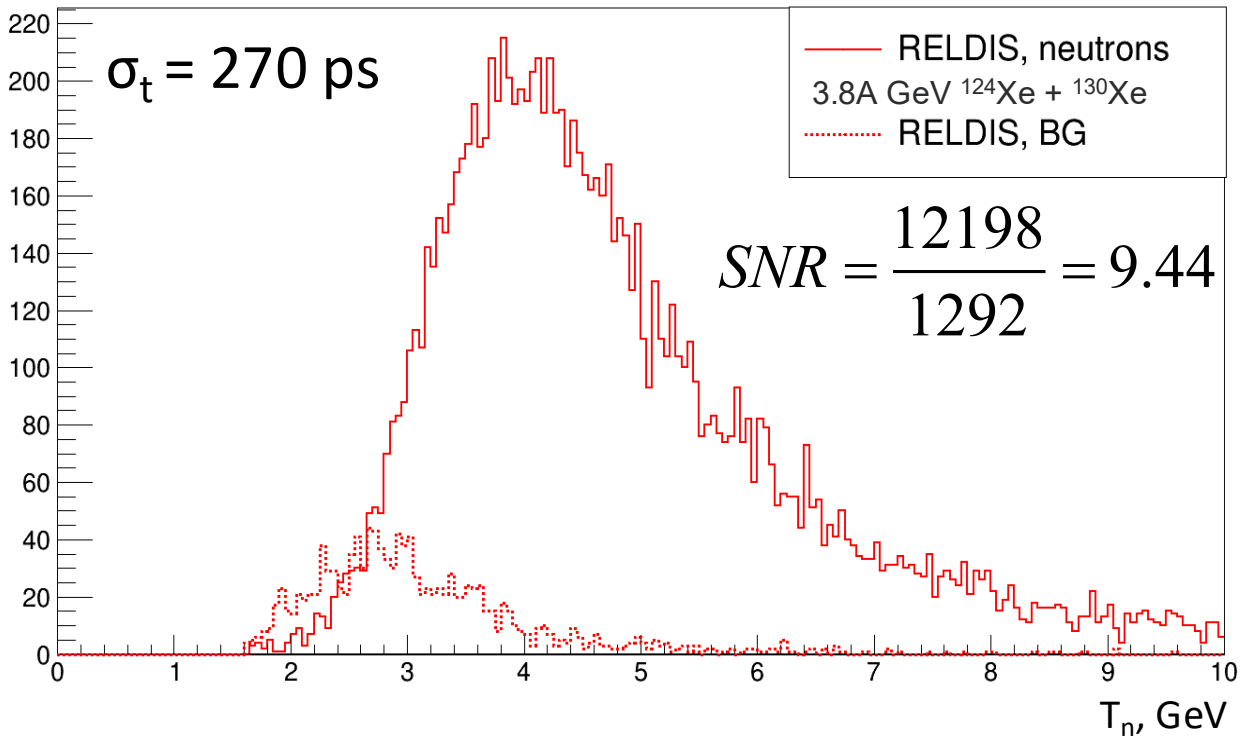
Средняя множественность нейтронов в акцептансе прототипа HGND:

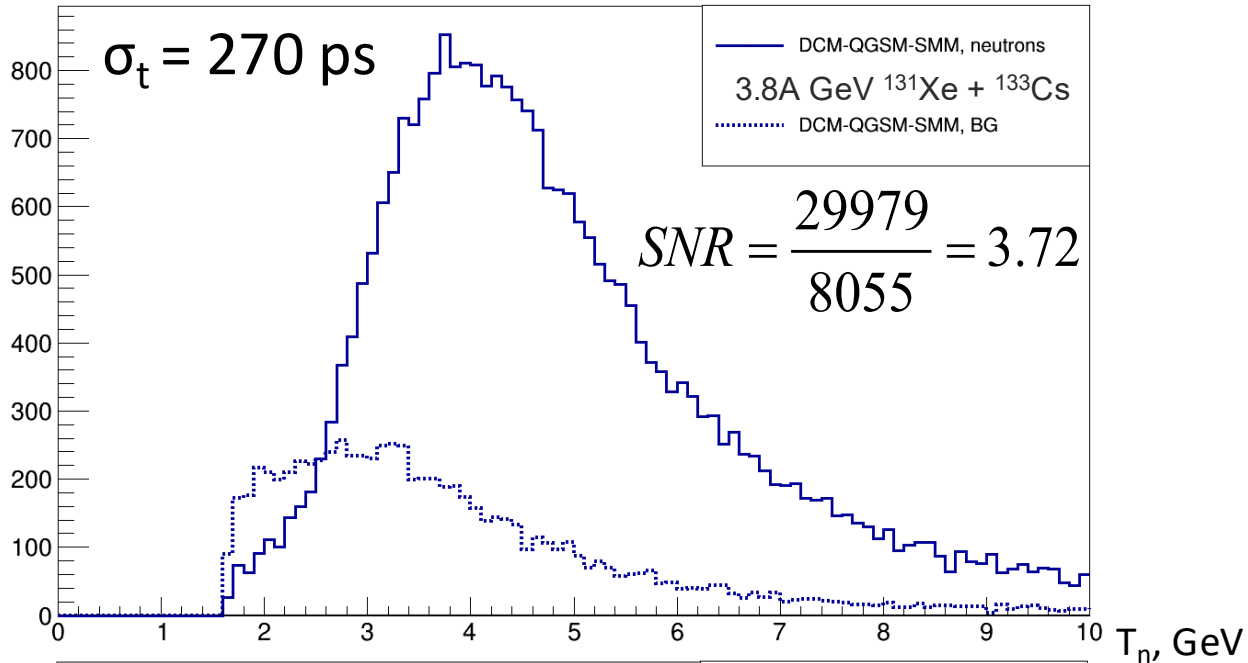
1.36 **1.51**

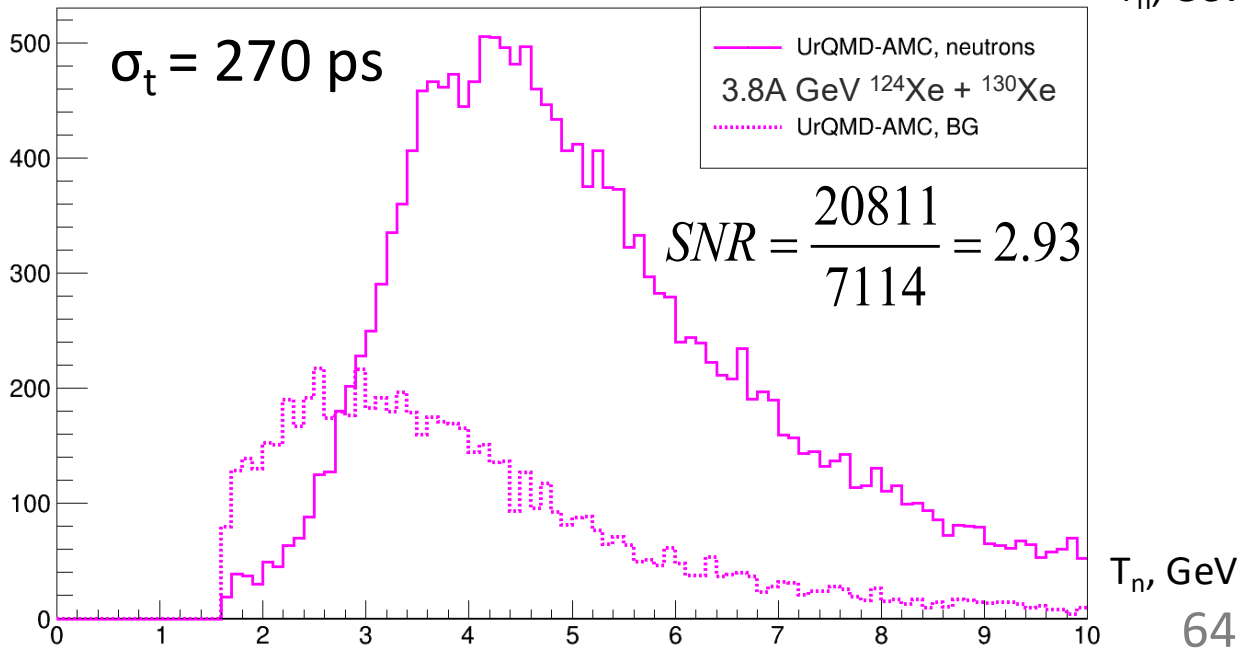
A.O. Svetlichnyi et al., Production of spectator neutrons, protons and light fragments on fixed targets at NICA. ArXiv:2510.02992v2 [Nucl-Th], **2025** 1–15.

M. Baznat et al., Monte-Carlo Generator of Heavy Ion Collisions DCM-SMM, *Phys. Part. Nucl. Lett.* **2020**, 17, 303.

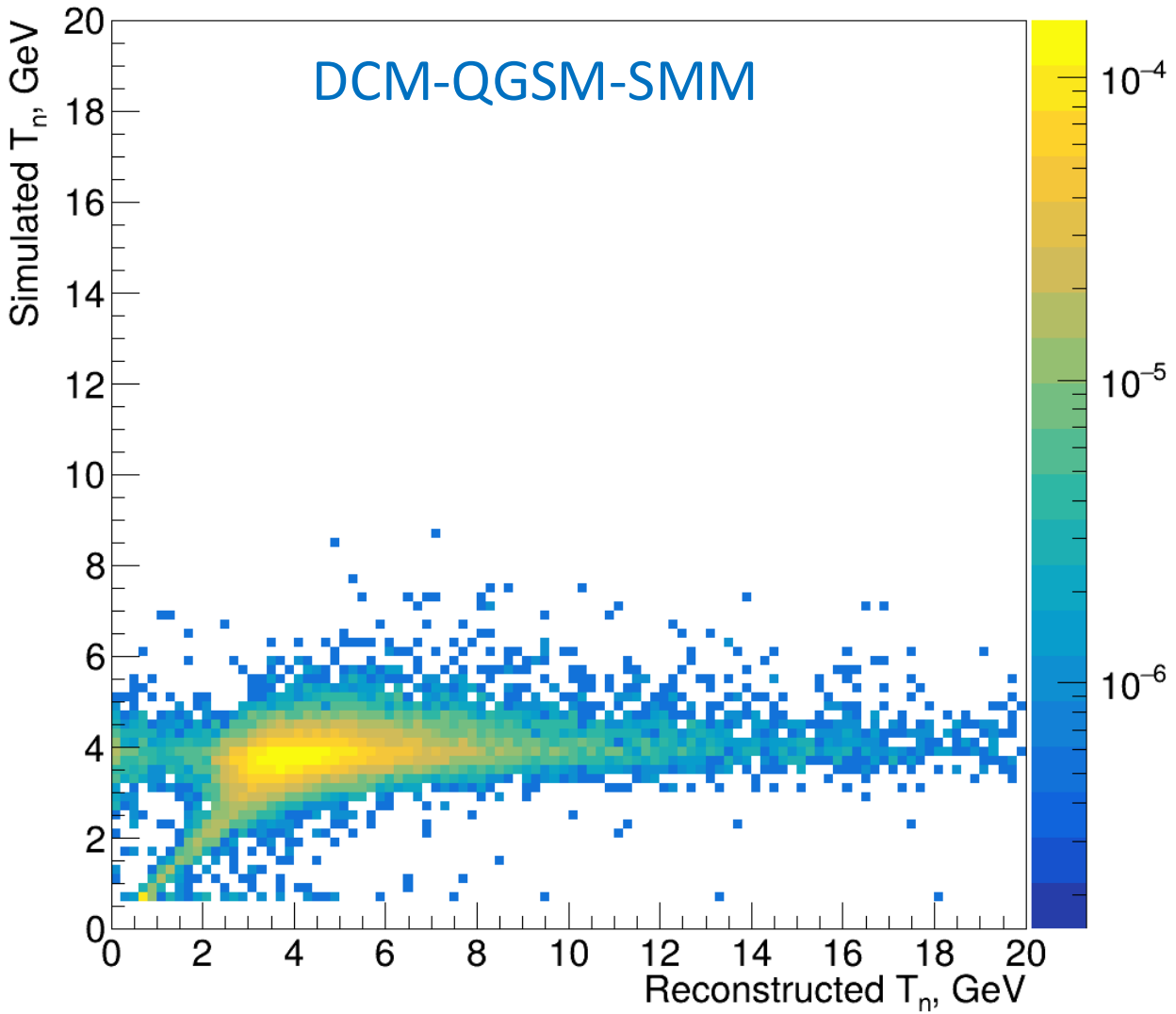
Background in simulation

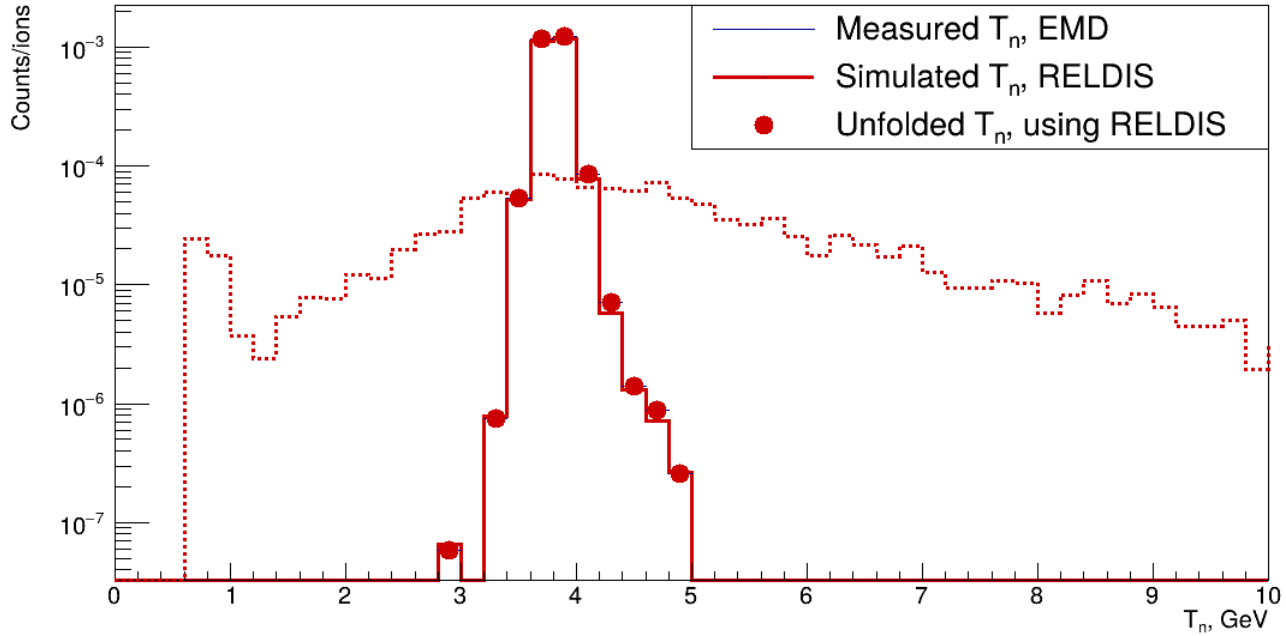


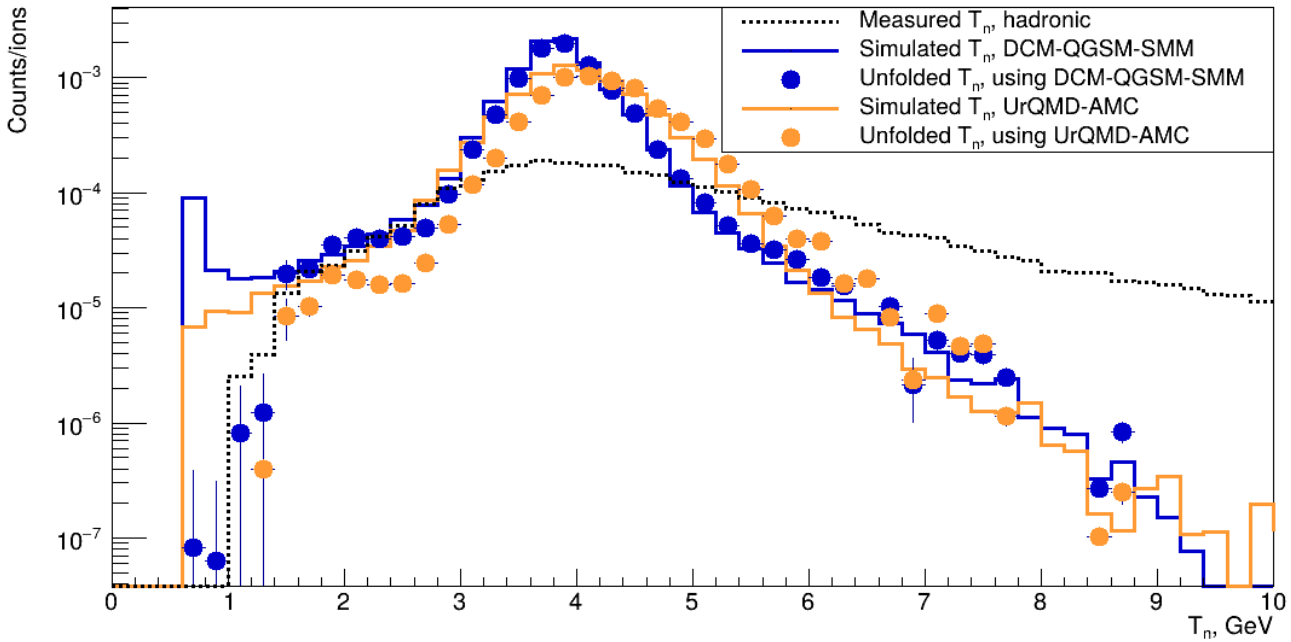




Unfolding using the response from DCM-QGSM-SMM for all

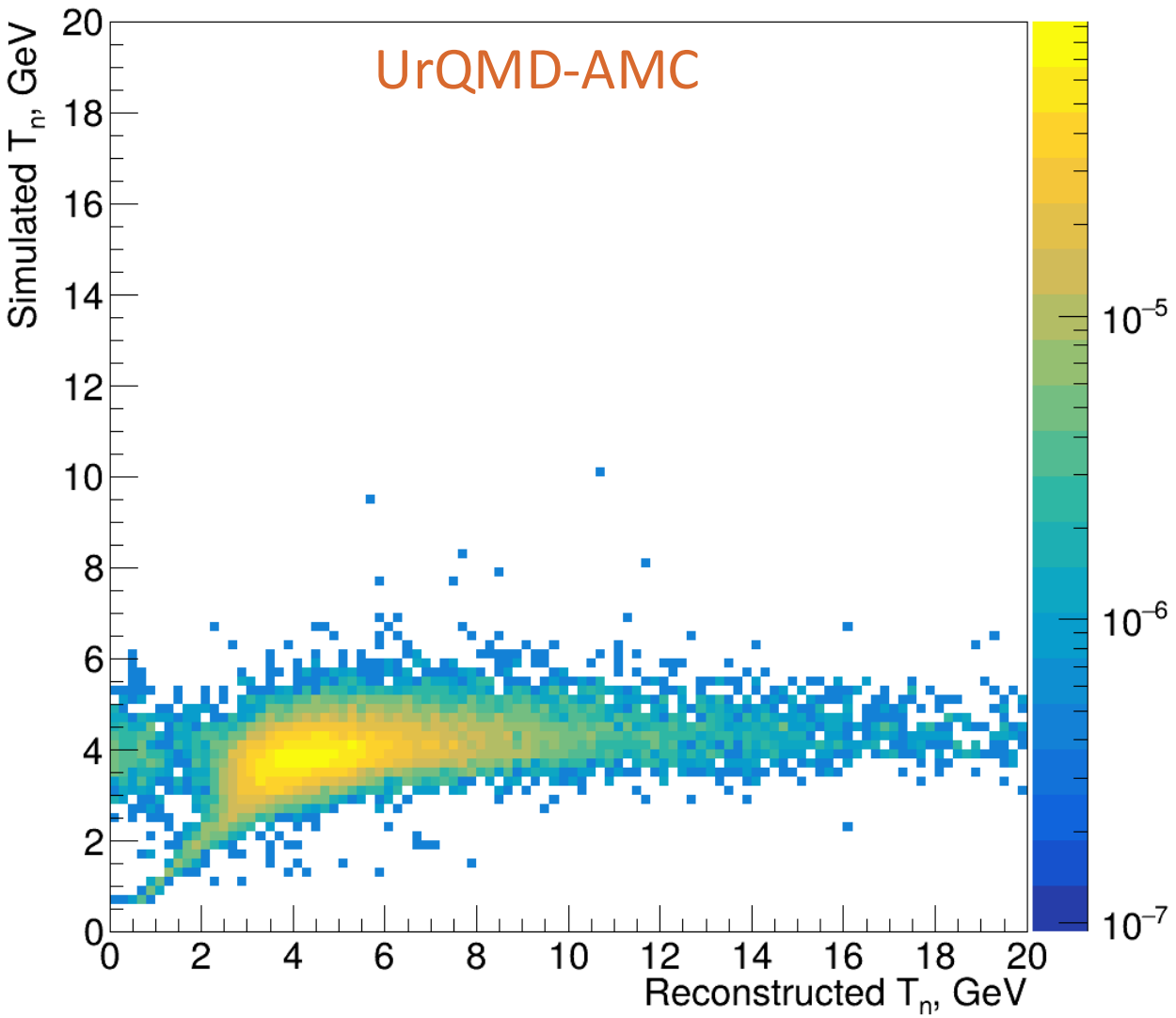


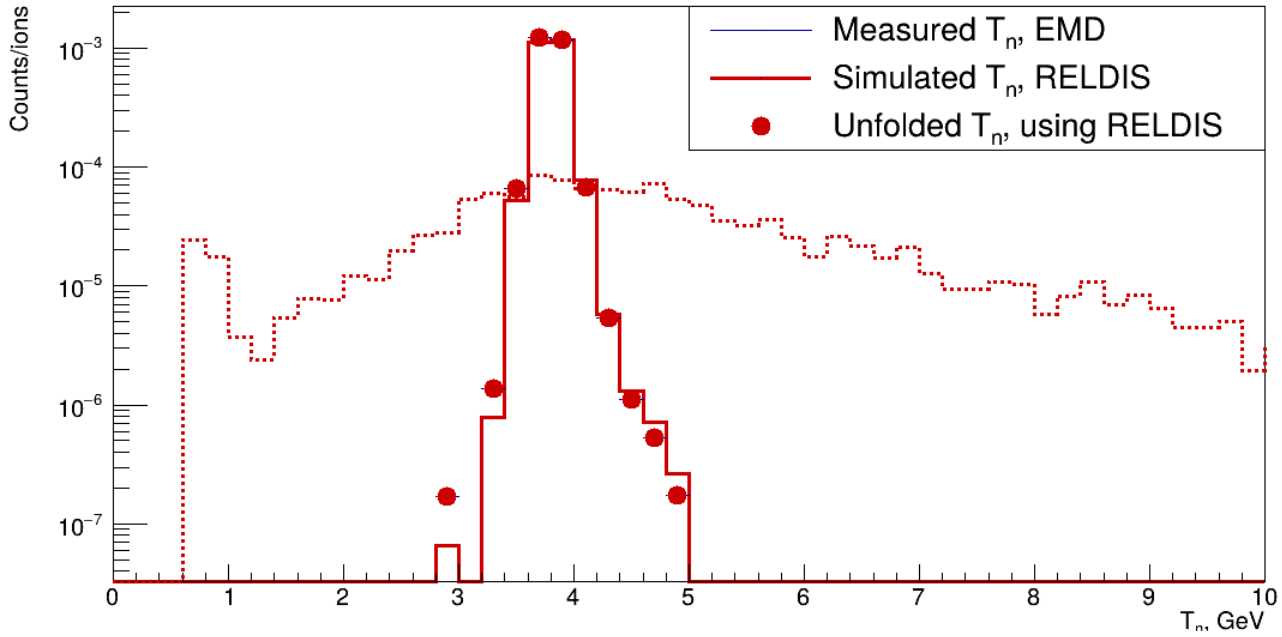


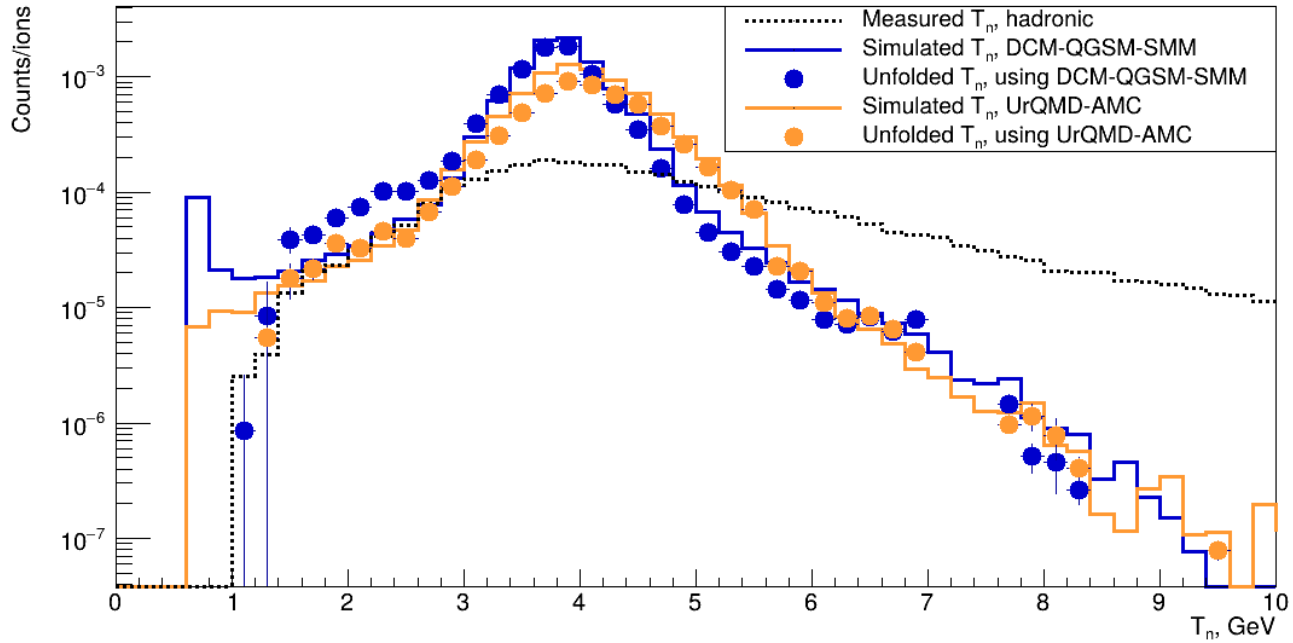


We can use the response matrix from other models with minor distortions.

Unfolding using the response from UrQMD-AMC for all



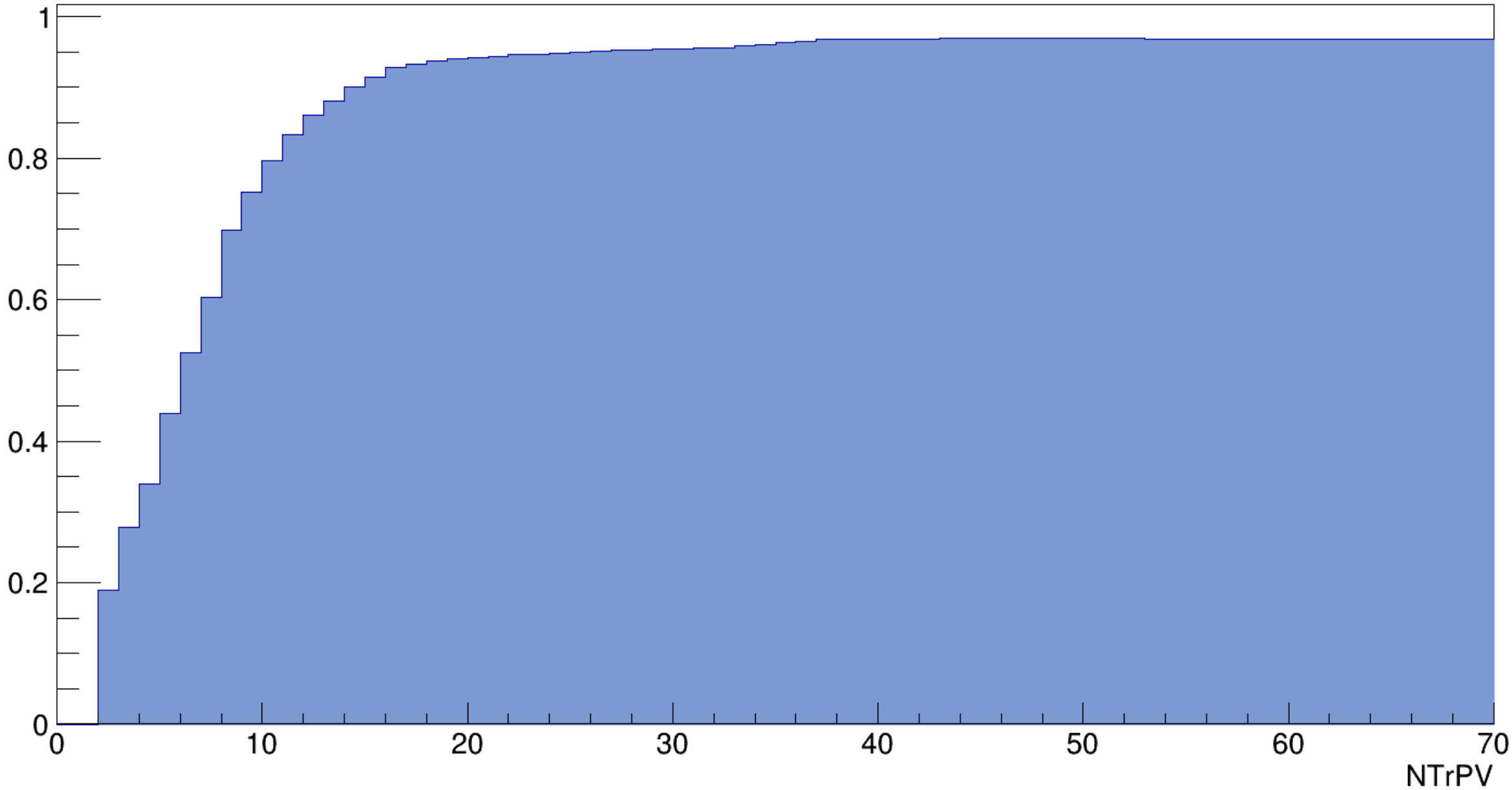




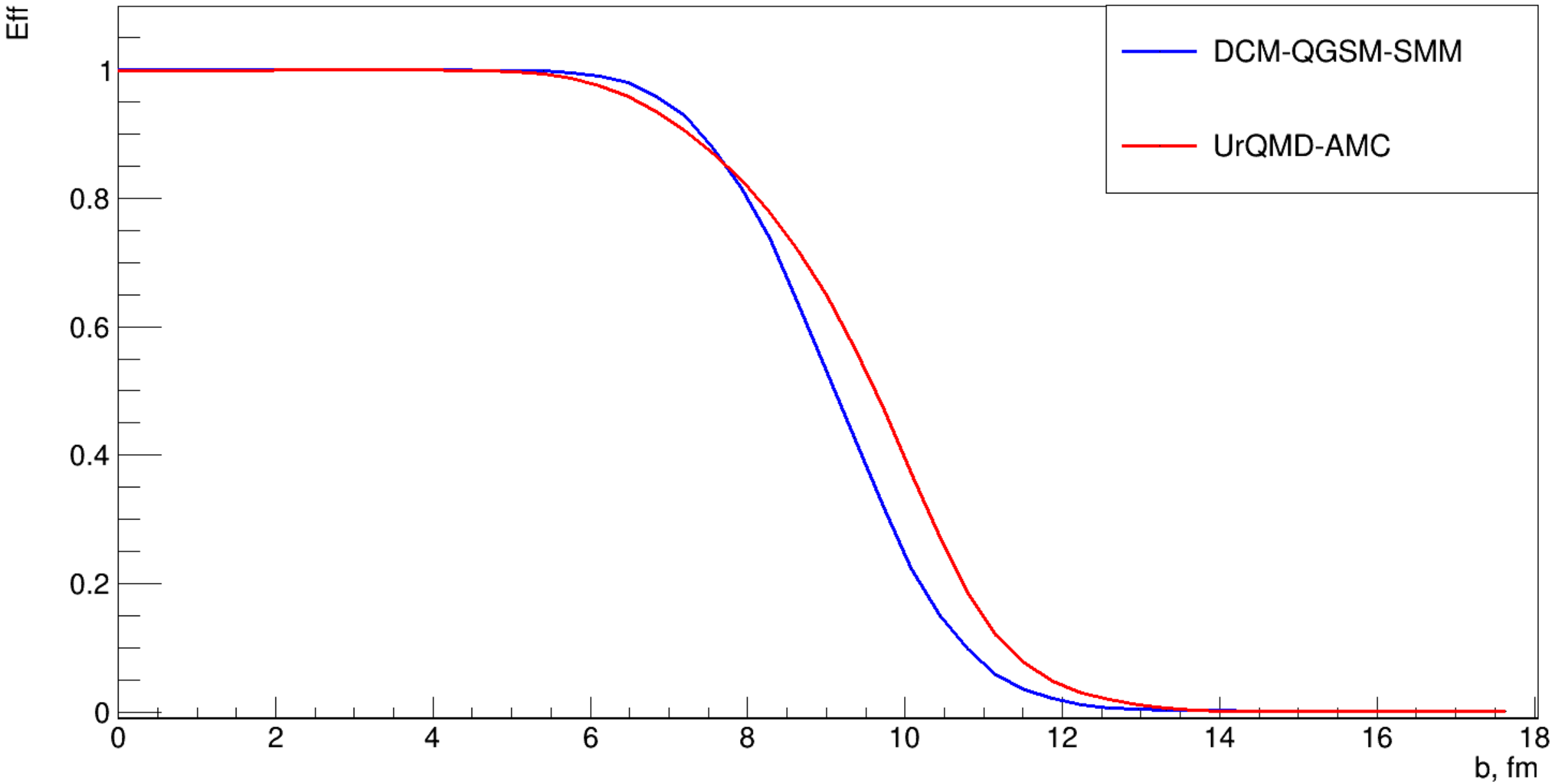
We can use the response matrix from other models with minor distortions.

Trigger efficiency

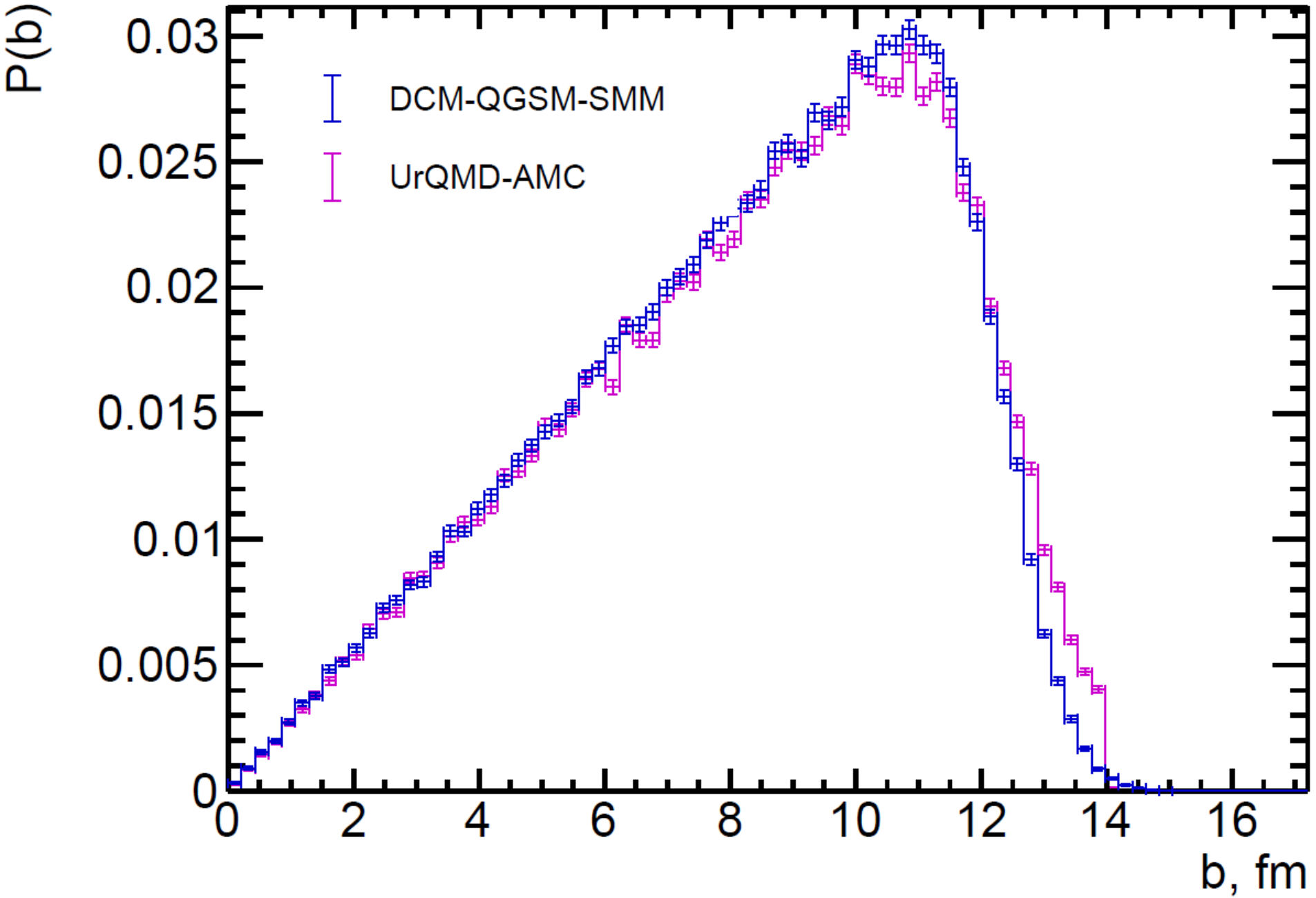
Trigger efficiency by V. Plotnikov



Trigger efficiency by D. Idrisov



Impact parameter distribution



Cross-section estimation

$$\begin{cases} P(d) = \dfrac{N_{ev} \cdot \langle N_n \rangle}{N_{ions}} \cdot (\Omega_n \times \varepsilon_n) \\ P(d) = 1 - \exp\left(-d/\lambda\right) \end{cases}$$

$$d = 0.175\,cm$$

$$N_A = 6.02 \cdot 10^{23}\ mol^{-1}$$

$$\rho = 4.53\,g/cm^3$$

$$\Omega_n = \frac{N_{hit}}{N_{gen}} \qquad \varepsilon_n = \frac{N_{rec}}{N_{hit}}$$

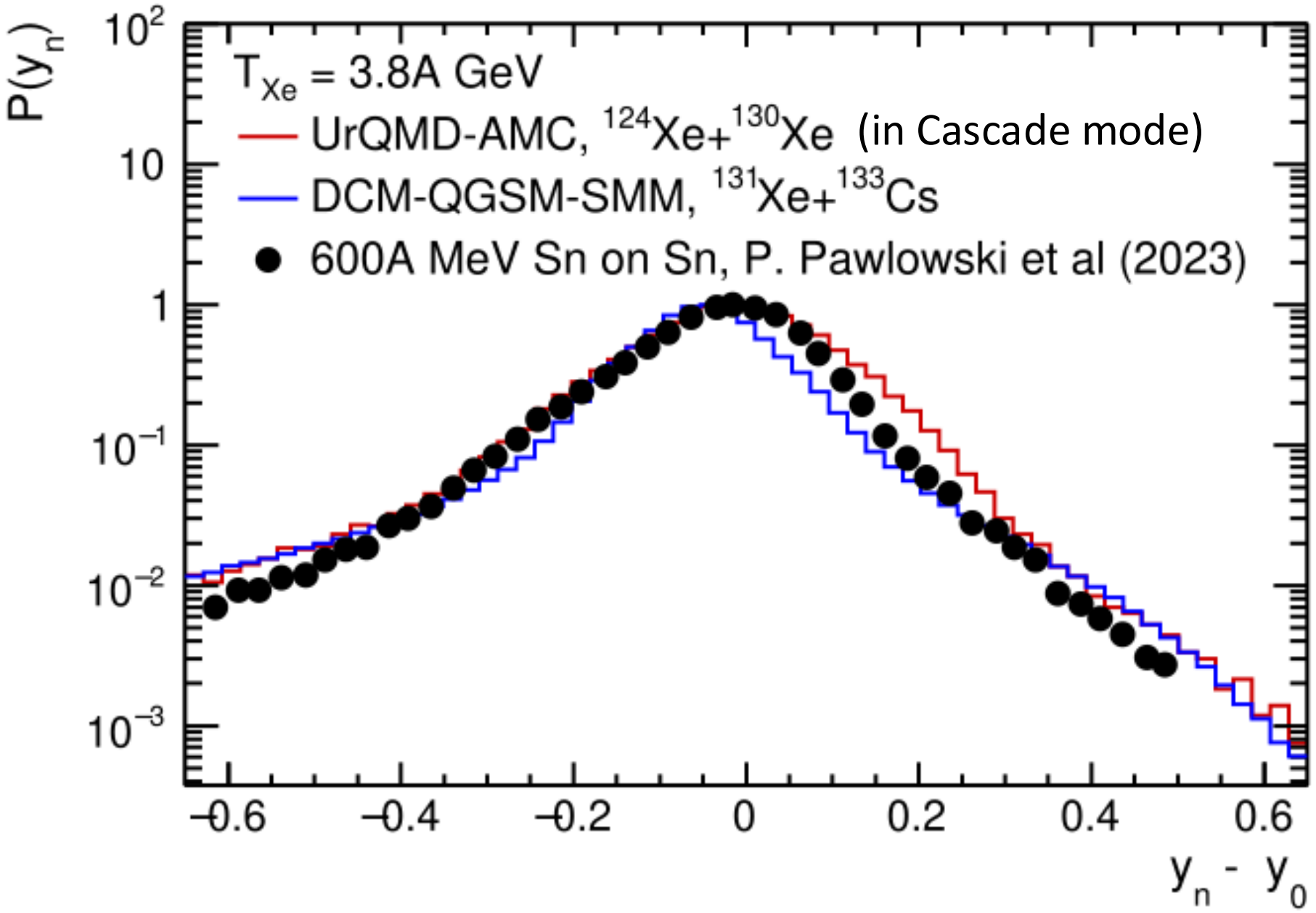
$d = \lambda$:

$$P(d) = \frac{d}{\lambda} = \frac{d \cdot N_A \cdot \rho \cdot \sigma}{A}$$

$$\sigma = \frac{N_{ev} \cdot \langle N_n \rangle}{N_{ions}} \cdot (\Omega_n \times \varepsilon_n) \cdot \frac{A}{d \cdot N_A \cdot \rho}$$

UrQMD-AMC

UrQMD-AMC vs DCM-QGSM-SMM



DCM-QGSM-SMM and UrQMD-AMC describe the experiment well in the rapidity region y_n-$y_0<0$.

In the region y_n-$y_0>0$, DCM-QGSM-SMM underestimates the data whereas UrQMD-AMC overestimates.

For DCM-QGSM-SMM, there is a shift in the rapidity relative to the beam rapidity.

Ablation Monte Carlo: decay code from AAMCC

- The excited nuclear fragments are formed by means of MST-clusterization algorithm after UrQMD
  - A few excited nuclear prefragments can be formed, in contrast with DCM-QGSM-SMM, where all the spectator nucleon remain bound in one prefragment.
- Excitation energy of prefragment is calculated by hybrid approximation: a combination of Ericson formula for peripheral collisions and ALADIN approximation otherwise[1)]
- Decays of prefragments are simulated as follows:
  - Fermi break-up model from Geant4 v9.2 [2)]
  - Statistical Multifragmentation Model (SMM) from Geant4 v10.4 [2)]
  - Weisskopf-Ewing evaporation model from Geant4 v10.4 [2)]
- They were validated and adjusted to describe the data[3)].

1) R. Nepeivoda, et al., Particles **5** (2022) 40
2) J. Alison et al. Nucl. Inst. A **835** (2016) 186
3) 55th Geant4 Techical Forum
https://indico.cern.ch/event/1106118/contributions/4693132/

Combining UrQMD and AAMCC

- AMC is developed to simulate secondary decays of spectator fragments created in other models, in particular UrQMD.
- It is assumed that spectator matter is formed out of nucleons that do not undergo any collisions.

UrQMD:

- Version 3.4
- Cascade mode in this work
- Offset radius 5 fm
- Evolution time – 100 fm/c
- Other parameters are set to default values

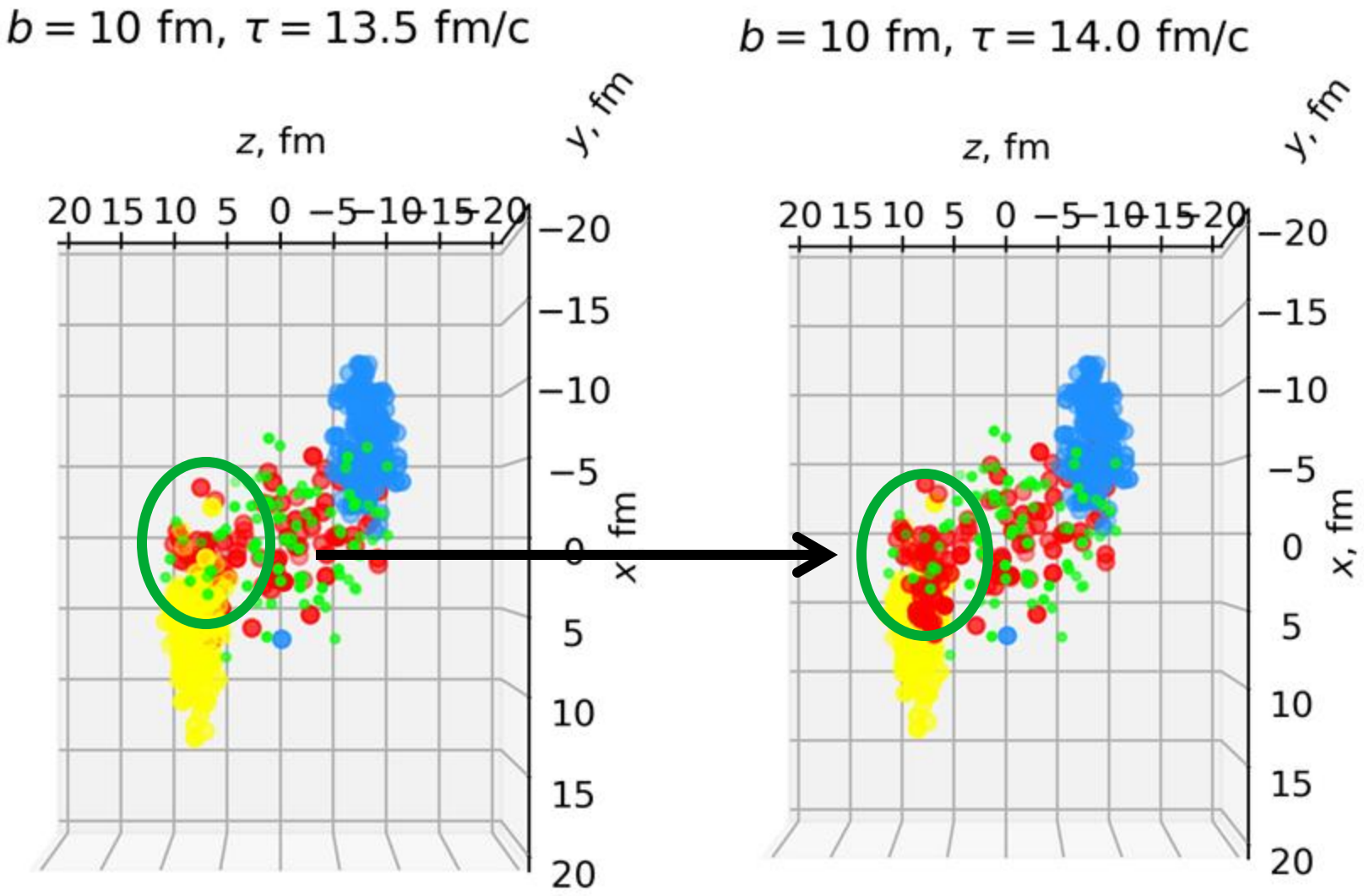
Unigen file

AMC:

- Find spectator nucleons
- Define prefragments via MST-clustering
- Constant d = 2.7 fm
- Model prefragments decays
- All the participant data remain intact

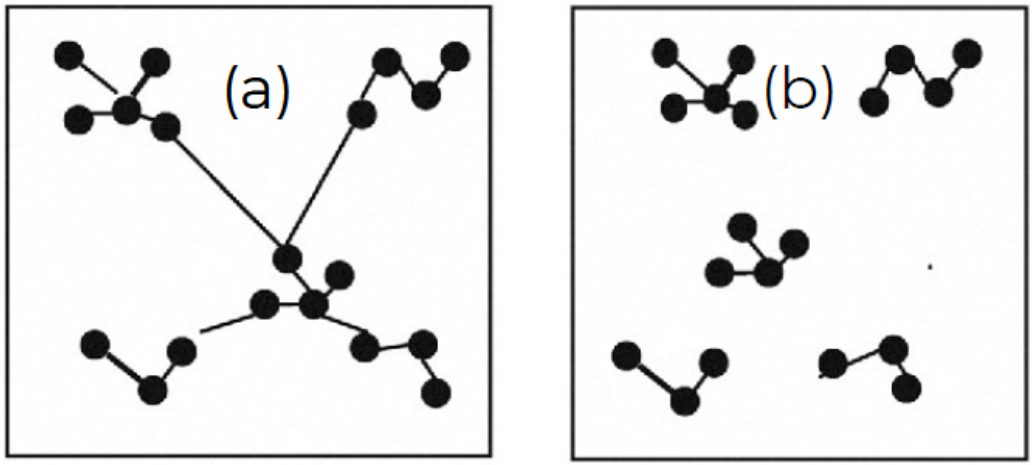
Unigen file

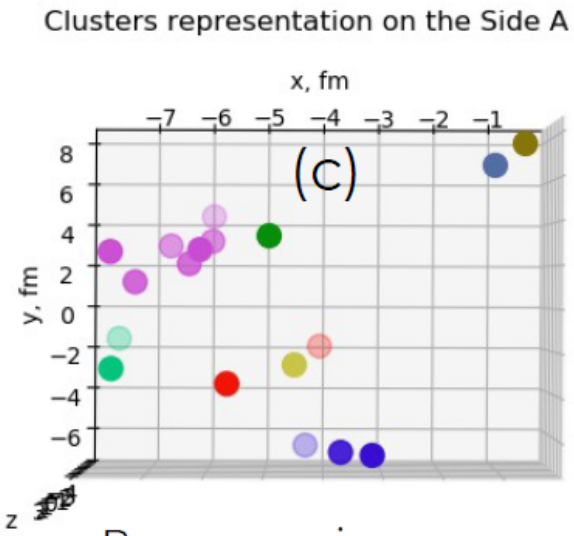
Knocking out some spectator nucleons by mesons



Blue and yellow – spectator nucleons, red – participant nucleons, green – produced mesons

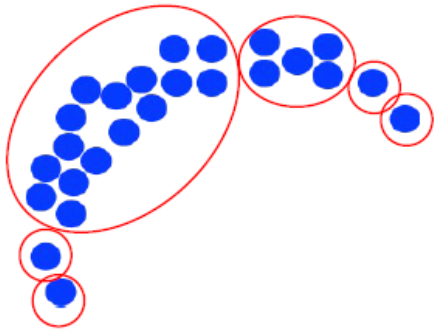
MST-clustering





Beam-eye view

- Graph vertexes – nucleons, edges weights – Cartesian distances between them.
- **(a)** The minimum spanning tree is selected from the complete graph
- **(b)** All edges with a weight greater than d are removed. d is the clustering parameter depending on the excitation energy
- **(c)** Connectivity components are separate (pre-)fragments

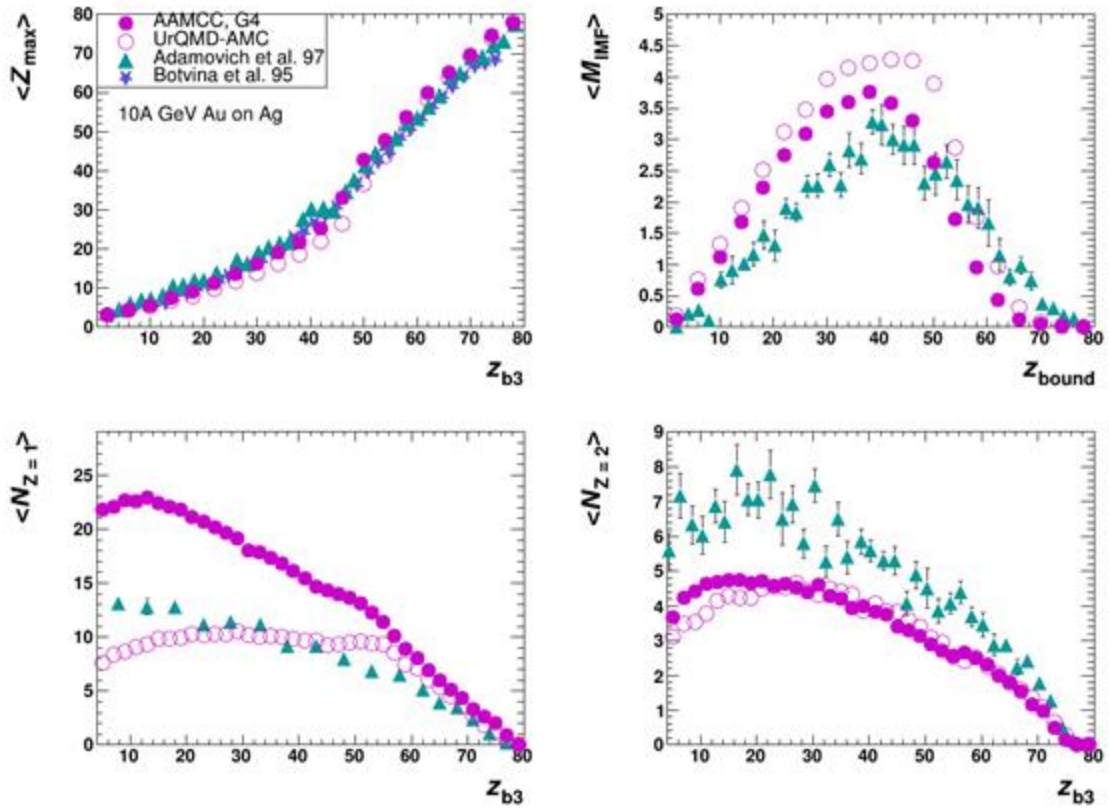


Prefragments in a central collision

AAMC^2

The prefragment is dynamically divided into several prefragments until thermodynamic equilibrium is reached.

^{197}Au fragmentation



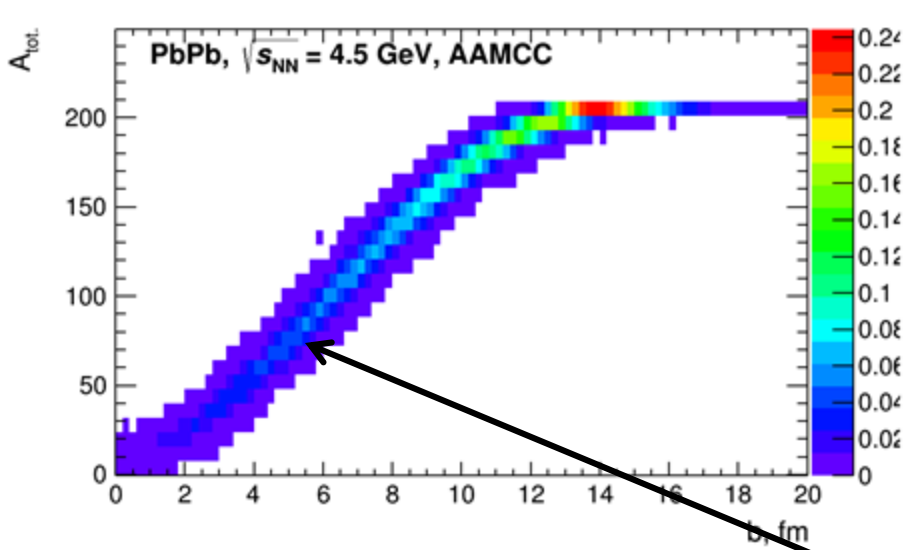
- UrQMD-AMC and AAMCC describe Z_{max}. Models give similar numbers of He

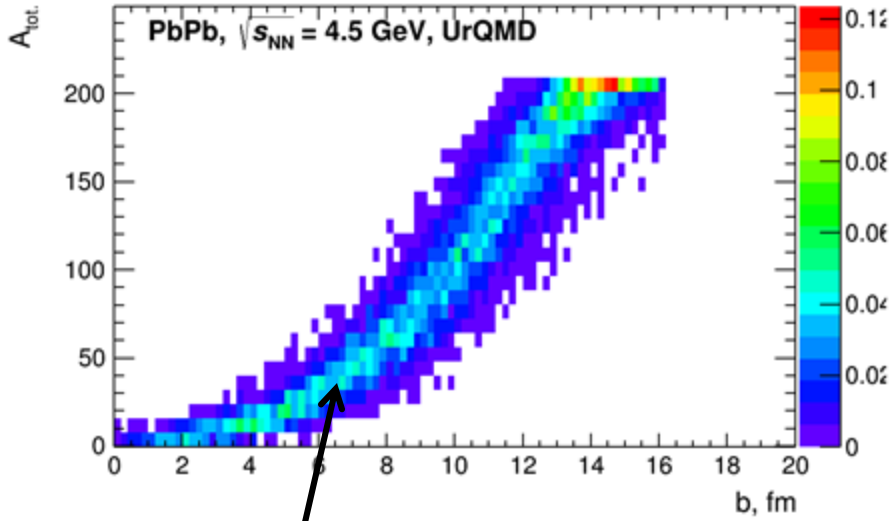
- UrQMD-AMC is systematically lower than AAMCC for $Z_{bound} < 50$. This is due to a smaller spectator volume in UrQMD.

- AAMCC is closer to data on M_{IMF}, while UrQMD-AMC overestimates M_{IMF} in semi-central collisions. This is because of higher excitation energy of prefragments since more nucleons are removed.

- The difference in H fragments can be attributed to the different number of participants, because of a larger contribution of protons from MST-clustering

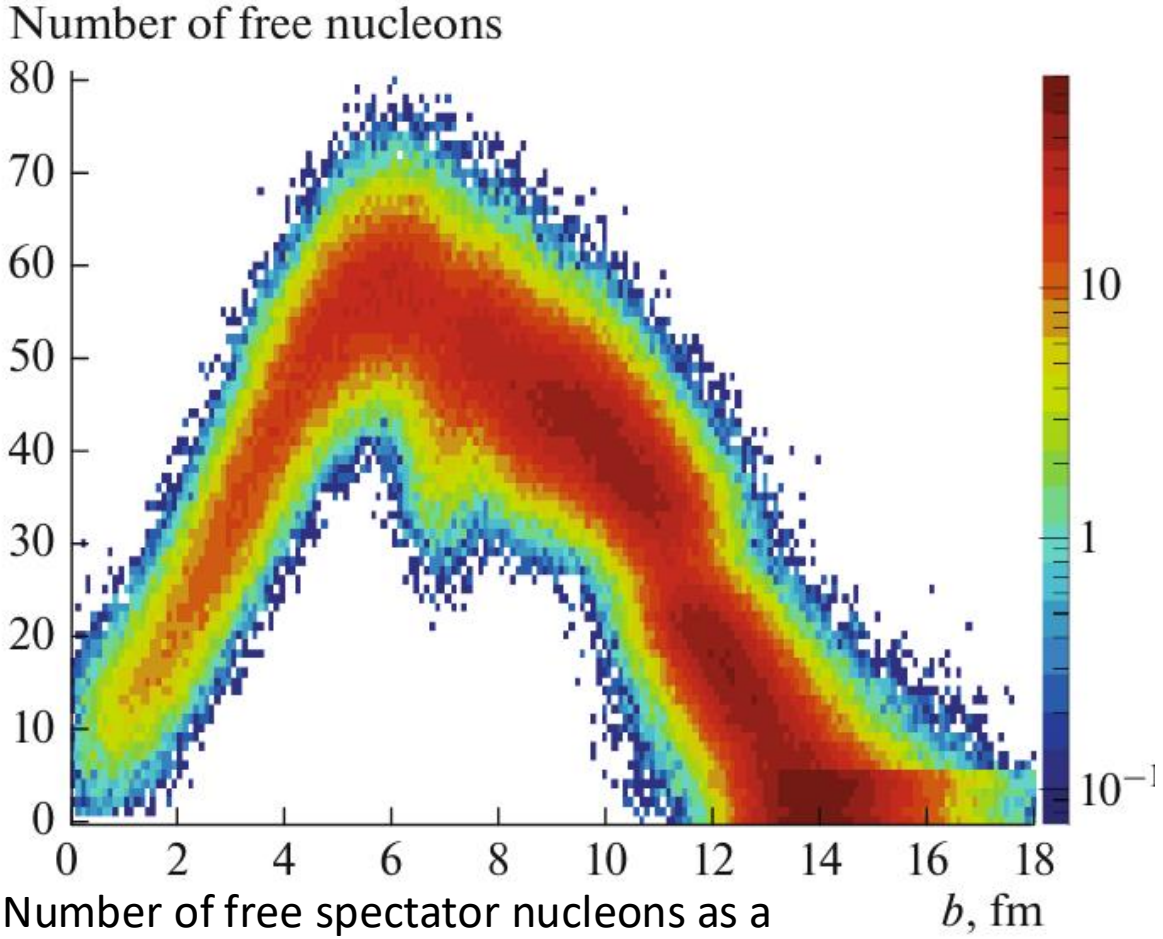
Spectator matter volume as a function of impact parameter





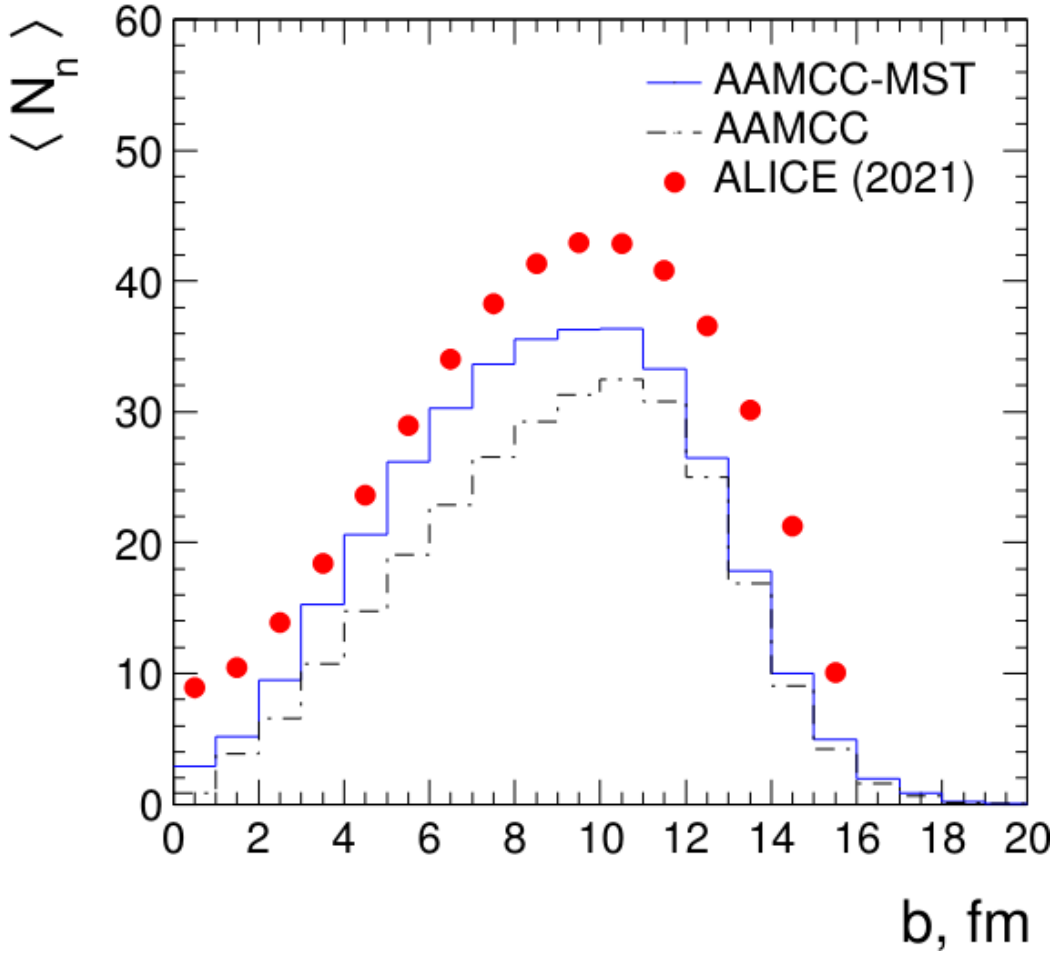
UrQMD gives less spectators than AAMCC for all b

Nuclear interaction



Number of free spectator nucleons as a function of the impact parameter in collisions between ^{197}Au nuclei at NICA at $\sqrt{s_{NN}}$ = 5 GeV

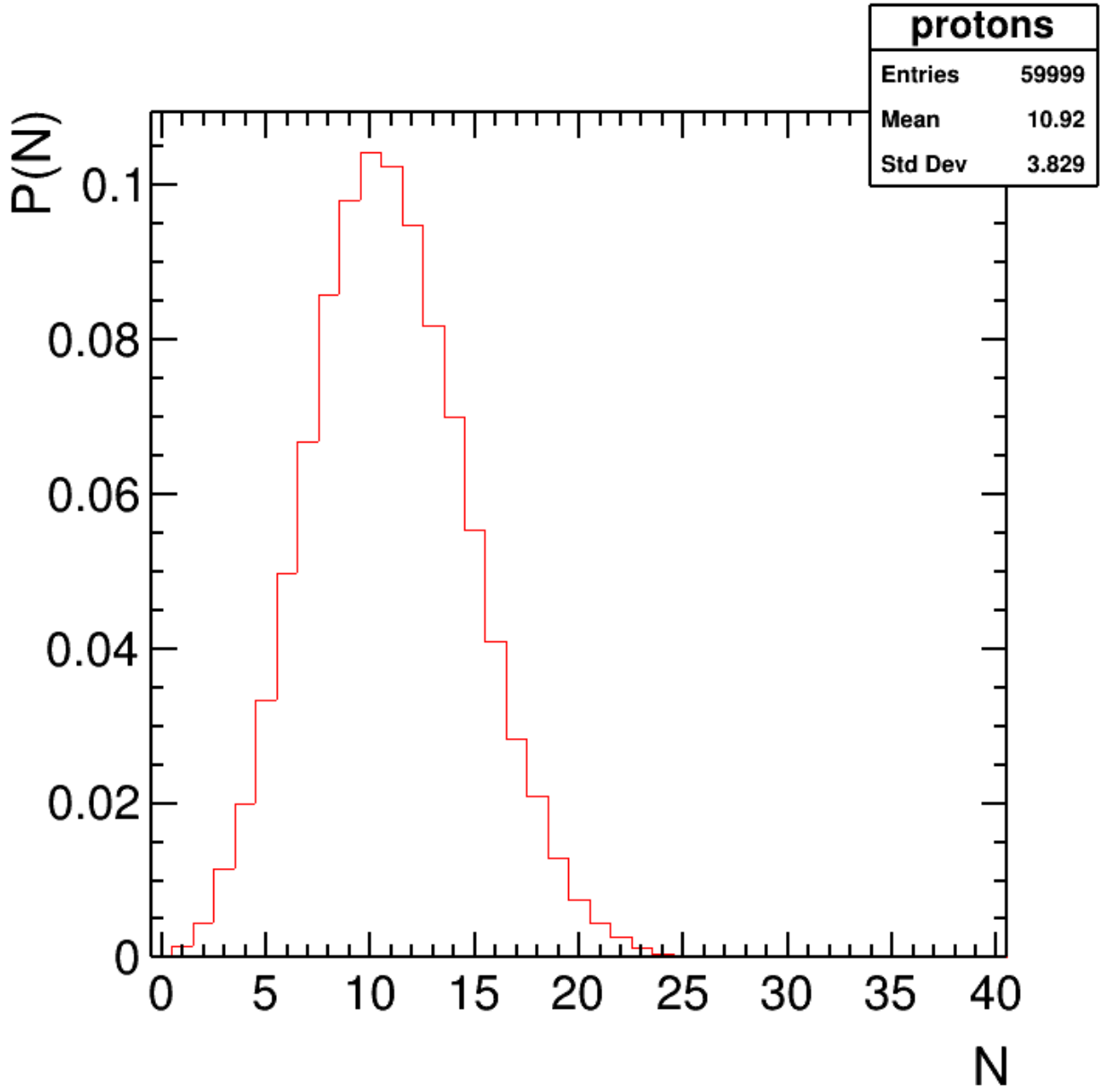
A. Svetlichnyi & I. Pshenichnov, Formation of Free and Bound Spectator Nucleons in Hadronic Interactions between Relativistic Nuclei. *Bulletin of the Russian Academy of Sciences: Physics* **2020**, 84 (8), 911–916.

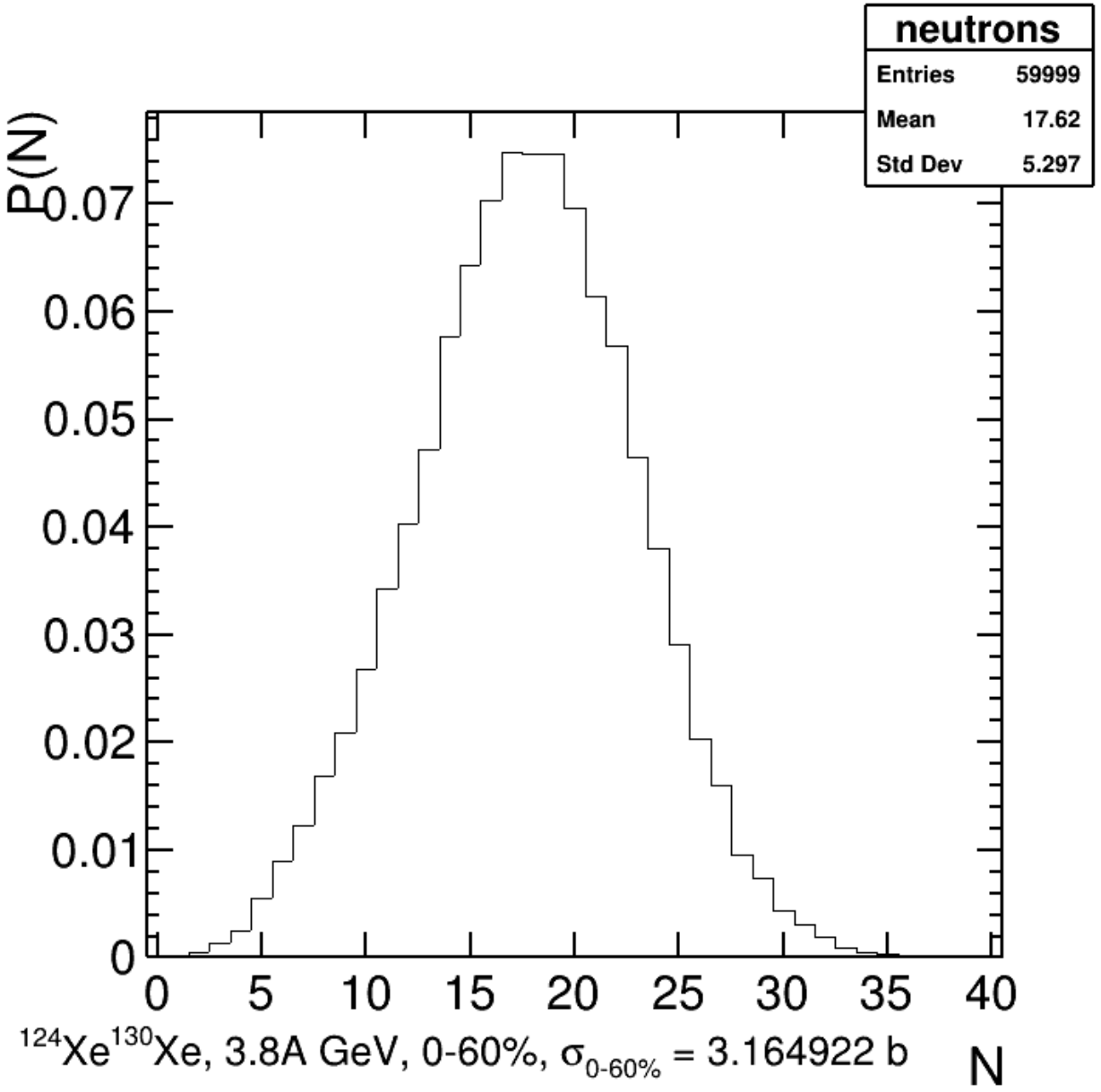


Average multiplicities of neutrons in ^{208}Pb–^{208}Pb collisions at $\sqrt{s_{NN}}$ = 5.02 TeV as functions of the collision impact parameter

Nepeivoda, R. et al., Pre-Equilibrium Clustering in Production of Spectator Fragments in Collisions of Relativistic Nuclei. *Particles* **2022**, 5, 40–51.

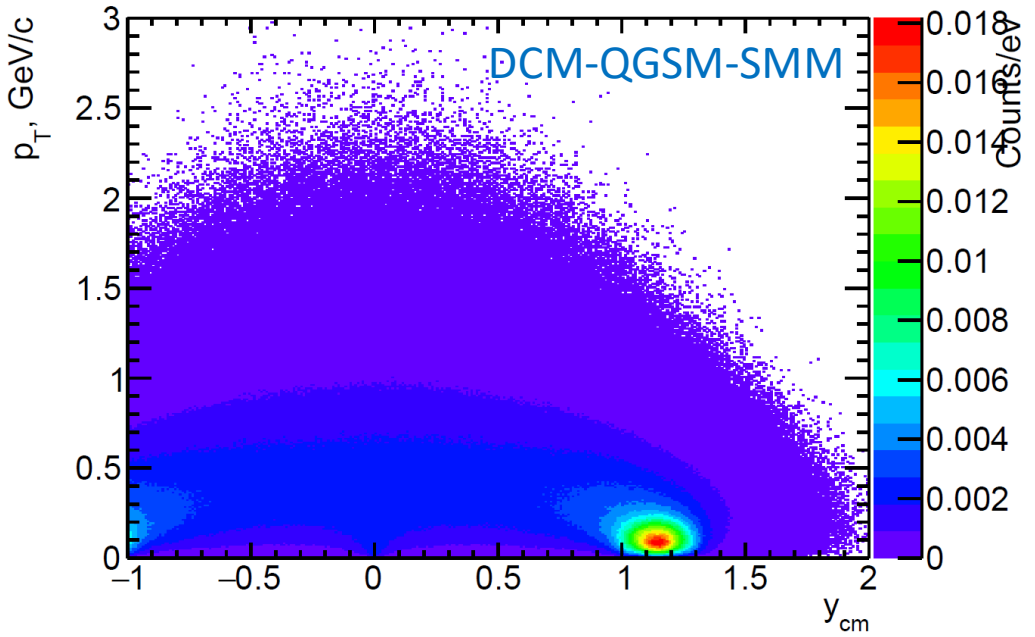
Nuclear interaction

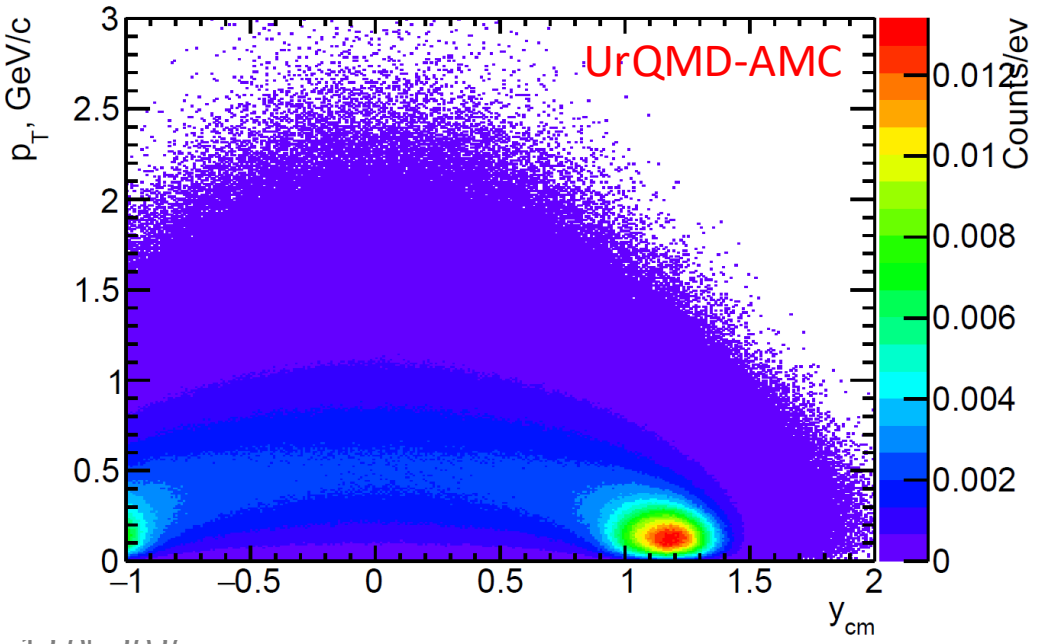


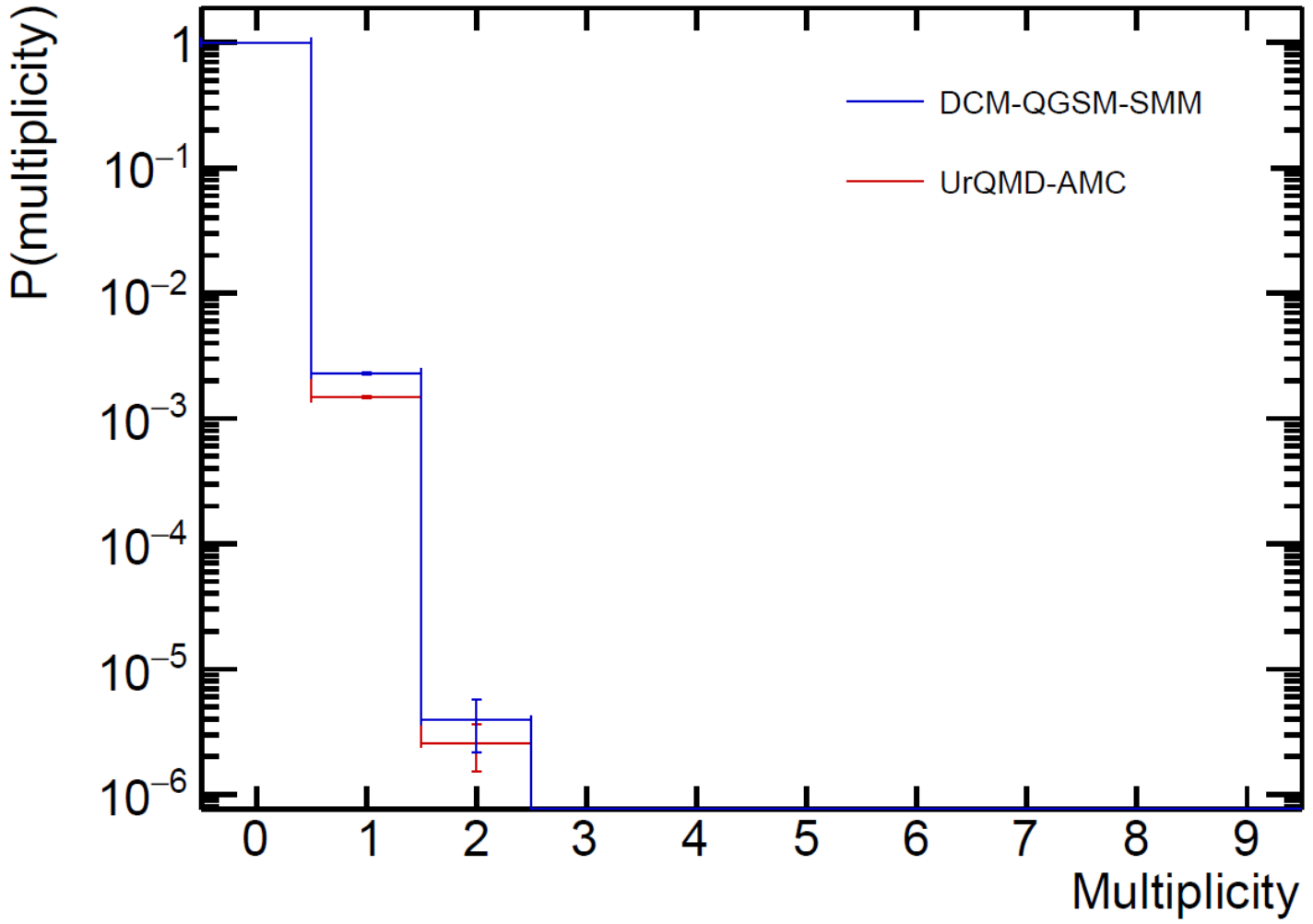


27°

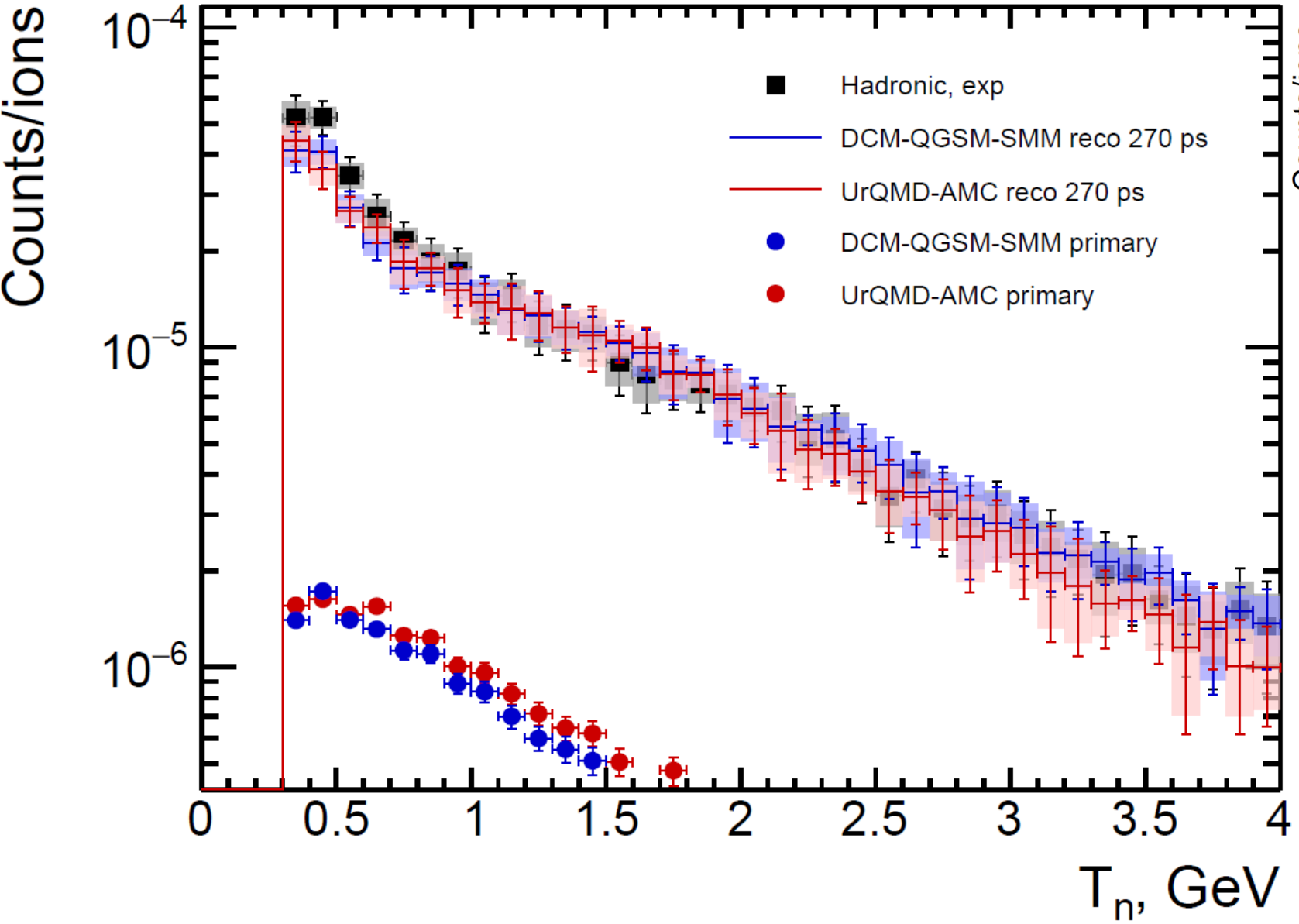
Neutron yields at 27°

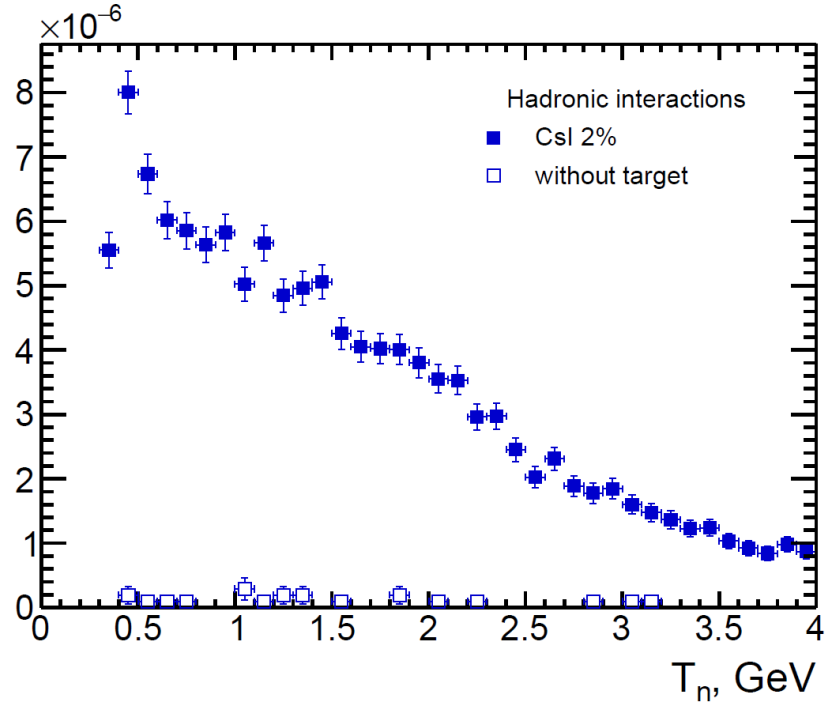




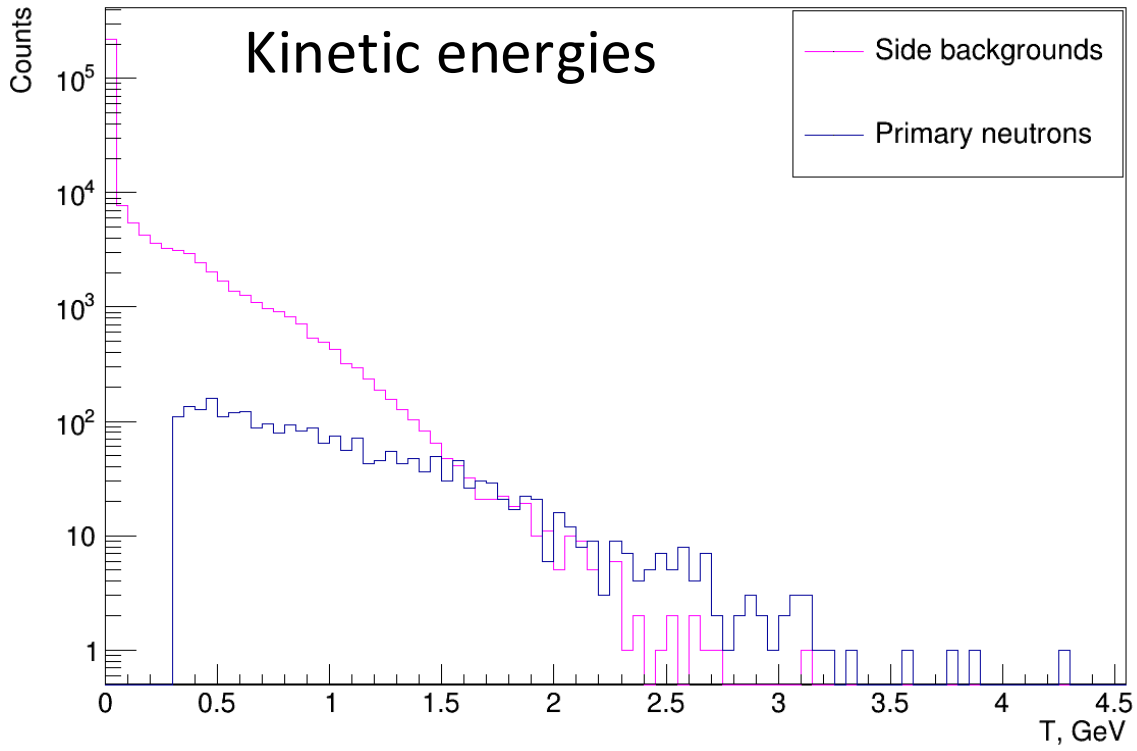


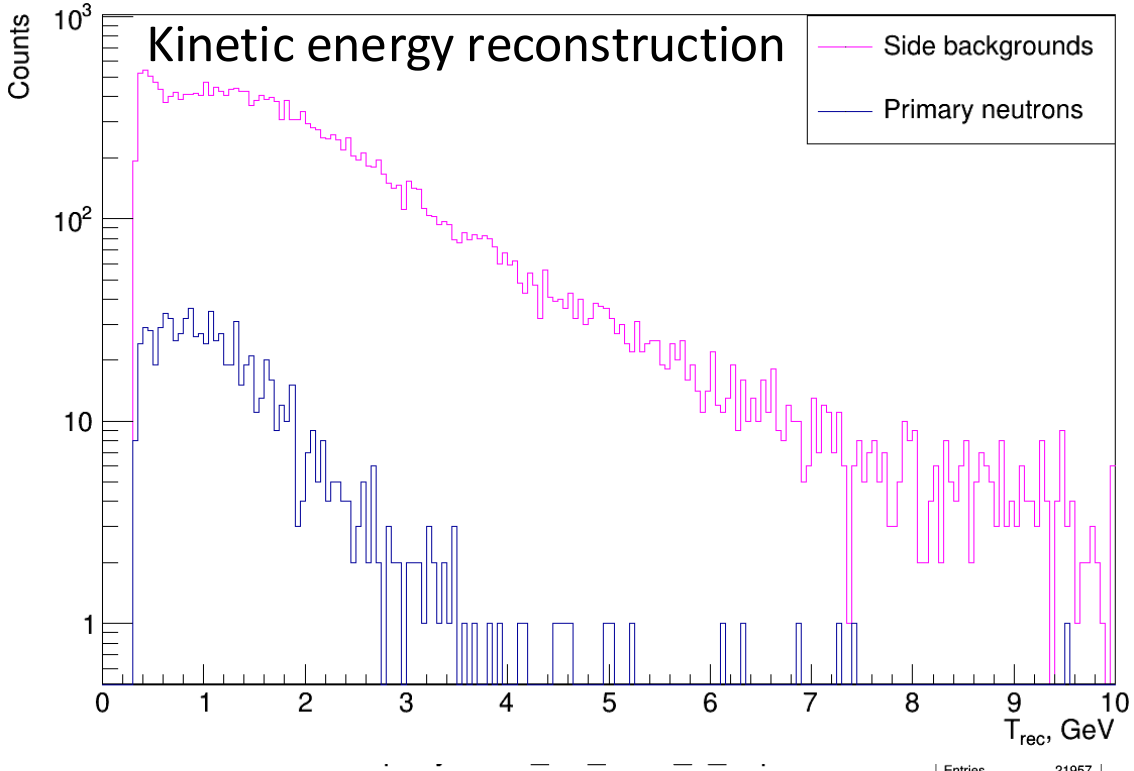
Neutron yields at 27°

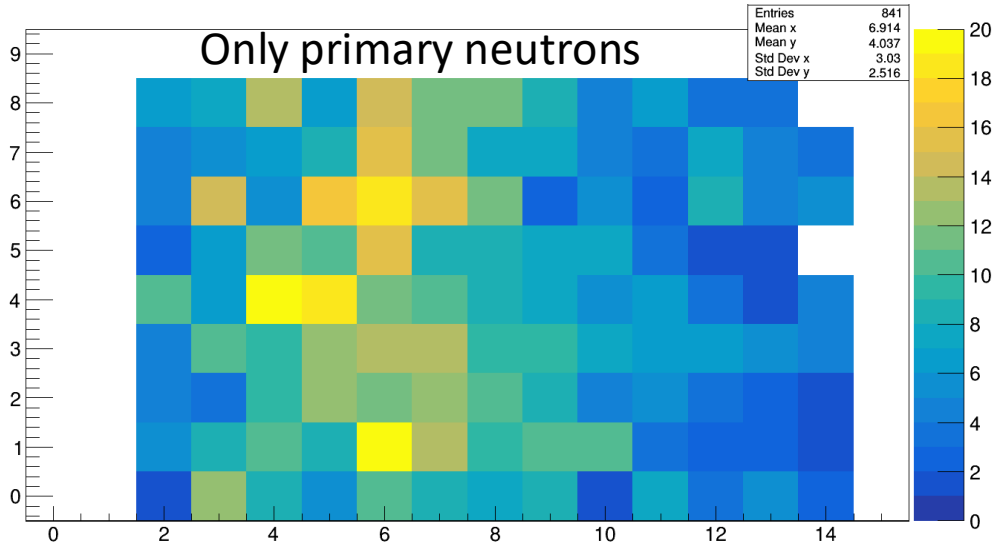


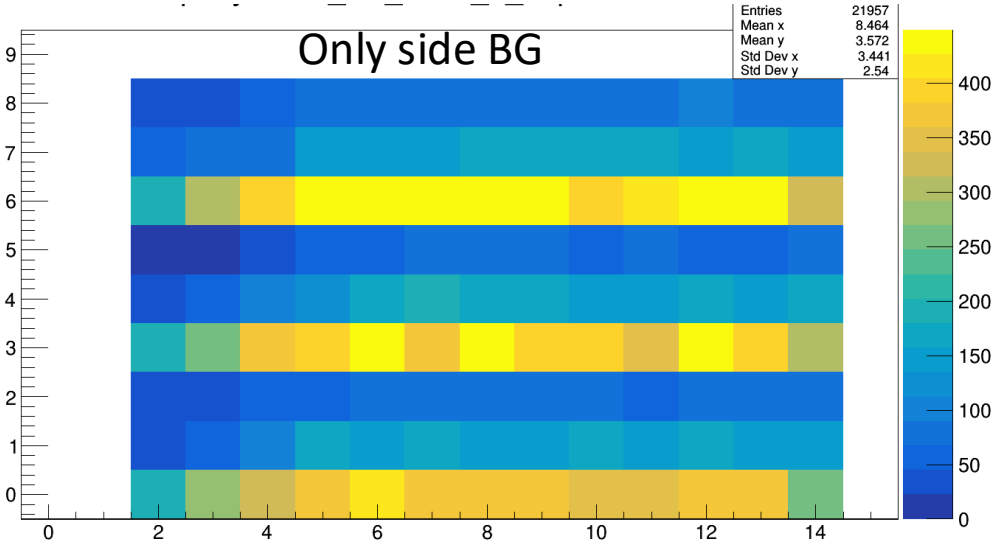


Backgrounds DCM-QGSM-SMM



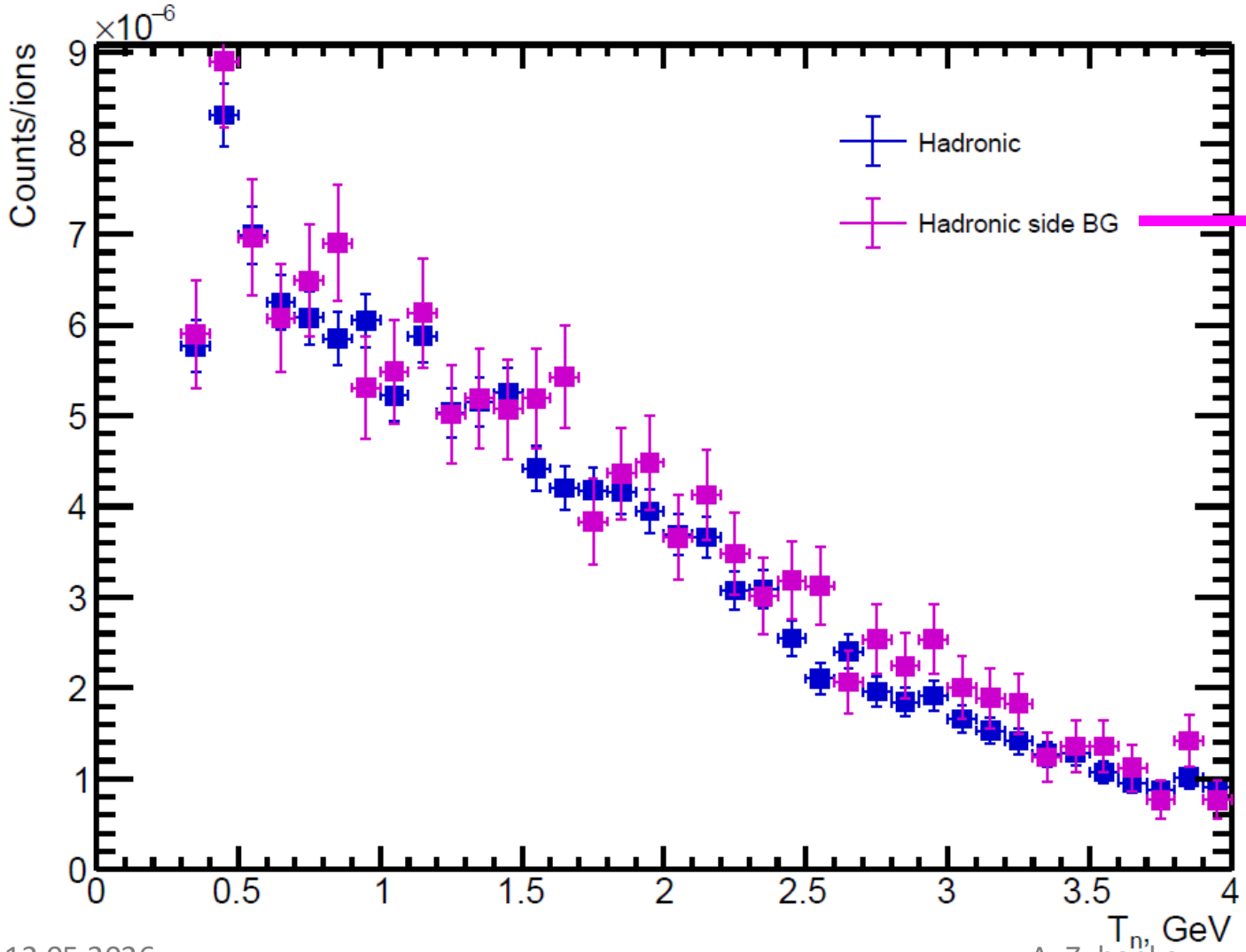


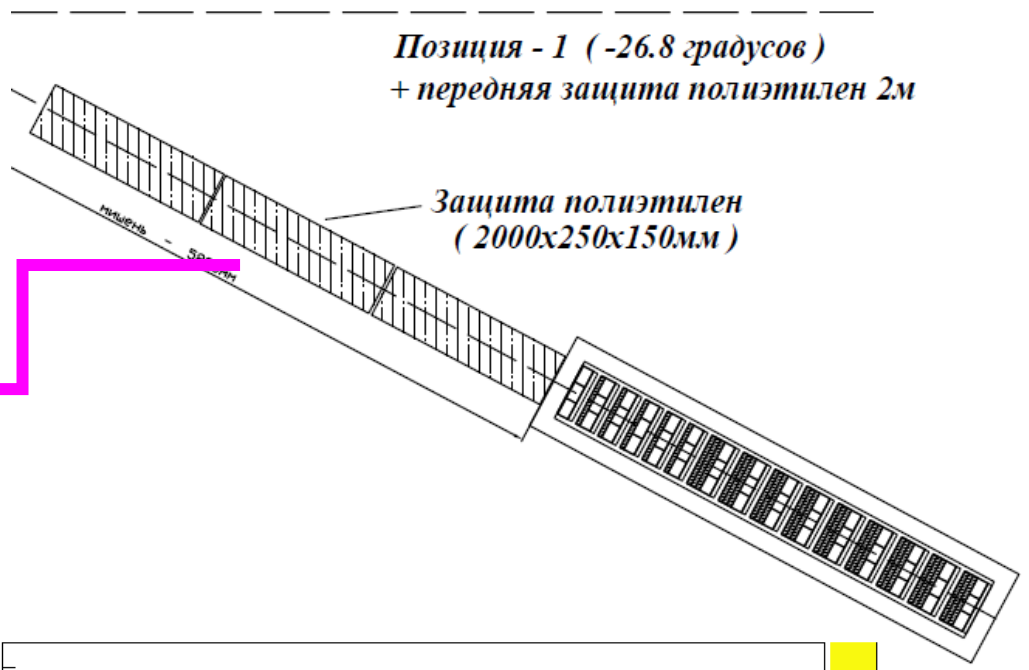


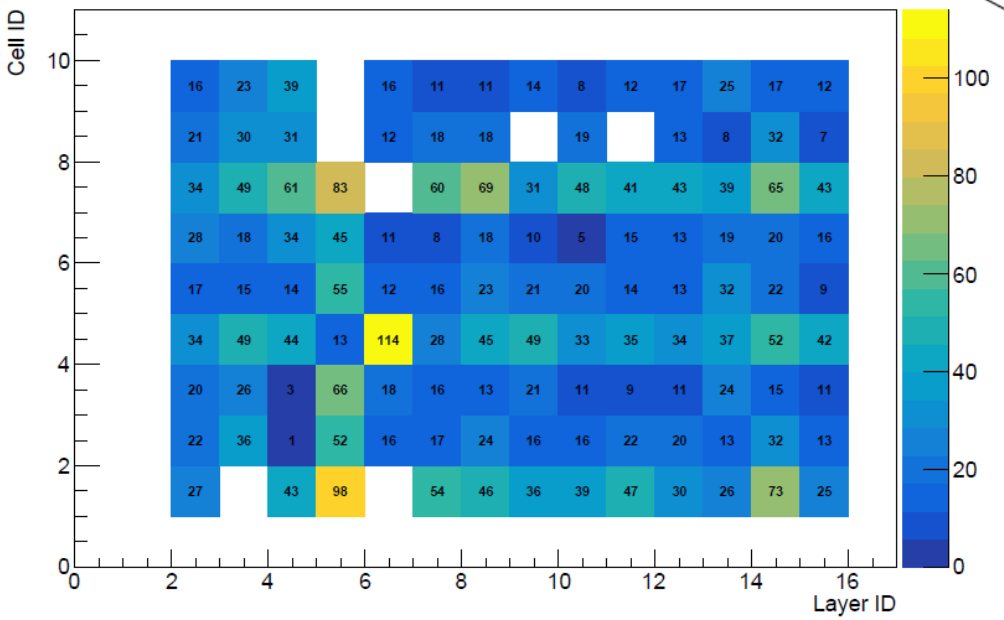


Backgrounds

Experimental data
Kinetic energy reconstruction



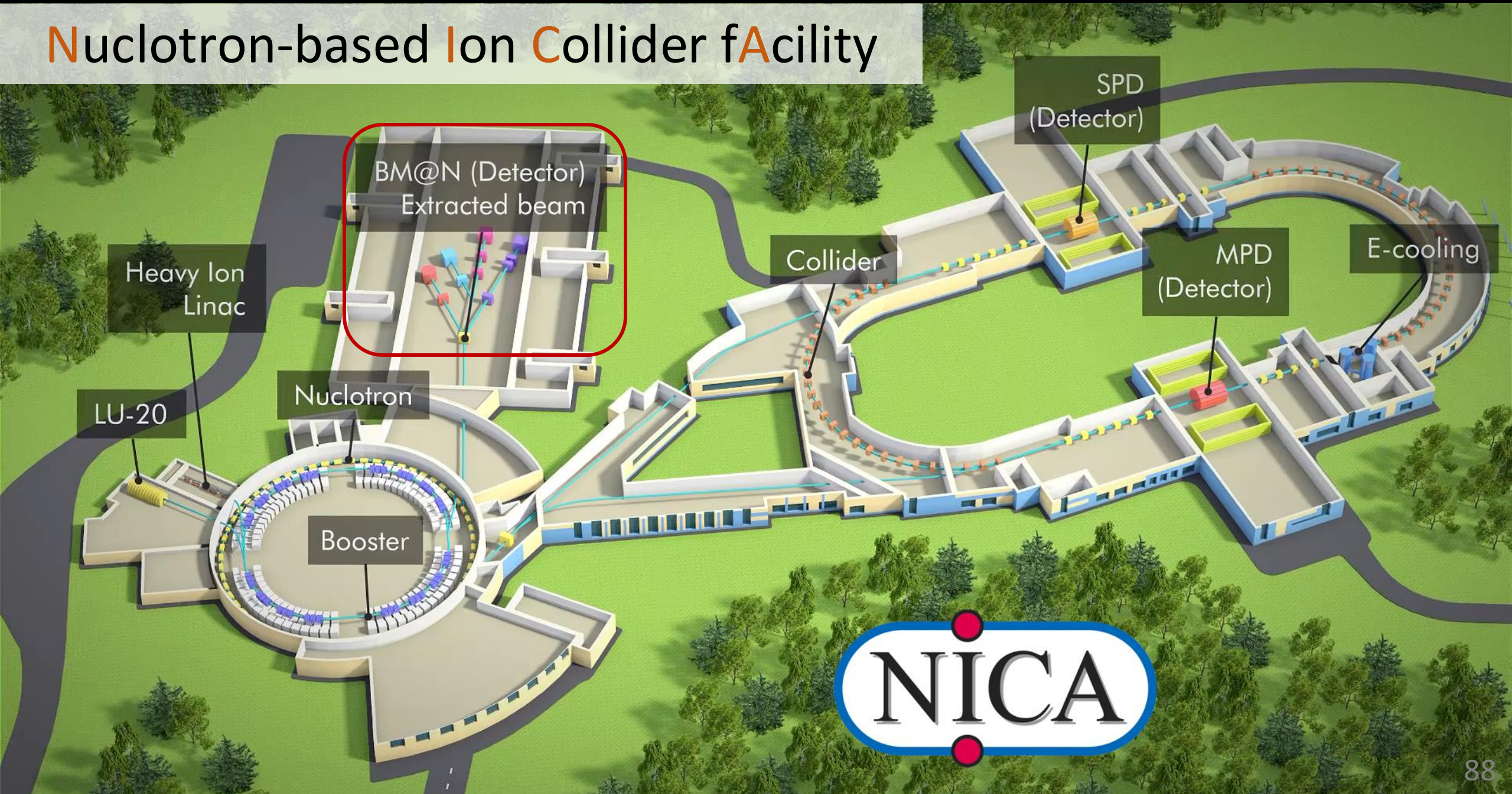




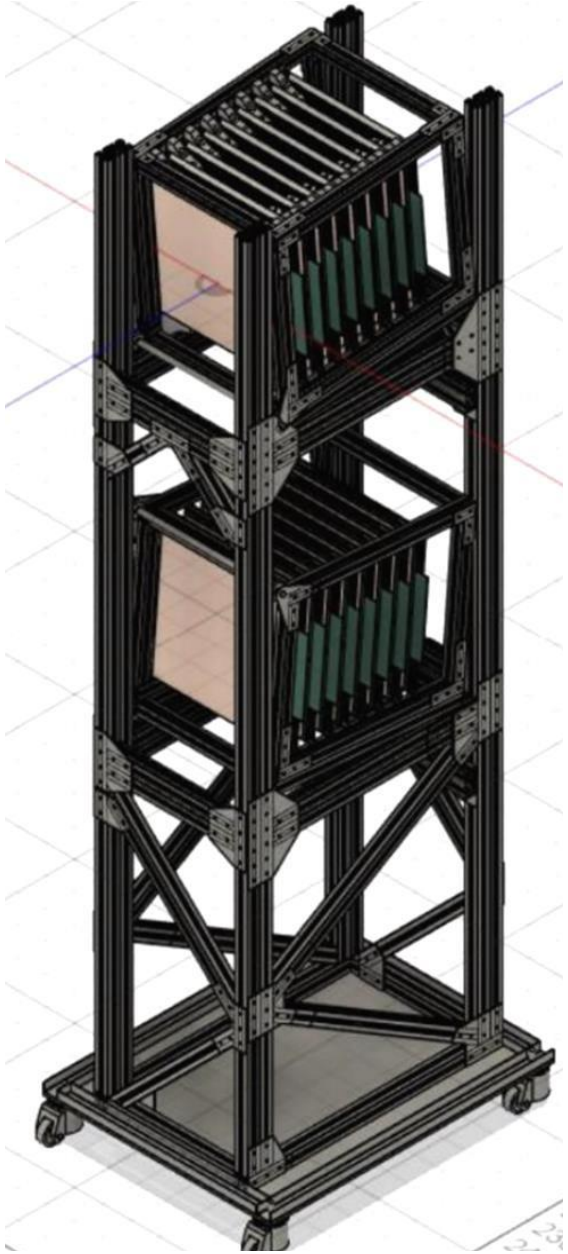
HGND

BM@N – первый действующий эксперимент на NICA

Nuclotron-based Ion Collider fAcility



Полномасштбаный HGND





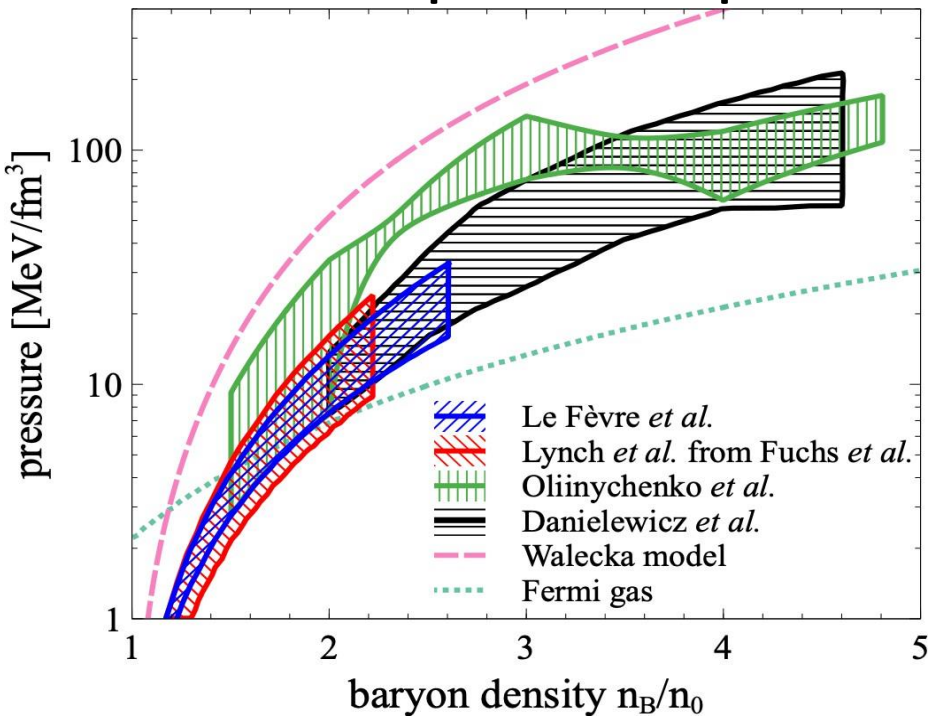
- HGND разрабатывается в ИЯИ РАН для измерения **азимутальных потоков и выходов нейтронов** с энергиями от 300 МэВ до 4 ГэВ в ядро-ядерных взаимодействиях при столкновениях тяжёлых ионов с энергиями до 4А ГэВ в эксперименте с фиксированной мишенью BM@N в ОИЯИ.
- Данные о потоке нейтронов в диапазоне энергий BM@N пока отсутствуют.

S. Morozov et al., The Highly-Granular time-of-flight Neutron Detector for the BM@N experiment, NIM A **2025**, 1072, 170152

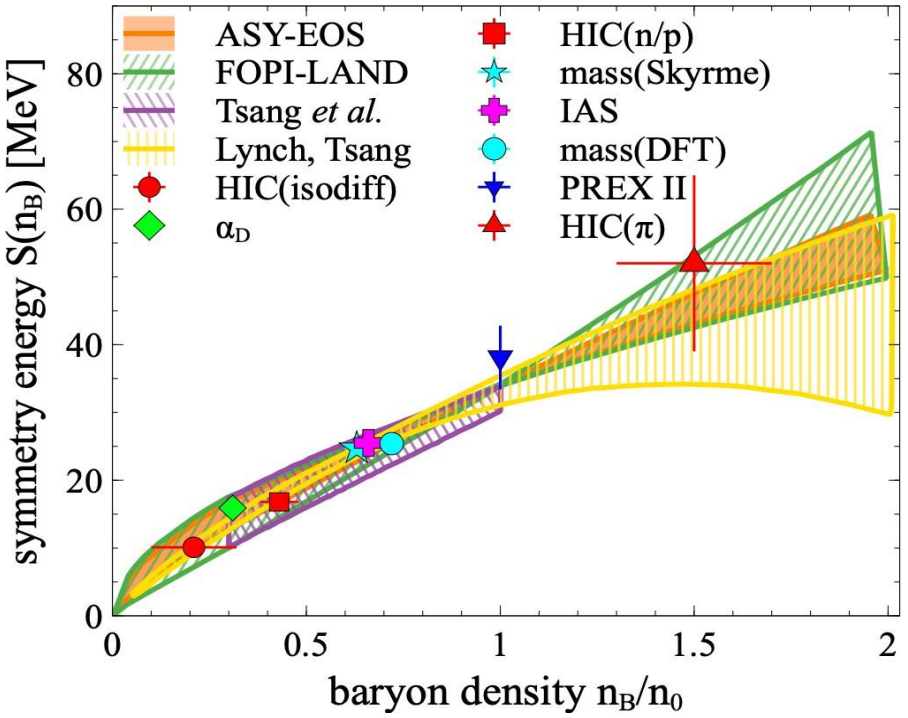
Исследовательская программа BM@N

Энергия связи на нуклон: $E_A(\rho,\delta) = E_A(\rho,0) + E_{sym}(\rho)\delta^2 + O(\delta^4)$

Симметричная материя



Энергия симметрии



$\delta = (\rho_n - \rho_p)/\rho$

Изоспиновая асимметрия

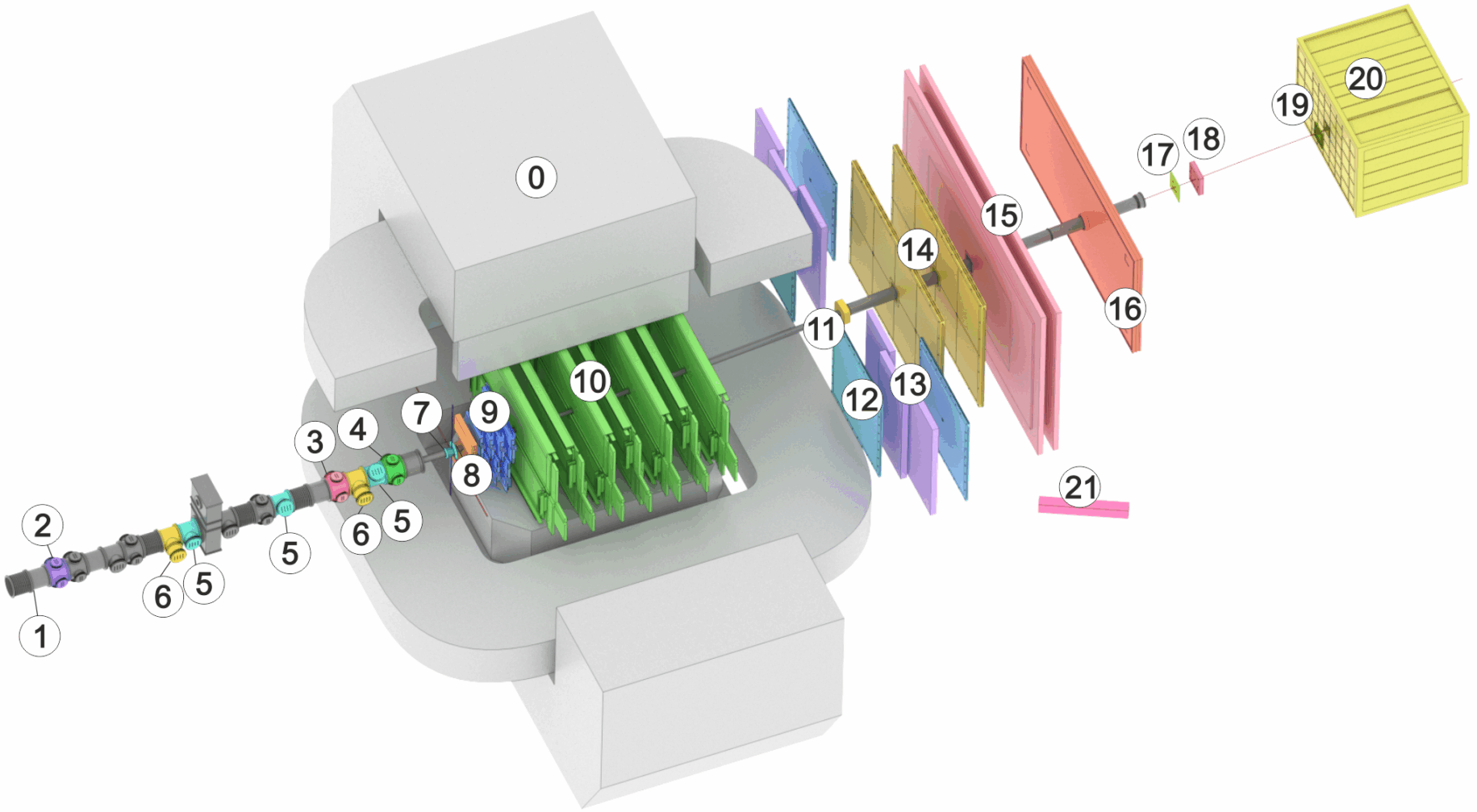
A. Sorensen et. al., Prog.Part.Nucl.Phys. 134 (2024) 104080

- Мало экспериментальных данных по вкладу энергии симметрии при энергиях выше 800 МэВ.
- Необходима реконструкция потока нейтронов и выходов.

- Изучение EoS необходимо для понимания свойств таких астрофизических объектов как нейтронные звезды.
- Отношение выходов и направленных потоков нейтронов к протонам чувствительно к вкладу энергии симметрии в уравнение состояния ядерной материи.

Установка BM@N

Baryonic **M**atter at **N**uclotron



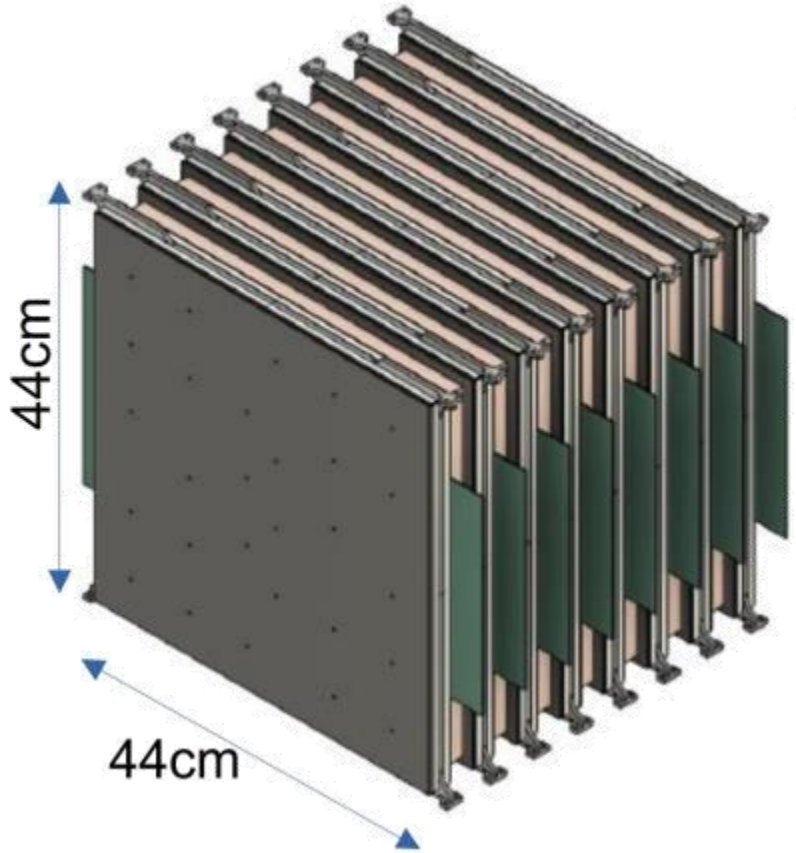
- Magnet SP-41 (0)
- Vacuum Beam Pipe (1)
- BC1, VC, BC2 (2-4)
- SiBT, SiProf (5, 6)
- BD (7)
- VSP, FSD, GEM (8, 9, 10)
- FD (11)
- 4 x CSC 1x1 m^2 (12)
- TOF 400 (13)
- 2 x CSC 2x1.5 m^2 (14)
- TOF 700 (15)
- ScWall (16)
- Small GEM (17)
- Beam Profilometer (18)
- FQH (19)
- FHCal (20)
- HGN (21)

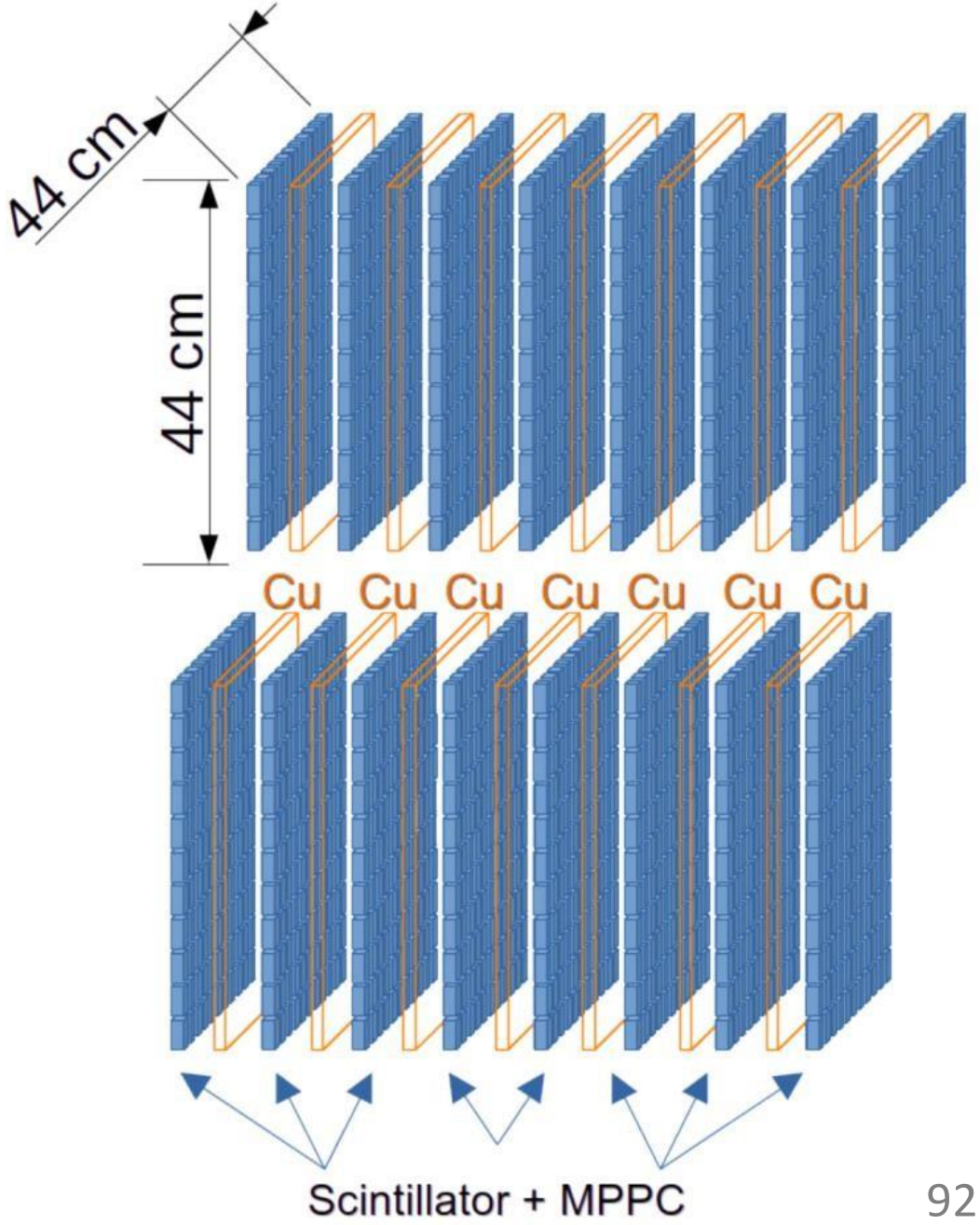
На BM@N измеряются анизотропные потоки протонов с помощью гибридной трекинговой системы совместно с времяпролетными детекторами TOF и передним адронным калориметром FHCal

Конструкция HGND

2 плеча по 8 слоев:

- 3 см Cu (поглотитель)
- 11x11 матрица сцинт. ячеек 2.5 см
- 0.5 см PCB
- Поперечный размер 44x44 см^2

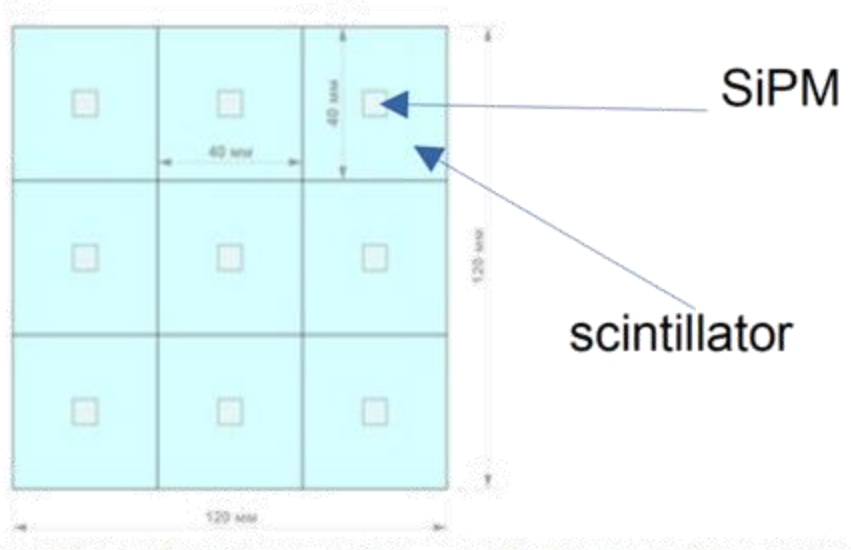




Конструкция HGND

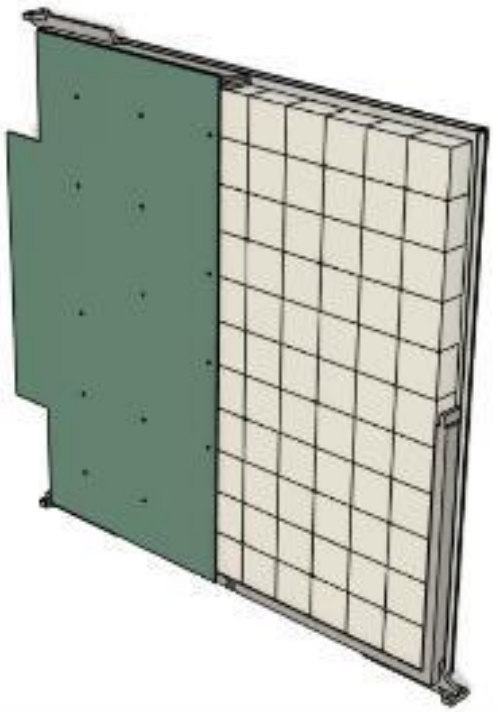
EQR15 11-6060D-S MPPC

- Активная площадь: 6x6 мм²
- Квантовая эффективность: 45% (420 нм)
- Усиление примерно 4×10^5



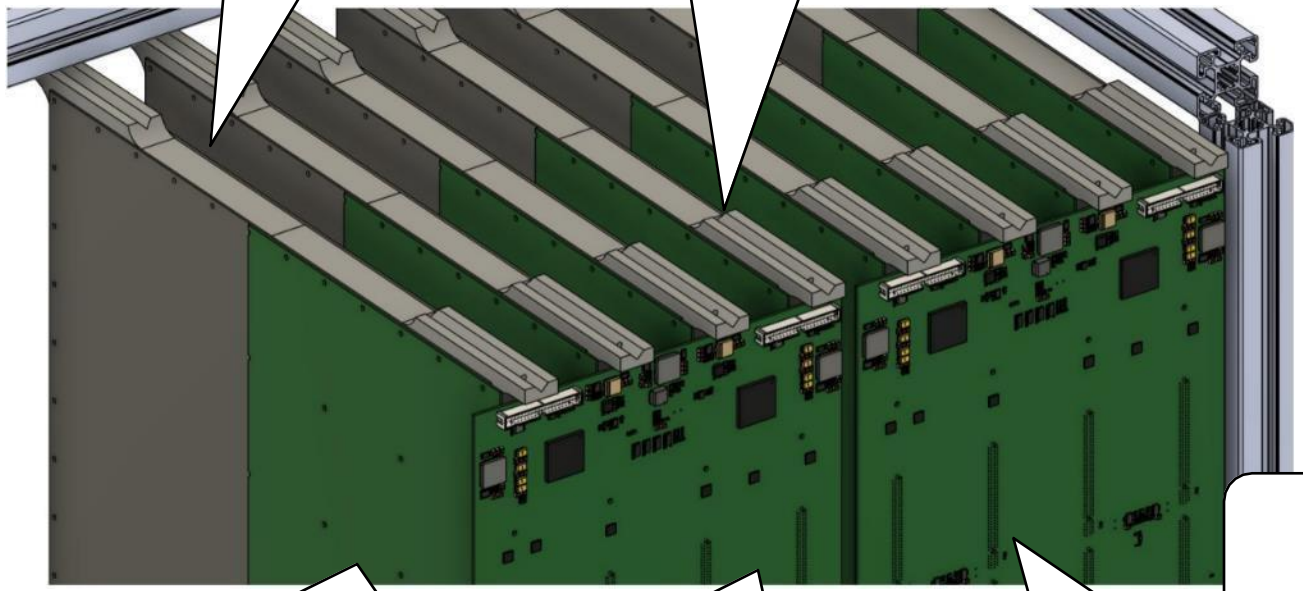
Сцинтилляторы на основе полистирола с POPOP

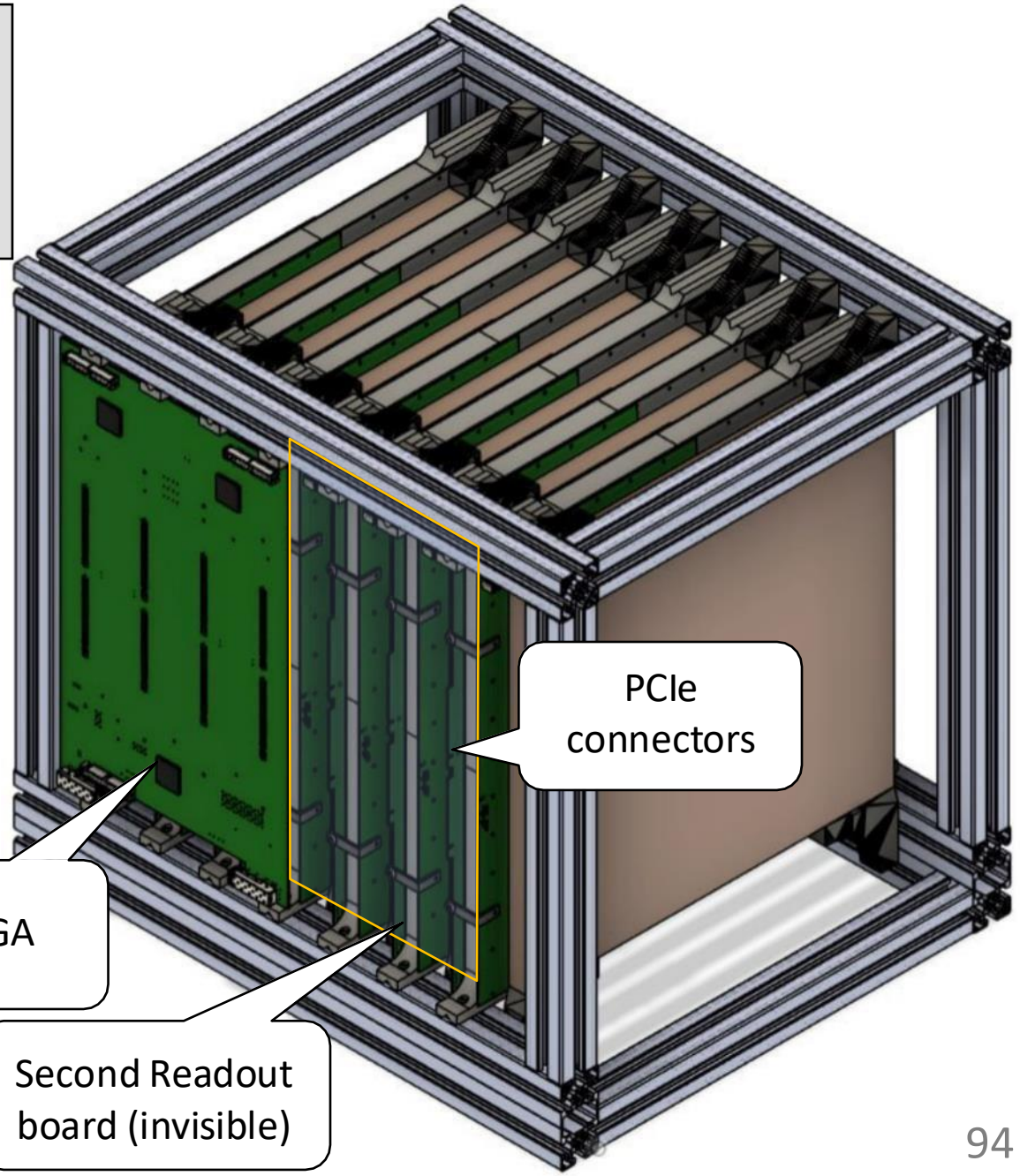
- Время высвечивания: 3,9±0,7 нс.
- Временное разрешение ячеек: 150 пс
- Полная длина детектора: ~0.5 м, ~1.5 λ_{int}
- Эффективность детектирования нейтронов: ~50% @ 1 GeV
- Энергетическое разрешение: - 2% (0.3 GeV); 20% (4 GeV)
- Световыход на MIP: 158±9 ф.э.
- Динамический диапазон: 1 – 8 MIP



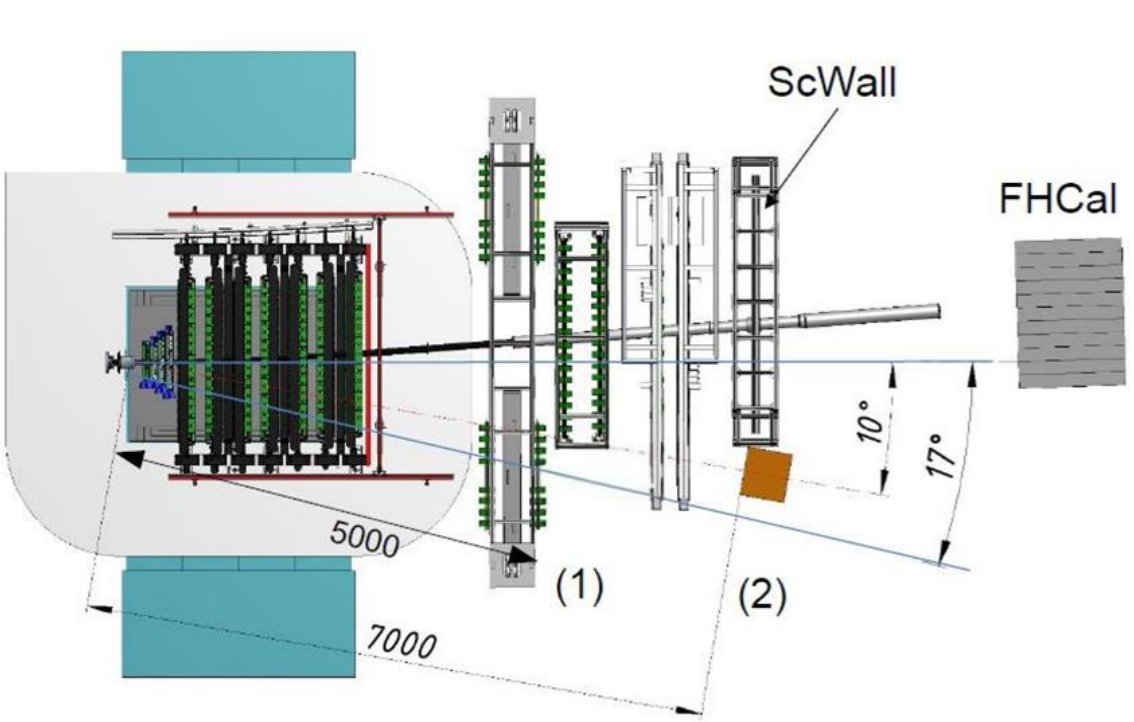
FEE & readout board

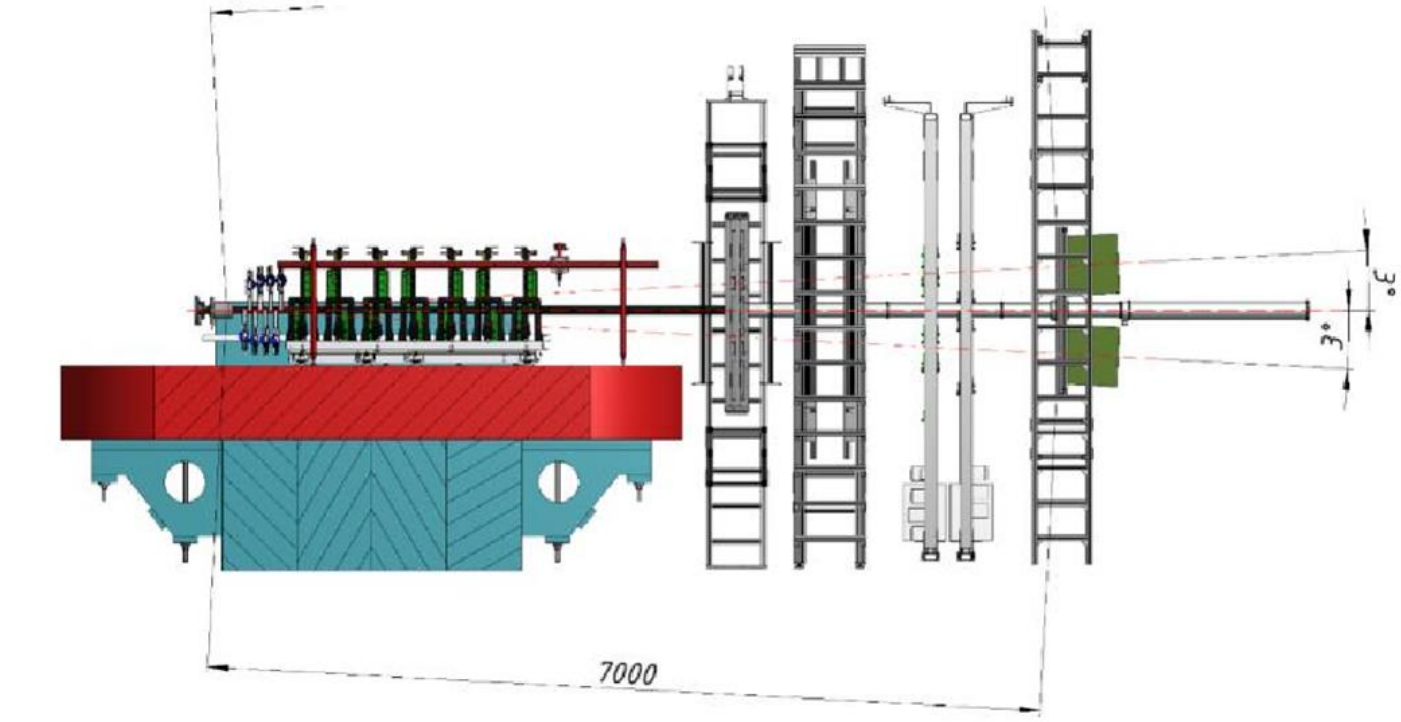
- 16 слоев ячеек
- 16 LED плат
- 32 FEE плат
- 8 считывающих плат
- 3 FPGA на плату
- 84 канала на FPGA
- 2000 каналов суммарно



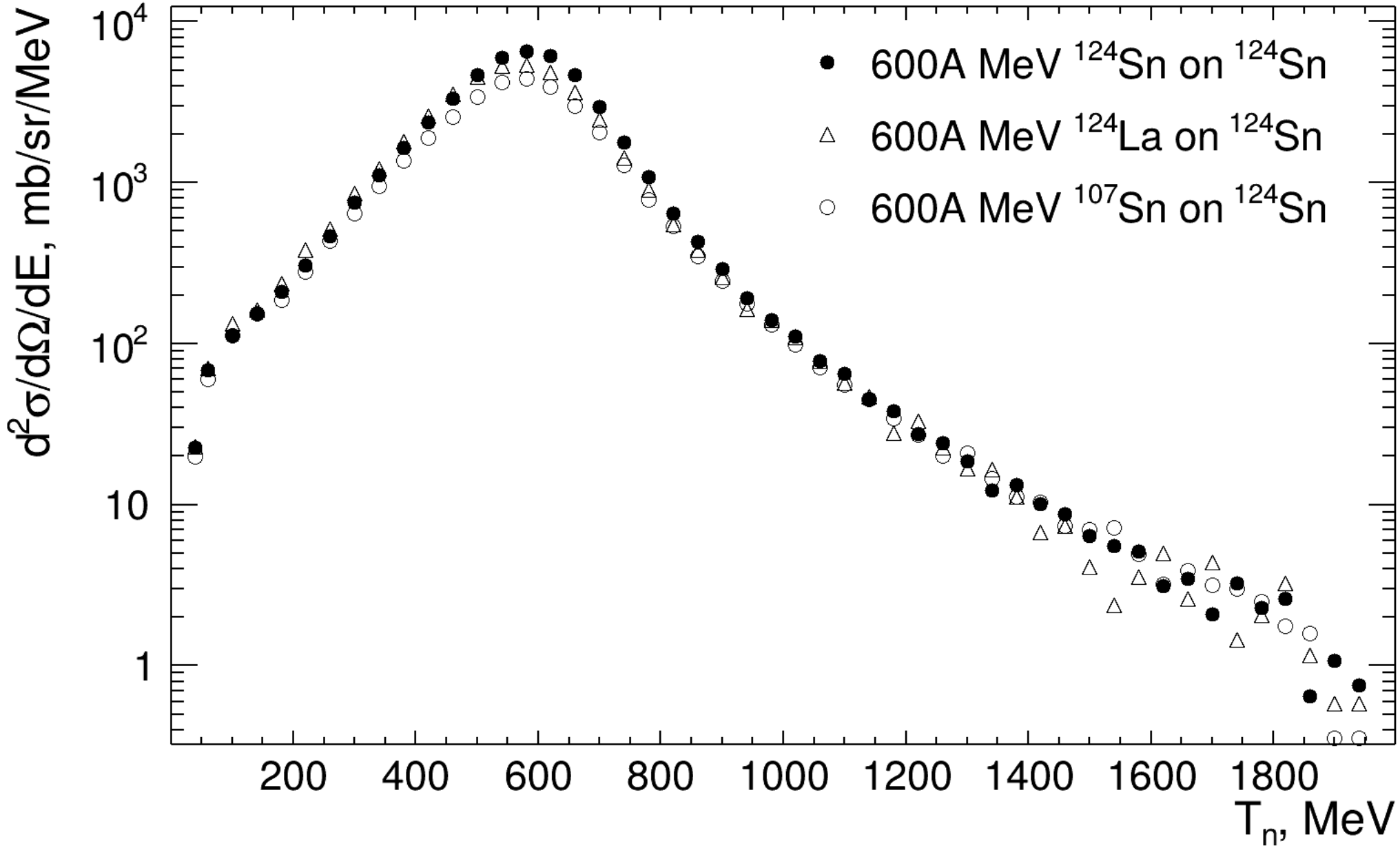


Планируемое положение HGND на BM@N





- ToF метод с T0 в качестве «стартового» времени
- Времяпролетная база ~ 7 м
- Детектор разделён на два «плеча» для увеличения акцептанса


600A MeV ^{124}Sn on ^{124}Sn
600A MeV ^{124}La on ^{124}Sn
600A MeV ^{107}Sn on ^{124}Sn
$d^2\sigma/d\Omega/dE$, mb/sr/MeV
T_n, MeV
10^4
10^3
10^2
10
1
200
400
600
800
1000
1200
1400
1600
1800

LAND acceptance

